

# The development of a diagnostic assay for nepoviruses in grapevine

by

**Lolita Frazenburg**



*Thesis presented in fulfilment of the requirements for the degree of  
Master of Science at the Department of Genetics, Faculty of Science,  
Stellenbosch University*

Supervisor: Prof. J.T. Burger  
Co-supervisor: Dr. R. Souza-Richards

March 2015

## Declaration

By submitting this thesis/dissertation electronically, I declare that the entirety of the work contained therein is my own, original work, that I am the sole author thereof (save to the extent explicitly otherwise stated), that reproduction and publication thereof by Stellenbosch University will not infringe any third party rights and that I have not previously in its entirety or in part submitted it for obtaining any qualification.

December 2014

Copyright © 2015 Stellenbosch University

All rights reserved

## Abstract

---

The nepoviruses are a group of nematode-transmitted plant viruses that are distributed worldwide and infect a wide range of plant species, including grapevine. Most of the nepoviruses are foreign to South Africa and to date, only *Grapevine fanleaf virus* (GFLV) is present. The Department of Agriculture, Forestry and Fisheries (DAFF), as the official National Plant Protection Organisation (NPPO) of South Africa, is committed to prevent the importation and spread of plant pathogens by administering the Agricultural Pests Act, 1983 (Act No. 36 of 1983). Effective measures are implemented by which the introduction of agricultural pests may be prohibited to safeguard the agricultural environment. One of the core functions of DAFF is to render a routine plant health diagnostic service for imported plants and plant products to prevent exotic pathogens from entering the country. The objective of this study was to develop a diagnostic assay for the detection of nepoviruses in grapevine. The project aimed to produce antibodies by recombinant DNA technology against bacterially expressed viral coat protein of a specific nepovirus [*Tomato ringspot virus* (ToRSV)] and subsequently develop a DAS-ELISA (Double Antibody Sandwich Enzyme-linked Immunosorbent) assay for the detection of the virus. The coat protein (CP) was successfully isolated from imported ToRSV-infected grapevine material. Two expression systems were utilised for expression of the ToRSV-CP, the GST gene fusion system and an *Agrobacterium*-mediated expression system. The GST gene fusion system was unsuccessful as insufficient soluble protein expression prevented the production of antibodies and thus the development of the DAS-ELISA assay. Tissue print immunoassay (TPIA) initially showed positive results for transient expression of the fusion protein in tobacco plants, but further confirmation proved to be inconclusive. The project also aimed to develop a real-time PCR assay for the specific detection and relative quantification of GFLV, based on a conserved region of the RNA-2 genome. A partial GFLV-RNA-2 from a South African isolate of grapevine was sequenced and used for the design of specific primers. The quantitative real-time PCR assay based on SYBR green technology proved to be sensitive in detecting levels as low as 0.11ng/reaction in infected plants, making it a highly effective diagnostic tool for the detection of GFLV.

## Opsomming

---

Die nepovirusse is 'n groep van nematode-oordraagbare plant virusse wat wêreldwyd versprei word en 'n wye verskeidenheid van plantspesies infekteer, insluitend wingerd. Die meeste van die nepovirusse is uitheems aan Suid-Afrika en tot op datum is net *Wingerd netelblaar virus* (GFLV) teenwoordig. Die Departement van Landbou, Bosbou en Visserie (DAFF), as die amptelike Nasionale Plant Beskermings Organisasie (NPBO) van Suid-Afrika, is daartoe verbind om die invoer en verspreiding van plantpatogene te voorkom deur administrasie van die Wet op Landbouplae, 1983 (Wet No. 36 van 1983). Doeltreffende maatreëls word geïmplementeer waardeur die invoer van landbouplae verbied word om sodoende die landbou-omgewing te beskerm. Een van die kernfunksies van DAFF is om 'n roetine plant gesondheid diagnostiese diens vir ingevoerde plante en plantprodukte te lewer om te verhoed dat eksotiese patogene die land binnedring. Die doel van hierdie studie was om 'n diagnostiese toets vir die opsporing van nepovirusse in wingerd te ontwikkel. Die projek was daarop gemik om antiliggame te vervaardig deur rekombinante DNA-tegnologie teen bakterieël-uitgedrukte virale mantelproteïen van 'n spesifieke nepovirus [*Tomato ringspot virus* (ToRSV)] en vervolgens 'n DAS-ELISA (Double Antibody Sandwich Enzyme-linked Immunosorbent) toets vir die opsporing van die virus te ontwikkel. Die mantelproteïen (CP) is met sukses geïsoleer vanaf ingevoerde ToRSV-besmette wingerdmateriaal. Twee uitdrukking stelsels is gebruik vir uitdrukking van die ToRSV-CP, die "GST gene fusion" stelsel en 'n *Agrobacterium*-bemiddelde uitdrukking stelsel. Die "GST gene fusion" stelsel was egter onsuksesvol aangesien onvoldoende oplosbare proteïen uitdrukking die produksie van antiliggame en dus die ontwikkeling van die DAS-ELISA toets verhoed het. "Tissue print immunoassay" (TPIA) het aanvanklik positiewe resultate getoon vir tydelike uitdrukking van die fusie proteïen in tabakplante, maar verdere bevestiging was onoortuigend. Die projek was ook daarop gemik om 'n in-tyd polimerase ketting reaksie (PKR) toets vir die spesifieke opsporing en relatiewe kwantifisering van GFLV, gebaseer op 'n gekonserveerde volgorde van die RNA-2 genoom, te ontwikkel. 'n Gedeeltelike GFLV-RNA-2 nukleïensuurvolgorde van 'n Suid-Afrikaanse wingerd isolaat is bepaal en gebruik vir die ontwerp van spesifieke inleiers. Die kwantitatiewe in-tyd PKR toets gebaseer op SYBR groen tegnologie was sensitief

genoeg om vlakke van so laag as 0.11ng/reaksie in geïnfekteerde plante op te spoor, wat dit 'n hoogs effektiewe diagnostiese hulpmiddel vir die opsporing van GFLV maak.

## Acknowledgements

---

I wish to express my sincere gratitude to the following people and institutions:

*Prof. Johan Burger*, for his guidance and the opportunity to perform this study.

*Dr. Rose Souza-Richards*, for excellent supervision and guidance. Without your invaluable support I would not have been able to complete this study.

*Dr. Hano Maree* and members of the *Vitis* lab for their assistance.

*Melanie Arendse* for continuous support, advice and encouragement.

*The Department of Agriculture, Forestry and Fisheries* for financial support.

*My colleagues, friends and family*, for their continuous encouragement.

*My mother*, for her love and moral support.

*Marius and Micah*, for your unconditional love, encouragement and patience.

*To my Heavenly Father*, for His grace and favour.

# Table of Contents

---

<b>Declaration</b> .....	ii
<b>Abstract</b> .....	iii
<b>Opsomming</b> .....	iv
<b>Acknowledgements</b> .....	vi
<b>Table of Contents</b> .....	vii
<b>List of Abbreviations</b> .....	x
<b>List of Figures</b> .....	xiii
<b>List of Tables</b> .....	xvi
<b>Chapter 1: Introduction</b>	
1.1 Background .....	1
1.2 Aims and Objectives .....	2
<b>Chapter 2: Literature review</b>	
2.1 Introduction .....	4
2.2 The South African Grapevine Industry .....	5
2.2.1 Overview of the grapevine industry .....	5
2.2.2 The role of the Department of Agriculture, Forestry and Fisheries .....	5
2.3 The genus <i>Nepovirus</i> .....	6
2.3.1 <i>Tomato ringspot virus</i> (ToRSV) .....	7
2.3.1.1 <i>Genome organisation and morphology</i> .....	7
2.3.1.2 <i>Geographical distribution and transmission</i> .....	9
2.3.1.3 <i>Host range and symptomatology</i> .....	9
2.3.1.4 <i>Molecular diversity</i> .....	11
2.3.2 <i>Grapevine fanleaf virus</i> (GFLV) .....	13
2.3.2.1 <i>Genome organisation and morphology</i> .....	13
2.3.2.2 <i>Geographical distribution and transmission</i> .....	15
2.3.2.3 <i>Host range and symptomatology</i> .....	16
2.3.2.4 <i>Genome variability</i> .....	18
2.4 Diagnostic methods for plant virus detection .....	19
2.4.1 Detection methods based on biological properties .....	19
2.4.1.1 <i>Symptomatology</i> .....	19
2.4.1.2 <i>Transmission tests</i> .....	20
2.4.1.3 <i>Electron microscopy</i> .....	20
2.4.2 Serological testing methods .....	21
2.4.2.1 <i>Antibody production</i> .....	21
2.4.2.2 <i>Enzyme linked immunosorbent assay (ELISA)</i> .....	23

2.4.2.3	Immunoblotting .....	25
2.4.3	Nucleic -acid based detection methods .....	25
2.4.3.1	<i>Molecular hybridisation</i> .....	25
2.4.3.2	<i>Polymerase chain reaction</i> .....	26
2.4.3.3	<i>Real-time PCR (qPCR)</i> .....	27
2.4.3.4	<i>Microarrays</i> .....	27
2.4.3.5	<i>Next-generation sequencing</i> .....	28

### Chapter 3: The development of a DAS-ELISA assay for the detection of *Tomato ringspot virus*

3.1	Introduction .....	30
3.2	Materials and Methods .....	34
3.2.1	Plant material .....	34
3.2.2	Isolation of total RNA .....	34
3.2.3	Primer design and RT-PCR .....	35
3.2.4	Cloning of the ToRSV-CP gene into the pDRIVE cloning vector .....	37
3.2.4.1	<i>Ligation</i> .....	37
3.2.4.2	<i>Transformation</i> .....	37
3.2.4.3	<i>Screening of recombinants by PCR</i> .....	37
3.2.4.4	<i>Plasmid DNA isolation</i> .....	38
3.2.4.5	<i>Sequencing of recombinant DNA</i> .....	38
3.2.4.6	<i>Cloning of the full-length ToRSV CP gene</i> .....	39
3.2.5	Bacterial expression of the ToRSV-CP gene using the GST gene fusion system .....	39
3.2.5.1	<i>Preparation of the pGEX6P2 vector</i> .....	39
3.2.5.2	<i>Ligation and Transformation</i> .....	40
3.2.5.3	<i>Screening of pGEX-6P-2: ToRSV-CP constructs</i> .....	40
3.2.5.4	<i>Transformation of constructs into KRX competent cells</i> .....	42
3.2.5.5	<i>Recombinant Protein Expression</i> .....	42
3.2.5.6	<i>SDS-Page Analysis</i> .....	43
3.2.5.7	<i>Western Blot</i> .....	44
3.2.6	Agrobacterium-mediated transient expression of the ToRSV-CP gene .....	44
3.2.6.1	<i>PCR analysis</i> .....	44
3.2.6.2	<i>Cloning of GST:ToRSV-CP fragment into pDRIVE</i> .....	45
3.2.6.3	<i>Cloning of GST-ToRSV-CP fragment into pBIN61S</i> .....	47
3.2.6.4	<i>Transformation into Agrobacterium via electroporation</i> .....	47
3.2.6.5	<i>Agrobacterium-infiltration of N. benthamiana plants</i> .....	48
3.2.6.6	<i>Tissue-print Immuno Assay</i> .....	48
3.2.6.7	<i>SDS Page analysis &amp; Western Blot</i> .....	49
3.3	Results .....	51
3.3.1	Isolation and cloning of the ToRSV-CP gene .....	51
3.3.2	Expression of the ToRSV-CP gene using the GST gene fusion system .....	54
3.3.3	Agrobacterium-mediated transient expression of the ToRSV-CP gene .....	59
3.4	Discussion .....	65

**Chapter 4: Diagnostic assay for the detection and quantification of *Grapevine Fanleaf virus***

4.1	Introduction .....	69
4.2	Materials and Methods .....	71
4.2.1	Cloning and sequencing of the RNA2 from a South African isolate of GFLV .....	71
4.2.1.1	<i>RNA isolation</i> .....	71
4.2.1.2	<i>Primer design and RT-PCR</i> .....	71
4.2.1.3	<i>Cloning and plasmid DNA isolation</i> .....	73
4.2.1.4	<i>Sequencing and Analysis</i> .....	73
4.2.2	Relative quantification of GFLV by real-time PCR .....	74
4.2.2.1	<i>Sample collection and RNA isolation</i> .....	74
4.2.2.2	<i>DNase treatment of RNA and cDNA synthesis</i> .....	74
4.2.2.3	<i>Design of GFLV primers for real-time PCR analysis</i> .....	75
4.2.2.4	<i>Optimisation of the real-time PCR assay</i> .....	76
4.2.2.5	<i>Relative quantification of GFLV</i> .....	77
4.3	Results .....	79
4.3.1	Cloning of the GFLV-V7 RNA-2 isolate .....	79
4.3.2	Sequence analysis and phylogeny .....	79
4.3.3	Development of the real time PCR assay .....	81
4.3.4	Relative quantification of GFLV .....	86
4.4	Discussion .....	90

**Chapter 5: Conclusion .....** 94

**Chapter 6: References .....** 96

## List of Abbreviations

---

μF	microfarad
μg	microgram
μl	microlitre
μM	micromolar
A	Adenine
Amp	Ampicillin
AMV	Avian Myeloblastosis Virus
BLAST	Basic local alignment search tool
bp	base pair
BSA	Bovine Serum Albumin
C	Cytosine
CAF	Central Analytical Facility
cDNA	complementary DNA
CIAA	Chloroform: isoamylalcohol
CP	Coat protein
Ct	Cycle threshold
cv	cultivar
CTAB	Cetyltrimethylammonium bromide
DAFF	Department of Agriculture, Forestry and Fisheries
DAS	Double-antibody sandwich
DEPC	Diethylpyrocarbonate
DIBA	Dot Immunobinding assay
DNA	Deoxyribonucleotide acid
dNTP	Deoxyribonucleotide triphosphate
dpi	days post inoculation
DTT	Dithiothreitol
EDTA	Ethylene diamine tetra-acetic acid di-sodium salt
EF1α	Elongation factor 1-alpha
ELISA	Enzyme-linked immunosorbent assay
EM	Electron microscopy
EtBr	Ethidium bromide
G	Guanine
GAPDH	Glyceraldehyde 3-phosphate dehydrogenase
GDP	Gross domestic product
GFLV	Grapevine fanleaf virus
GST	Glutathione-S-Transferase
GYV	Grape yellow vein

HP	Homing protein
IAMB	Instituto Agronomico Mediterraneo di Bari
IC	immunocapture
ICVG	The International Council for the Study of Viruses and Virus-like Diseases of Grapevine
IPPC	International Plant Protection Convention
IPTG	Isopropyl $\beta$ -D-1-thiogalactopyranoside
ISEM	Immunosorbent Electron microscopy
Kan	Kanamycin
kb	kilobase
KCl	Potassium chloride
kDa	kilo-Daltons
kV	kilovolts
LB	Luria Bertoni broth
M	Molar
mA	milliampere
MEGA	Molecular Evolutionary Genetics Analysis
MES	2-(N-morpholino)ethanesulfonic acid
ml	millilitre
mM	millimolar
MP	Movement protein
Mr	Relative molecular mass
ms	millisecond
NC	Negative control
ng	nanogram
NGS	Next generation sequencing
nm	nanometer
NPPO	National Plant Protection Organisation
nt	nucleotide
NTC	No template control
OD	Optical density
ORF	Open reading frame
PAGE	Polyacrylamide gel electrophoresis
PBS	Phosphate buffered saline
PCR	Polymerase chain reaction
PMSF	Phenylmethanesulphonylfluoride
PVP	Polyvinyl pyrrolidone
PYB	peach yellow bud
qPCR	quantitative real-time PCR
R <sup>2</sup>	Correlation coefficient

RNA	Ribonucleic acid
rpm	revolutions per minute
rRNA	ribosomal RNA
RT	Reverse transcriptase
S	Svedberg units (indicates sedimentation coefficients)
SAWIS	South African Wine Industry and Systems
SDS	Sodium dodecyl sulfate
spp	species
SU	Stellenbosch University
TBE	Tris, boric acid and EDTA
TBIA	Tissue blot immunoassay
TBRV	Tomato blackring virus
T-DNA	transfer DNA
TEMED	Tetramethylenediamine
ToRSV	Tomato ringspot virus
TRSV	Tobacco ringspot virus
U	Units
UBC	Ubiquitin-conjugating enzyme
UTR	Untranslated region
UV	Ultraviolet
VPg	Virus genome-linked protein
X-gal	5-bromo-4-chloro-3-indolyl-beta-D-galacto-pyranoside

## List of Figures

---

- Figure 2.1:** Genome organisation of ToRSV. The ORFs are boxed and functions of the proteins released by proteolysis are indicated. **MP**, movement protein; **CP**, coat protein; **Hel**, helicase; **Pro**, proteinase; **Pol**, polymerase. Dashed lines represent the proteolytic cleavage sites. RNA-1 is cleaved at 5 sites to release 6 mature proteins and several intermediate precursors and RNA-2 is cleaved at 3 sites to release 4 protein domain and possible precursors. The ovals at the 5'-end of the RNAs represents the VPg, and **An** at the 3'-end the poly-A. [Adapted from Virus taxonomy (8<sup>th</sup> report) Fauquet C.M. *et al* 2005, pg 814] ..... 7
- Figure 2.2:** Electron micrograph of purified ToRSV virus particles stained in 2% uranyl acetate showing a mixture of middle and bottom components. The bar represents 100nm. [Photo obtained from <http://www.dpvweb.net/dpv/showdpv.php?dpvno=290>] ..... 8
- Figure 2.3:** (A) *Tomato ringspot virus* symptoms on plants and leaves of red currants in Corvallis, Oregon. This virus causes yellow mottling, yellow lines or yellow mosaic patterns in leaves. (B) *Tomato ringspot virus* in *Prunus* spp. The first symptoms on newly infected peach or nectarine trees is the development of yellow blotches or spots on the leaf blades that are irregular in outline and usually follow the main veins. [Photos obtained from <http://www.ars-grin.gov/cor/ribes/ribsymp/virus2.html> (A) and [http://www.oregon.gov/ODA/CID/PLANT\\_HEALTH/pages/tomato\\_ringspot\\_virus.aspx](http://www.oregon.gov/ODA/CID/PLANT_HEALTH/pages/tomato_ringspot_virus.aspx) (B)] ..... 10
- Figure 2.4:** Typical yellow vein symptoms on grapevine caused by ToRSV. Yellow vein banding leaf symptoms vary but are most drastic in cold climates. Symptoms of yellow vein resemble those described for GFLV, and they can be easily confused. [Photo obtained from [http://iv.ucdavis.edu/Viticultural\\_Information/?uid=198&ds=351](http://iv.ucdavis.edu/Viticultural_Information/?uid=198&ds=351)] ..... 11
- Figure 2.5:** Phylogenetic analysis of ToRSV isolates. The result of the parsimony analysis is shown. Numbers indicate the degree of confidence at a specific node as tested by 100 bootstrap replications. (A) Phylogenetic tree derived from the deduced amino acid sequence of the VPg-Pro-Pol domain using all available ToRSV isolate sequences. (B) Phylogenetic tree derived from the deduced amino acid sequence of the Coat protein domain using all available ToRSV isolate sequences. In both cases, the GVV isolate are grouped separate from the other ToRSV isolates. [Figure obtained from Wang & Sanfaçon (2000)] ..... 13
- Figure 2.6:** Genome organisation of GFLV. The ORFs are boxed and functions of the proteins released by proteolysis are indicated. **MP**, movement protein; **CP**, coat protein; **Hel**, helicase; **Pro**, proteinase; **Pol**, polymerase. Dashed lines represent the proteolytic cleavage sites. The ovals at the 5'-end of the RNAs represents the VPg, and **An** at the 3'-end the poly-A. [Adapted from Virus taxonomy (8<sup>th</sup> report) Fauquet C.M. *et al* 2005, pg 814] ..... 14
- Figure 2.7:** Purified virus particles of GFLV mounted in uranyl acetate. Particles are serologically identical and an empty virus particle is also present. The bar represents 50nm. [Photo obtained from <http://www.dpvweb.net/dpv/showdpv.php?dpvno=385>] ..... 15
- Figure 2.8:** Typical foliar symptoms of GFLV. (A) Vines showing stunted and zigzag shoots with fan-shaped leaves (B) Yellow mosaic pattern on leaf (C) Bright yellow vein banding on leaf [Photos courtesy of William M. Brown Jr., [Bugwood.org](http://bugwood.org) (A) and Canadian Food Inspection Agency (B & C); obtained from <http://www.extension.org/pages/33064/grapevine-fanleaf-degeneration-disease>] ..... 17
- Figure 2.9:** (A) Chardonnay vineyard in France infected with GFLV showing patchy distribution of the virus as a result of plant-to-plant virus transmission by the ectoparasitic nematode *Xiphinema index*. (B) Comparison of healthy (left) and GFLV-infected (right) grapevine showing fruit clusters reduced in size and number in infected grapevine. [Photos obtained from Andret-Link *et al.*, 2004] ..... 18
- Figure 2.10:** Schematic diagram illustrating two of the most common ELISA formats: Indirect detection system of the Plate-trapped antigen (PTA-ELISA) and the Double antibody sandwich (DAS-ELISA). Diagram from Ward *et al.*, (2004) ..... 24
- Figure 3.1:** Plasmid map of pGEX-6P-2 showing the inserted ToRSV-CP gene at the *SalI* restriction site as well as the binding sites for the ToRSV-*SalI* and pGEX primers used. [Created using SnapGene® software from GSL Biotech; available at [snapgene.com](http://snapgene.com)] ..... 41
- Figure 3.2:** Plasmid map of pBIN61S indicating the inserted GST:ToRSV-CP sequence (blue arrow) at the *SacI* and *XbaI* restriction sites. [Created using SnapGene® software from GSL Biotech; available at [snapgene.com](http://snapgene.com)] ..... 46
- Figure 3.3:** Total RNA isolated from ToRSV-infected leaf material. Lane 1:100bp plus DNA marker; Lane 2: Total RNA isolated from infected grapevine material ..... 51

**Figure 3.4:** One-step RT-PCR to amplify partial ToRSV-CP fragment. Lane 1: 100bp+ DNA marker; Lanes 2: ToRSV positive control; Lane 3-4: 1684bp fragment amplified from ToRSV positive sources. Lane 5: Negative control; Lane 6: No template control; Lane 7: 1kb DNA ladder ..... 52

**Figure 3.5:** Amplification of the full-length ToRSV-CP. Lane 1: 1kb DNA marker; Lane 2: No template control; Lanes 3, 5 & 7: left blank; Lanes 4, 6 & 8: 1702bp fragment amplified ..... 53

**Figure 3.6:** Restriction digest of pDRIVE:ToRSV-CP construct with *Sa*I enzyme. Lane 1: 1kb DNA marker; Lane 2: pDRIVE vector, uncut; Lane 3: pDRIVE vector, digested; Lanes 4-9 & 11-14: pDRIVE-ToRSVcp constructs, digested; Lane 10: Negative control; Lane 15: blank; Lane 16: 100bp+ DNA marker ..... 53

**Figure 3.7:** Sequencing result of the pDRIVE:ToRSV-CP construct showing the *Sa*I sequence (underlined) and the extra 'A' nucleotide that was inserted to maintain the frame ..... 54

**Figure 3.8:** Orientation screening of recombinant clones by PCR using primers pGEX-F and ToRSV-*Sa*I-R (lanes 2-10) and primers pGEX-F and ToRSV-*Sa*I-F (lanes 11-19). Lane 1: 100bp plus DNA marker. Lanes 2-19: Recombinant clones. Lane 20: 1kb DNA marker. Clones in the correct orientation should yield a band of ~1800bp with the first primer set (as seen in lanes 8 and 9) and not with the second primer set (as seen in lanes 17 and 18) ..... 54

**Figure 3.9:** Rhamnose control of T7 RNA Polymerase in KRX cells. Expression of T7 RNA polymerase is controlled by the *rha*P<sub>BAD</sub> promoter. This promoter undergoes catabolite repression by glucose and is activated by the addition of rhamnose. In addition, rhamnose induces the activator RhaR, resulting in the production of active RhaS. In turn, RhaS bind to rhamnose activating transcription from *rha*P<sub>BAD</sub>. [from Promega Technical Bulletin, Part# TB352] ..... 55

**Figure 3.10:** SDS-Page analysis of GST:ToRSV-CP fusion protein. Lane 5: Unstained protein ladder. Lanes 1-4: Uninduced insoluble (1) and soluble (2) fractions of pGEX-6P-2 without the fusion protein and uninduced insoluble (3) and soluble (4) fractions of the expressed GST:ToRSV-CP. Lane 6: Total cell protein. Lanes 7-10: Induced insoluble (10) and soluble (9) fractions of vector and soluble (7) and insoluble (8) fractions of the expressed fusion protein ..... 56

**Figure 3.11:** SDS-Page analysis of GST:ToRSV-CP fusion protein with different parameters. Lane 1: Uninduced fusion protein, soluble. Lane 2: Uninduced fusion protein, insoluble. Lane 3: Unstained protein ladder. Lane 4: Induced fusion protein (+ rhamnose, + IPTG, no sarkosyl), soluble. Lane 5: Induced fusion protein (+ rhamnose, + IPTG, no sarkosyl), insoluble. Lane 6: Induced fusion protein (+ rhamnose, + IPTG, 0.5% sarkosyl), soluble. Lane 7: Induced fusion protein (+ rhamnose, + IPTG, 0.5% sarkosyl), insoluble ..... 57

**Figure 3.12:** SDS-Page analysis of GST:ToRSV-CP fusion protein with different parameters. Lane 1: Induced fusion protein (+ rhamnose, + IPTG, 1% sarkosyl), soluble. Lane 2: Induced fusion protein (+ rhamnose, + IPTG, 1% sarkosyl), insoluble. Lane 3: Induced fusion protein (+ rhamnose, no sarkosyl), soluble. Lane 4: Induced fusion protein (+ rhamnose, no sarkosyl), insoluble. Lane 5: Unstained protein ladder. Lane 6: Induced fusion protein (+ rhamnose, 0.5% sarkosyl), soluble. Lane 7: Induced fusion protein (+ rhamnose, 0.5% sarkosyl), insoluble. Lane 8: Induced fusion protein (+ rhamnose, 1% sarkosyl), soluble. Lane 9: Induced fusion protein (+ rhamnose, 1% sarkosyl), insoluble ..... 57

**Figure 3.13:** SDS-Page analysis of GST:ToRSV-CP fusion protein with lysozyme added to lysis buffer. Lane 3: Unstained protein ladder. Lanes 1-2: Uninduced soluble and insoluble fractions of pGEX-6P2. Lanes 4-6: Uninduced TCP, soluble and insoluble fractions of the fusion protein. Lanes 7-9: Induced TCP, soluble and insoluble fractions of pGEX-6P-2. Lanes 10-12: Induced TCP, soluble and insoluble fractions of the fusion protein ..... 58

**Figure 3.14:** Restriction digest of the pDRIVE:GST-ToRSV-CP fragment with *Sac*I and *Xba*I enzymes to facilitate cloning into pBIN61S vector. Lane 1: 1kb DNA ladder. Lane 2: pBIN61S vector uncut. Lane 3: Vector DNA, digested with *Sac*I. Lane 4: Vector DNA, digested with *Xba*I. Lane 5: Insert DNA, uncut. Lane 6: Insert DNA digested with *Sac*I. Lane 7: Insert DNA digested with *Xba*I showing 2.5kb fragment (indicated by arrow) ..... 60

**Figure 3.15:** Restriction digest of the pBIN61S:GST-ToRSV-CP fragment with *Eco*RI and *Sa*I enzymes to confirm successful cloning. Lanes 1 & 8: 1kb DNA ladder. Lane 2: pBIN61S uncut. Lanes 3-4: pBIN61S digested with *Eco*RI and *Sa*I. Lane 5: pBIN61S:GST:ToRSV-CP uncut. Lane 6: Construct digested with *Eco*RI showing the expected bands at ~523bp and ~1423bp (indicated with arrows). Lane 7: Construct digested with *Sa*I with the arrow indicating the band at ~1693. The band of 35kb is too small to be seen on the gel ..... 60

**Figure 3.16:** *N.benthamiana* plants infiltrated with *Agrobacterium* transformed with the pBIN61S:GST-ToRSV-CP construct. **A-C:** Leaves infiltrated with transformed *Agrobacterium* culture. **D-E:** Negative control – leaves infiltrated with re-suspension solution ..... 61

- Figure 3.17:** TPIA results for the mesophyll tissue of *N.benthamiana* after agroinfiltration. **1:** Negative control shows no reaction to the ToRSV antibodies. **2-3:** Leaves infiltrated with *Agrobacterium* containing the pBIN61S:GST-ToRSV-CP construct shows a definite reaction to the antibodies, indicating the presence of ToRSV..... 62
- Figure 3.18:** SDS-Page analysis of *N.benthamiana* after agroinfiltration on a 10% polyacrylamide gel.. Lanes **1& 8:** Unstained Protein ladder. Lanes **2-4, 6:** Leaves infiltrated with *Agrobacterium* containing the pBIN61S:GST-ToRSV-CP construct. Lane **5:** Prestained Protein ladder Lane **7:** Negative control – leaves infiltrated with buffer only..... 63
- Figure 3.19:** (A) SDS-Page analysis of *N.benthamiana* after agroinfiltration on a 8% polyacrylamide gel. Lanes 1 & 10: Prestained protein ladder. Lanes 2 – 6: Leaves infiltrated with *Agrobacterium* containing the pBIN61S:GST-ToRSV-CP construct. Lane 7: Unstained Protein ladder. Lane 8: ToRSV-ch positive control. Lane 9: Negative control, crude leaf extract of *N. benthamiana*. (B) Western Blot analysis of 8% polyacrylamide gel ..... 63
- Figure 3.20:** 10% polyacrylamide gel to detect the GST fragment of the fusion protein. Lanes 1 & 10: Prestained protein ladder. Lanes 2 – 6: Leaves infiltrated with *Agrobacterium* containing the pBIN61S:GST-ToRSV-CP construct. Lane 7: Unstained Protein ladder. Lane 8: rGST positive control. Lane 9: Negative control, *N. benthamiana* ..... 64
- Figure 4.1:** Regions of the sequenced GFLV-Vak 7 RNA-2 genome compared to GFLV-SAPCS3 RNA-2. The region of the Vak7 RNA-2 that was successfully sequenced is indicated in grey and the nucleotide positions of where it aligns to SAPCS3 are indicated below. Regions not sequenced are indicated in purple. The SAPCS3 RNA-2 genome is shown with the sizes of the ORF, 5'UTR and 3'UTR indicated inside the blocks ..... 80
- Figure 4.2:** Alignment of the 2C<sup>CP</sup> of the two South African isolates GFLV-SACH44 and GFLV-SAPCS3 with GFLV-Vak7 showing nucleotide differences between the three sequences. Each coloured line is a SNP representing a different nucleotide. The alignment was performed using Geneious 6.1.6 software .....80
- Figure 4.3:** Phylogenetic tree based on the 2C<sup>CP</sup> of isolates from the genus *Nepovirus* (Richards *et al.*, 2014). Analysis was conducted using the Neighbour-joining method. The percentage of replicate trees in which the sequences clustered together in the bootstrap test (1000 replicates) is indicated next to the branches. Influenza A virus was used as an outgroup. Phylogenetic analysis was conducted in MEGA5 (Tamura *et al.*, 2011) ..... 81
- Figure 4.4:** Standard curve using primers to amplify the GFLV gene. (A) Amplification profile of the five-fold dilution series of the calibrator sample (B) Standard curve of the Ct values of each triplicate plotted against the logarithm of the relative concentration of the sample (C) 2% agarose gel of the five –fold dilution series (lanes 1-5) and the NTC (lane 6) ..... 82
- Figure 4.5:** Standard curve using primers to amplify the Actin gene. (A) Amplification profile of the five-fold dilution series of the calibrator sample (B) Standard curve of the Ct values of each triplicate plotted against the logarithm of the relative concentration of the sample (C) 2% agarose gel of the five –fold dilution series (lanes 1-5) and the NTC (lane 6) ..... 83
- Figure 4.6:** Standard curve using primers to amplify the UBC gene. (A) Amplification profile of the five-fold dilution series of the calibrator sample (B) Standard curve of the Ct values of each triplicate plotted against the logarithm of the relative concentration of the sample (C) 2% agarose gel of the five –fold dilution series (lanes 1-5) and the NTC (lane 6) ..... 84
- Figure 4.7:** Standard curve using primers to amplify the GAPDH gene. (A) Amplification profile of the five-fold dilution series of the calibrator sample (B) Standard curve of the Ct values of each triplicate plotted against the logarithm of the relative concentration of the sample (C) 2% agarose gel of the five –fold dilution series (lanes 1-5) and the NTC (lane 6) ..... 85
- Figure 4.8:** Grapevine samples tested with GFLV primers. (A) Amplification curves of the grapevine samples diluted 1:5 (B) Melting curve analysis confirming amplification of the correct amplicon with melting peaks of between 85.3 – 85.5°C (C) Ct values of amplified samples imported onto the GFLV standard curve ..... 87
- Figure 4.9:** Bar chart representing the relative expression of GFLV in each sample. Values on the y-axis indicate ng/reaction. The different samples are indicated on the x-axis. Samples in green represents greenhouse samples and samples in purple represents field samples. I 3798 represent the negative sample ..... 89

## List of Tables

---

<b>Table 2.1:</b> Comparison of different techniques in detection of plant viruses .....	29
<b>Table 3.1:</b> Characteristics of primers used in this chapter .....	35
<b>Table 3.2:</b> Primer sets used for orientation screening of the pGEX-6P-2 expression vector containing the ToRSV-CP gene .....	41
<b>Table 3.3:</b> Characteristics of primers to facilitate pBIN61S cloning .....	45
<b>Table 4.1:</b> Characteristics of primers used for sequencing .....	72
<b>Table 4.2:</b> Characteristics of primers used for real-time PCR .....	76
<b>Table 4.3:</b> Calculated concentration values of the grapevine samples in ng/reaction. Column 7 represents the geometric mean value for the three reference genes: Actin, GAPDH and UBC. ....	88

# CHAPTER 1

---

## Introduction

### 1.1 Background

Grapevine (*Vitis vinifera*) is one of the most ancient and widely cultivated crops produced in the world and remains the most important crop economically as more than 7.9 million hectares are planted in temperate and tropical climatic regions worldwide (Bouquet, 2011). Grapevine is a host to more than 60 different viruses, of which 15 belongs to the genus *Nepovirus* (nematode-transmitted polyhedral virus). In addition, grapevines also host mixed infections of different viruses as well as mixed infections of different sequence variants of the same virus. Fanleaf degeneration/decline disease is one of the most severe viral disease complexes affecting grapevine worldwide. The fundamental agents of fanleaf degeneration and decline are members of the genus *Nepovirus*, including *Grapevine fanleaf virus* (GFLV) and *Tomato ringspot virus* (ToRSV) (Martelli and Boudon-Padieu 2006).

Nepoviruses have a significant economic impact and some cause severe disease that leads to reduction of growth, yield losses and ultimately plant necrosis. Nepovirus-incurred symptoms vary from fan-like leaves, vein banding and chlorotic ringspots on leaves, to severe decline in vigour and fruit production of vines (Martelli, 1993). These viruses are distributed worldwide, although, as a result of their transmission via nematodes, the geographical range of many individual members of the genus is rather restricted. Most of the nepoviruses are foreign to South Africa and to date, only *Grapevine fanleaf virus* is present in the country.

South Africa is among the top ten wine producing countries in the world and grapevine is one of its most important commodities. GFLV is widespread in the Breede River valley of the Western Cape Province in South Africa (Malan and Hugo, 2003), which contributes to approximately one-third of the wine economy (South African Wine Industry and Systems [SAWIS] Statistics 2014). Proper control measures are therefore

essential to prevent the unrestricted spread of GFLV as it could have major economical impact and a significant effect on the wine industry.

The Department of Agriculture, Forestry and Fisheries (DAFF), as the official National Plant Protection Organisation (NPPO) of South Africa, undertakes to implement effective measures to prevent the importation and distribution of plant pathogens. The Directorate Inspection Services as part of DAFF administers the Agricultural Pests Act, 1983 (Act No. 36 of 1983) to provide measures by which the introduction of agricultural pests may be prevented and combated to safeguard our agricultural environment. One of the functions of Inspection Services is to render a routine plant health diagnostic service for imported plants and plant products to prevent exotic pathogens from entering South Africa.

At the Plant Quarantine station of the Directorate Inspection Services, screening techniques employed to test for the presence of nepoviruses in grapevine samples include PCR (polymerase chain reaction), ELISA (Enzyme-linked immunosorbent assay) and biological indexing of herbaceous host plants. Of the 15 nepoviruses infecting grapevine, samples are routinely screened for seven of these nepoviruses. Currently, the samples are screened for a specific nepovirus per test, which can be laborious and time-consuming and also costly as most samples are often received as mass consignments. All these factors contribute to the necessity to develop alternative identification methods for the diagnosis of nepoviruses that is sensitive, more rapid and reliable.

## **1.2 Aims and objectives**

The aim of the study was to develop a diagnostic assay for the detection of nepoviruses in grapevine. We aimed to produce antiserum by recombinant DNA technology against a specific nepovirus (ToRSV) and subsequently develop an ELISA kit for the detection of the virus. ToRSV is currently not present in South Africa but is of great concern as it not only infects grapevine but deciduous crops as well. Furthermore, we aimed to

develop a qPCR assay for the detection of GFLV in grapevine. GFLV is currently restricted to the Western Cape of South Africa and a sensitive detection assay is imperative to prevent uncontrolled spread of the virus. The following objectives were set out to achieve these aims:

- To obtain a positive ToRSV source for isolation and cloning of the ToRSV coat protein gene.
- To express the ToRSV coat protein gene in order to produce antiserum for the development of an ELISA kit.
- To generate a complete GFLV RNA-2 sequence of a South African grapevine isolate to facilitate the design of GFLV-specific primers.
- To design a qPCR assay for the rapid and reliable detection and relative quantification of GFLV.

## CHAPTER 2

---

### Literature Review

#### 2.1 Introduction

Grapevine is a valuable agricultural commodity and one of the most widely grown horticultural crops worldwide. Fanleaf degeneration and decline disease is one of the most severe viral disease complexes that affects grapevine and was reported in Europe as early as 1841 (Martelli, 1993). The viruses responsible for decline are closely related and grouped in the genus *Nepovirus*, of which grapevine hosts 15 species.

The nepoviruses are a group of about 46 viruses that infect a wide range of plant species, producing symptoms that include ringspots, mottles, mosaics and systemic necrosis. Transmission of its members is through free-living, soil-inhabiting nematodes, principally of *Longidorus* or *Xiphinema* species, feeding on plant roots (Lamberti, Taylor & Seinhorst, 1975). Viruses belonging to this group include *Tomato ringspot virus* (ToRSV), *Tomato black ring virus* (TBRV), *Grapevine fanleaf virus* (GFLV) and *Tobacco ringspot virus* (TRSV).

In this chapter, a brief description of the grapevine industry in South Africa and the role of the Department of Agriculture, Forestry and Fisheries (DAFF) as the official National Plant Protection Organisation (NPPO) are given. This is followed by a detailed discussion of the nepoviruses ToRSV and GFLV. The chapter concludes with a review of the diagnostic methods available for the detection of plant viruses.

## **2.2 The South African Grapevine Industry**

### **2.2.1 Overview of the grapevine industry**

The grapevine industry is one of the largest agricultural export industries in South Africa. In 2013, 525.6 million litres of wine were exported, which is 57.4% of the total wine produced in that year. The total surface area under wine grape vineyards in South Africa is currently 99 680 hectares with Stellenbosch and Paarl being the two largest regions under cultivation. A 2009 study on the macro-economic impact of the wine industry on the economy of South Africa showed that the industry contributes R26 billion a year to the annual GDP of South Africa ([http://www.sawis.co.za/info/download/Macro\\_study\\_2009.pdf](http://www.sawis.co.za/info/download/Macro_study_2009.pdf)). The report also indicated that 275 606 people are employed either directly or indirectly in the wine industry, while an additional R4.2 billion is generated indirectly through wine tourism.

In terms of world wine production, South Africa ranks ninth in overall volume production of wine and contributes 4% to total world wine production (<http://www.sawis.co.za/info/annualpublication.php>). On the international front, South Africa's wines are highly competitive, with the industry showing a sustainable and increasingly positive trend over the years.

### **2.2.2 The role of the Department of Agriculture, Forestry and Fisheries (DAFF)**

Viral, fungal and bacterial diseases pose a serious threat to the future growth and international competitiveness of the grapevine industry and can result in severe economic losses and may even devastate the industry. As the official NPPO of South Africa, DAFF undertakes to prevent the spread and introduction of foreign pests of plants and plant products and to promote appropriate measures for their control. The Directorate Inspection Services issues regulations and control measures to protect and improve plant health and plant quarantine by administering the Agricultural Pests Act

(Act No. 36 of 1983). This act regulates the importation of controlled goods in accordance with the objectives of the International Plant Protection Convention (IPPC).

Agricultural products imported into South Africa must comply with the specific import conditions as set out in the import permit and is inspected before admission at prescribed ports of entry across the country. Material is then submitted to Inspection Services where it is again inspected before being established and will remain in quarantine for up to two growing seasons depending on its phytosanitary certificate compliance. During this time the material is subjected to regular visual inspections and diagnostic testing for pathogens not occurring in the country.

### **2.3 The genus *Nepovirus***

The genus *Nepovirus* (**N**ematode-transmitted **P**olyhedral viruses) is one of three genera in the family *Comoviridae*. By definition, nepoviruses are a group of viruses that are transmitted from plant to plant by soil nematodes (*Longidorridae*) in a semi-persistent manner. There are however nepoviruses with other types of vectors, e.g. *Blackcurrant reversion virus* is transmitted by mites, and several nepoviruses are transmitted by pollen and/or by seed (Le Gall *et al.*, 2007; Sanfacon *et al.*, 2009).

Members of the genus *Nepovirus* are characterised by their bipartite single-stranded RNA genome encapsidated in isometric particles, with each genome producing a polyprotein. Definitive nepoviruses have coat proteins with an approximate Mr of 55 kDa, larger than those of other small isometric plant viruses (Description of Plant Viruses, <http://www.dpvweb.net>). Nepoviruses are classified into three subgroups, A, B and C, based on their sequence similarities, serological relationships and the length and arrangement of their RNA-2 genome (Fauquet *et al.*, 2005).

### 2.3.1 Tomato ringspot virus (ToRSV)

*Tomato ringspot virus* (ToRSV) belongs to subgroup C, whose members are characterised by having a larger RNA-2, which includes considerable regions of shared sequence similarity with RNA-1 (Mayo & Robinson, 1996).

#### 2.3.1.1 Genome structure and morphology

The genome of ToRSV contains two positive sense single stranded RNA segments, RNA-1 and RNA-2, which are 8214 and 7273 nucleotides (nt) in length, respectively (Figure 2.1). ToRSV RNA-1 contains the domain for the replication proteins which are the RNA-dependent RNA polymerase, the proteinase, the genome-linked viral protein (VPg), the putative helicase (also termed NTB), which has a putative nucleoside triphosphate binding activity, and X1 and X2 for which the functions are unknown (Rott *et al.*, 1995; Wang and Sanfacon, 2000b). RNA-2 encodes structural proteins, which include coat protein (CP) and movement protein (MP), as well as the X4 and X3 proteins of unknown function (Carrier *et al.*, 2001; Hans and Sanfacon, 1995).

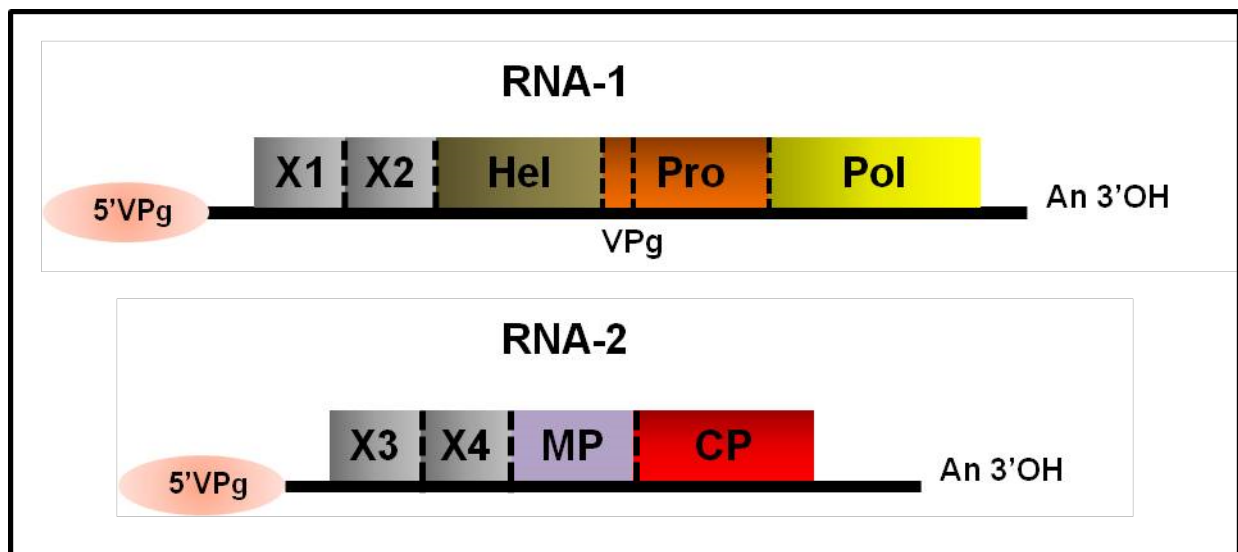


**Figure 2.1:** Genome organisation of ToRSV. The ORFs are boxed and functions of the proteins released by proteolysis are indicated. **MP**, movement protein; **CP**, coat protein; **Hel**, helicase; **Pro**, proteinase; **Pol**, polymerase. Dashed lines represent the proteolytic cleavage sites. RNA-1 is cleaved at 5 sites to release 6 mature proteins and several intermediate precursors and RNA-2 is cleaved at 3 sites to release 4 protein domain and possible precursors. The ovals at the 5'-end of the RNAs represents the VPg, and **An** at the 3'-end the poly-A. [Adapted from Virus taxonomy (8<sup>th</sup> report) Fauquet C.M. *et al* 2005, pg. 814]

In 2001, Carrier *et.al* characterised a third cleavage site in the N-terminal region of the RNA-2-encoded polyprotein (P2) of ToRSV. Cleavage at this site results in the release of two proteins: a 34 kDa protein located at the N-terminus of P2 and a 71kDa protein located immediately upstream of the MP domain. In comparison, only one protein domain is present in the equivalent region of the P2 polyprotein of other characterised nepoviruses.

ToRSV has isometric particles with angular outlines that are approximately 28 nm in diameter (Figure 2.2). The particles have a conspicuous capsomere arrangement and sediments as three components, top (T), middle (M) and bottom (B) in sucrose density gradients (Schneider *et al.*, 1974). T-particles are empty virus particles without an RNA component and sediments at 50S. M-particles sediments at 86-128S and contains a single molecule of RNA-2 while B-particles contain a single molecule of RNA-1 and sediments at 115-134S (Allen & Dias, 1977).

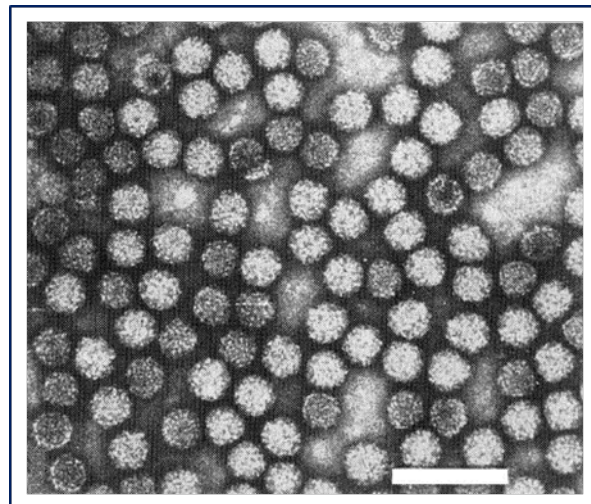


**Figure 2.2:** Electron micrograph of purified ToRSV virus particles stained in 2% uranyl acetate showing a mixture of middle and bottom components. The bar represents 100nm. [Photo obtained from <http://www.dpvweb.net/dpv/showdpv.php?dpvno=290>]

### 2.3.1.2 Geographical distribution and transmission

ToRSV is transmitted by the American dagger nematode, *Xiphinema americanum sensu lato*, a species complex containing more than 20 distinct species. Adults, as well as three larval stages, can transmit the virus, acquiring and inoculating it into healthy plants within one hour. For nematode transmission to occur, the virus must first dissociate from its retention site, a specific area in the nematode food canal. The dissociated viruses are injected to the plant root during the nematode feeding. *X. americanum* requires at least one year to complete its life cycle and can mature and survive (but not multiply) in soil in the absence of a host plant. ToRSV is also reported to be seed-transmitted in several host plants and can be spread from pollen to seed or by pollen to the pollinated plant (Rosenberger *et al.*, 1983). The virus is also readily transmissible by grafting and by sap inoculation to herbaceous hosts.

The virus appears to be prevalent in North America, especially around the Great Lakes region and along the Pacific coast from California to British Columbia. This natural spread is restricted to areas where moderate to high populations of its nematode vector occurs. ToRSV has also been isolated from ornamentals and berry crops in other parts of the world namely Central & South America, Asia, Australia, New Zealand and the European Union. In 2003, Pourrahim *et al.* reported the first occurrence of ToRSV in grapevines in Iran. To date, ToRSV has not been identified or isolated in South Africa.

### 2.3.1.3 Host range and symptomatology

*Tomato ringspot virus* has a wide host range – it affects about 285 plant species in 159 genera of 55 botanical families (Edwardson & Christie, 1997). In nature, ToRSV occurs mostly in woody or semi-woody and ornamental plants, rather than in herbaceous hosts, including *Ribes*, *Prunus*, *Perlagonium* and *Vitis*.

The most severe diseases caused by ToRSV are those on fruit crops, including yellow bud mosaic in peach and almond (*Prunus spp.*) – this causes pale-green to yellow blotches to develop along the main vein or large lateral veins of the leaves (Figure 2.3).

Fruits are often deformed and buds can either produce small leaves or are pale yellow and dies.

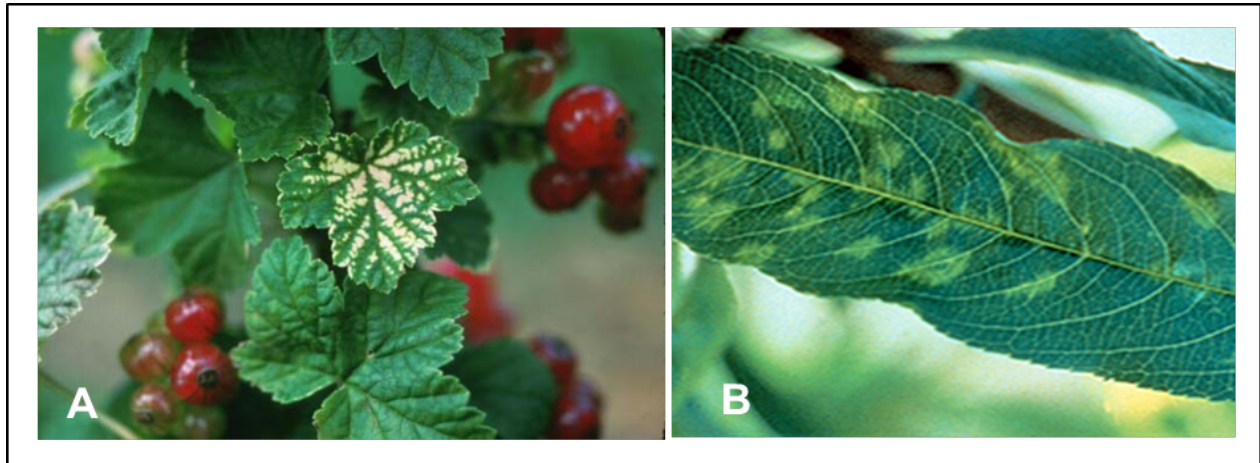


**Figure 2.3:** (A) *Tomato ringspot virus* symptoms on plants and leaves of red currants in Corvallis, Oregon. This virus causes yellow mottling, yellow lines or yellow mosaic patterns in leaves. (B) *Tomato ringspot virus* in *Prunus* spp. The first symptoms on newly infected peach or nectarine trees is the development of yellow blotches or spots on the leaf blades that are irregular in outline and usually follow the main veins. [Photos obtained from <http://www.ars-grin.gov/cor/ribes/ribsymp/virus2.html> (A) and [http://www.oregon.gov/ODA/CID/PLANT\\_HEALTH/pages/tomato\\_ringspot\\_virus.aspx](http://www.oregon.gov/ODA/CID/PLANT_HEALTH/pages/tomato_ringspot_virus.aspx) (B)]

On grapevines, severely infected vines will display weak and stunted shoot growth early in the season. Shoot and foliage symptoms (Figure 2.4) become more prominent with later vine growth, with leaves developing ringspots and mottling and becoming reduced in size (Yang *et al.*, 1986).

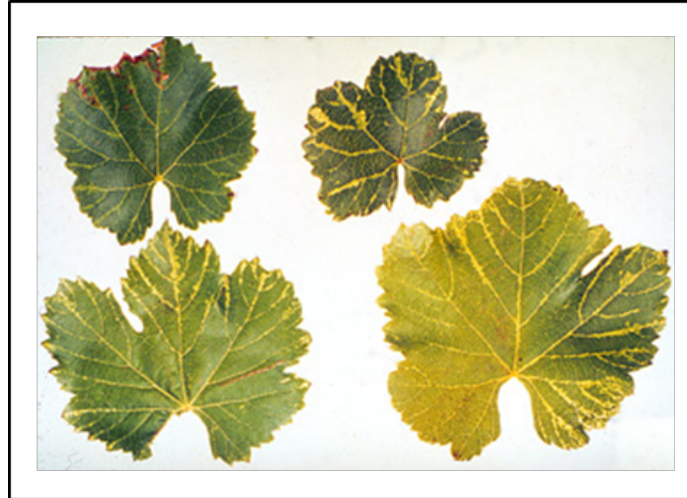


**Figure 2.4:** Typical yellow vein symptoms on grapevine caused by ToRSV. Yellow vein banding leaf symptoms vary but are most drastic in cold climates. Symptoms of yellow vein resemble those described for GFLV, and they can be easily confused. [Photo obtained from [http://iv.ucdavis.edu/Viticultural\\_Information/?uid=198&ds=351](http://iv.ucdavis.edu/Viticultural_Information/?uid=198&ds=351)]

#### 2.3.1.4 Molecular diversity

Plant RNA viruses generally have a large population of diversity since they have an error-prone replication mechanism and a short generation time. The genetically diverse populations of RNA viruses are referred to as quasispecies (Roossinck, 1997). Maintaining diverse quasispecies is advantageous because when the virus is exposed to a new environmental niche or selective regimen, the variant in the population that is more fit to the new environment can survive (Roossinck, 2003; Schneider and Roossinck, 2001).

ToRSV isolates are diverse and vary with regard to their natural hosts, symptoms expressed on indicator plants, diseases induced, specificity of nematode transmission and geographical origin (Cadman and Lister 1961; Hoy *et al.*, 1984; Brown *et al.*, 1993).

In 1988, Bitterlin and Gonsalves classified ToRSV isolates into five serogroups using polyclonal antibodies in a direct double-antibody sandwich ELISA assay. Very little cross-reactivity was noted among some of these serogroups, indicating that ToRSV

isolates may differ significantly in the sequence of their genomes, at least in the coat protein-coding region.

In 2000, Wang and Sanfaçon examined the biological and genetic diversity of four ToRSV isolates: isolate Rasp-1 (originally purified from infected raspberry plants), isolate GYV (grape yellow vein, originally isolated from infected grapevines from California), isolate PYB-1 (peach yellow bud-1, originally collected from an infected peach orchard in California), as well as T392, an isolate of unknown origin. These isolates were inoculated onto cucumber and after five to seven days post inoculation (dpi) local chlorotic lesions appeared on the inoculated cotyledons for all tested isolates. However, the symptoms on true leaves differed between the isolates. For isolates Rasp-1, T392, and PYB-1, infected plants showed severe systemic symptoms, including chlorotic and necrotic lesions, distorted leaves, and stunting of the plants. Isolate GYV, in contrast, caused milder systemic symptoms, which included chlorotic spots, mottle and intraveinal chlorosis, but necrotic lesions and stunting of plants were not observed. In about 20% of the plants infected by isolates Rasp-1, T392, and PYB-1 apparent recovery from the infection was observed, but not in plants infected with isolate GYV. This correlates with the findings of Bitterlin and Gonsalves (1988) who observed that GYV induced symptoms on *Nicotiana benthamiana* that were distinct from those induced by other ToRSV isolates, including raspberry and peach isolates.

They also compared the nucleotide sequences for the VPg, Pro, Pol, and CP coding regions among these isolates and found that the deduced amino acid sequence of the VPg-Pro-Pol protein domain was more conserved than that of the CP domain. The published sequences of the VPg-Pro-Pol coding region of isolate Rasp-2 and of the CP coding region of isolates Rasp-2 and PYB-2 were included for phylogenetic analysis. Overall, the level of sequence identity among five of the isolates (Rasp-1, Rasp-2, PYB-1, PYB-2, and T392) was very high at both the nucleotide and amino acid levels (between 96 and 99% identity), but in contrast, isolate GYV had a lower level of sequence identity to the other isolates (78 to 81% at the nucleotide level and 84 to 89% at the amino acid level). A parsimony analysis was conducted using the amino acid sequences of the VPg-Pro-Pol and CP domains of the ToRSV isolates and in both

instances isolate GYV was grouped on a separate branch from the other isolates (Figure 2.5).

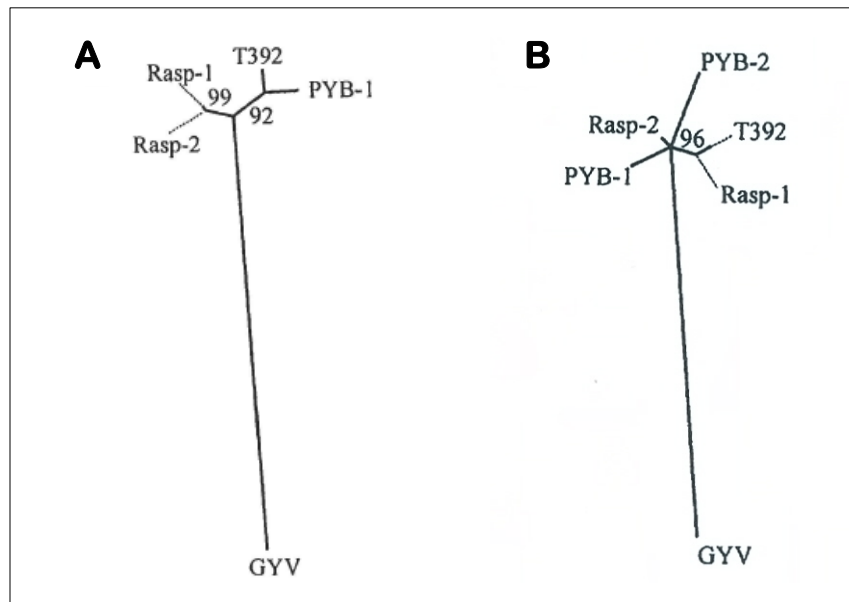


**Figure 2.5:** Phylogenetic analysis of ToRSV isolates. The result of the parsimony analysis is shown. Numbers indicate the degree of confidence at a specific node as tested by 100 bootstrap replications. (A) Phylogenetic tree derived from the deduced amino acid sequence of the VPg-Pro-Pol domain using all available ToRSV isolate sequences. (B) Phylogenetic tree derived from the deduced amino acid sequence of the Coat protein domain using all available ToRSV isolate sequences. In both cases, the GYV isolate are grouped separate from the other ToRSV isolates. [Figure obtained from Wang & Sanfaçon (2000)]

### 2.3.2 Grapevine fanleaf virus (GFLV)

*Grapevine fanleaf virus* (GFLV) belongs to subgroup A, whose members are characterised by having the smallest RNA-2, which is present in both the middle and bottom components of the virus particle.

#### 2.3.2.1 Genome structure and morphology

The genome of *Grapevine fanleaf virus* consists of two positive sense single stranded RNA fragments, RNA-1, with a molecular weight (Mr) of  $2.4 \times 10^6$  and RNA-2 with a Mr of  $1.4 \times 10^6$  (Quacquarelli *et al.*, 1976). RNA-1 is approximately 7342nt in length and encodes the proteins necessary for replication (Ritzenthaler *et al.*, 1991) while the RNA-

2 is variable between 3774nt and 3806nt and encodes the proteins needed for cell-to-cell movement and coating of the viral RNAs (Serghini *et al.*, 1990; Wetzel *et al.*, 2001). The two genomic RNAs are monocistronic and carry a small covalently linked viral protein (VPg) at the 5' terminus and a poly(A) tail at the 3' terminus (Pinck *et al.*, 1988). GFLV RNA-1 is proteolytically cleaved into the proteinase co-factor (also known as protein 1A), a helicase and NTP-binding domain (1B<sup>Hel</sup>), the viral genome-linked protein (1C<sup>VPg</sup>), a proteinase (1D<sup>Pro</sup>) and the RNA-dependant RNA polymerase (1E<sup>Pol</sup>) (Margis *et al.*, 1994; Pinck *et al.*, 1991) (Figure 2.1). GFLV-RNA-2 encodes the homing protein (2A<sup>HP</sup>), a movement protein (2B<sup>MP</sup>), and the coat protein (2C<sup>CP</sup>) (Margis *et al.*, 1993) (Figure 2.6).

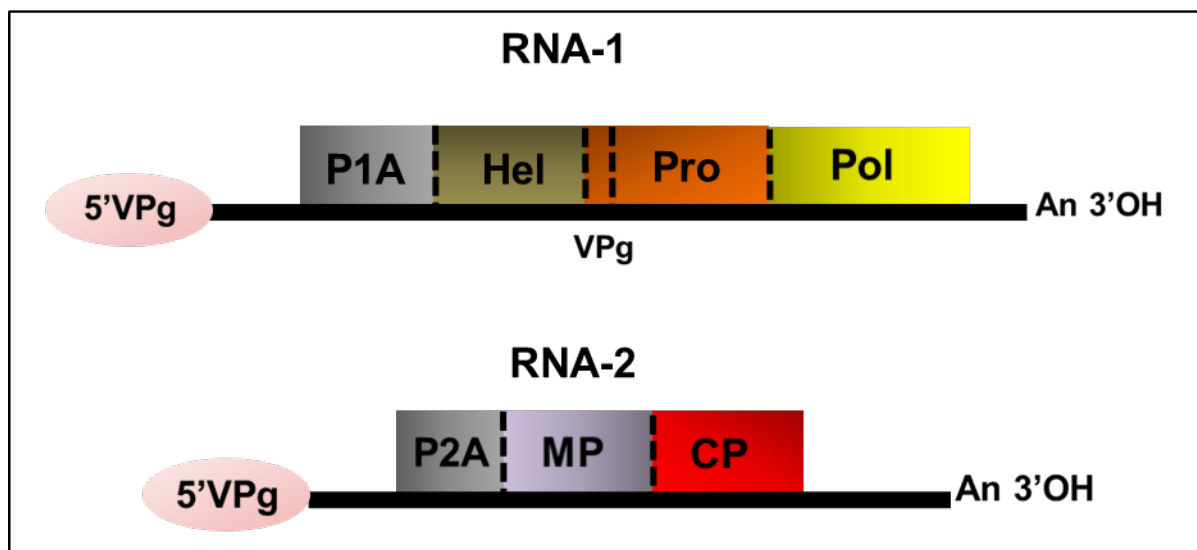


**Figure 2.6:** Genome organisation of GFLV. The ORFs are boxed and functions of the proteins released by proteolysis are indicated. **MP**, movement protein; **CP**, coat protein; **Hel**, helicase; **Pro**, proteinase; **Pol**, polymerase. Dashed lines represent the proteolytic cleavage sites. The ovals at the 5'-end of the RNAs represents the VPg, and **An** at the 3'-end the poly-A. [Adapted from Virus taxonomy (8<sup>th</sup> report) Fauquet C.M. *et al* 2005, pg. 814]

Various GFLV isolates have been associated with satellite RNA molecules (Pinck *et al.*, 1988; Saldarelli *et al.*, 1993; Gottula *et al.*, 2013; Lamprecht *et al.*, 2013). Satellite RNA is usually small RNA molecules that are dependent on cognate helper viruses for replication, encapsidation, movement and transmission (Murant and Mayo, 1982). The satellite RNA associated with GFLV strain F13, referred to as RNA-3, is 1114nt in length and also carries a 5' VPg and 3' poly-A tail as the two genomic RNAs (Pinck *et al.*, 1988).

Virus particles are polyhedral with a diameter of approximately 28nm and an angular outline. The particles consist of three density components that are serologically identical (Figure 2.7). The top (T) component particles are empty protein shells, the middle (M) component particles consists of RNA-2 and the bottom (B) component particles contains both RNA-1 and RNA-2 species (Quacquarelli *et al.*, 1976). The viral coat protein gene accounts for approximately 70% of the weight of M particles and 58% of B particles with a Mr of 56 019 as calculated from the nucleotide sequence (Serghini *et al.*, 1990).

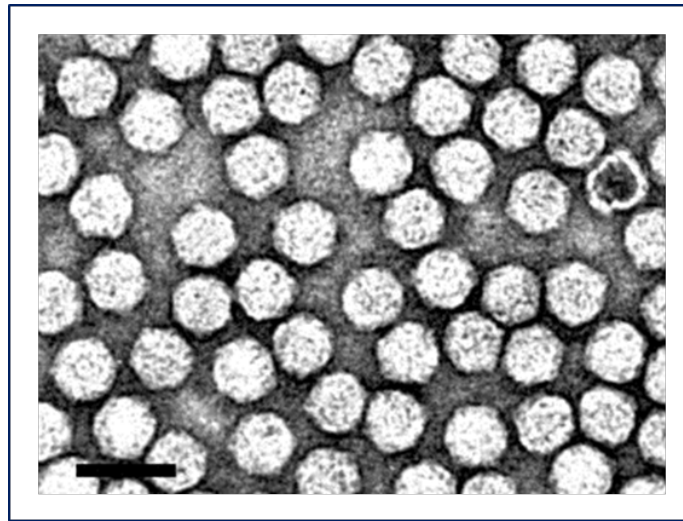


**Figure 2.7:** Purified virus particles of GFLV mounted in uranyl acetate. Particles are serologically identical and an empty virus particle is also present. The bar represents 50nm. [Photo obtained from <http://www.dpvweb.net/dpv/showdpv.php?dpvno=385>]

### 2.3.2.2 Geographical distribution and transmission

*Grapevine fanleaf virus* is among the most widespread of grapevine viruses and occurs worldwide in nearly every temperate region where *Vitis vinifera* is cultivated. It has been reported in Africa, Asia, North and South America, Europe, New Zealand and Australia (Martelli and Savino, 1990; Bovey *et al.*, 1990).

In nature, GFLV is transmitted by the ectoparasitic nematode *Xiphinema index* that feeds on the growing root tips of grapevine (Raski *et al.*, 1983; Wyss, 2000). *X. index*, also known as the California dagger nematode, was the first example of a nematode

acting as a vector for a plant viral disease (Hewitt *et al.*, 1958). During feeding, the nematode ingests the virus from infected vines and retains it in the odontophore, oesophagus and oesophageal pump from where it can be released into neighbouring vines (Taylor and Robertson, 1970). *X. index* is prevalent in continents with viticulture production and is spread by contaminated seed and the grafting of infected rootstocks (Martelli and Holland, 1987). In a study done by Demangeat *et. al* (2005) it was determined by RT-PCR that GFLV can persist in juveniles of *X. index* for over four years in the absence of host plants.

### **2.3.2.3 Host range and symptomatology**

The natural host range for GFLV is mostly limited to species of the genus *Vitis*, although the virus can sometimes be detected in weeds in infected vineyards (Izadpanah *et al.*, 2003). GFLV can be readily transmitted to herbaceous hosts by inoculation of plant sap and its experimental host range includes over 30 species in seven dicotyledonous families (Horvart *et al.*, 1994).

GFLV causes a range of symptoms in grapevines that varies in type and severity (Martelli, 1993). Leaves are severely deformed and asymmetrical with prominent toothed margins, closer primary veins and an open petiolar sinus (Martelli *et al.*, 2001). These symptoms cause the leaves to resemble a fan, hence the name of the virus (Figure 2.8A). Other foliar symptoms include chlorotic mottling, partial or complete yellow mosaic and yellowing of leaf veins (Figure 2.8B & C). Canes are also malformed, showing abnormal branching, short internodes and zigzag growth (Figure 2.3A) (Raski *et al.*, 1983).

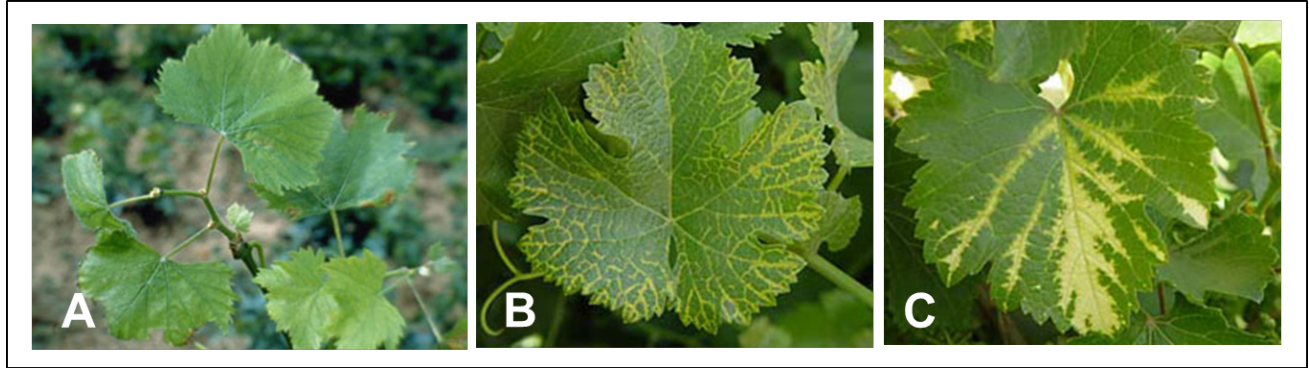


**Figure 2.8:** Typical foliar symptoms of GFLV. **(A)** Vines showing stunted and zigzag shoots with fan-shaped leaves **(B)** Yellow mosaic pattern on leaf **(C)** Bright yellow vein banding on leaf [Photos courtesy of William M. Brown Jr., Bugwood.org (A) and Canadian Food Inspection Agency (B & C); obtained from <http://www.extension.org/pages/33064/grapevine-fanleaf-degeneration-disease>]

Due to the limited movement of its nematode vector, vines infected with GFLV are usually seen in patches within a vineyard (Figure 2.9A) (Andret-Link *et al.*, 2004). Typical foliar symptoms develop in early spring and usually persist throughout the vegetative season although fading may occur during high summer temperatures (Martelli, 1993). GFLV infection leads to a reduction in crop yield as fruit clusters are reduced in size and number (Figure 2.9B).



**Figure 2.9:** (A) Chardonnay vineyard in France infected with GFLV showing patchy distribution of the virus as a result of plant-to-plant virus transmission by the ectoparasitic nematode *Xiphinema index*. (B) Comparison of healthy (left) and GFLV-infected (right) grapevine showing fruit clusters reduced in size and number in infected grapevine. [Photos obtained from Andret-Link *et al.*, 2004]

#### 2.3.2.4 Genome variability

*Grapevine fanleaf virus*, like most plant RNA viruses, has great potential for genetic variation because host plants remain infected for a long period, and the possibility of high mutation rates occurring within the viral genome due to the lack of proof-reading activity within the RNA polymerase gene. The diversity of the GFLV genome has been reviewed in several countries and divergence of up to 17% at the nucleotide level and up to 9% at amino acid level have been observed within the GFLV 2C<sup>CP</sup> gene (Lamprecht *et al.*, 2012; Liebenberg *et al.*, 2009; Mekuria *et al.*, 2009; Pompe-Novak *et al.*, 2007; Naraghi-Arani *et al.*, 2001). The limited variability at amino acid level indicates

a strong genetic stability within the GFLV 2C<sup>CP</sup> gene, validating its role in particle structure and stability, virus movement and host-vector interactions (Vigne *et al.*, 2004).

Sequence comparisons have also revealed a high amino acid diversity of up to 15% in the 2A<sup>HP</sup> gene, which is necessary for RNA-2 replication. It was found that the 2A<sup>HP</sup> gene varies in size between isolates, and is not as genetically conserved as the 2B<sup>MP</sup> and 2C<sup>CP</sup> genes (Oliver *et al.*, 2010). It has also been reported that the genetic variability between GFLV isolates, specifically at the 2A<sup>HP</sup> level, may be responsible for the wide range of symptoms expressed by infected vines (Elbeaino *et al.*, 2014; Terlizzi *et al.*, 2004).

## **2.4 Diagnostic methods for plant virus detection**

The most critical step in managing a virus disease is correct diagnosis. The attributes of a good diagnostic technique are accuracy, specificity, sensitivity and speed. Several techniques are available for plant virus diagnosis, each with its own particular advantages and disadvantages (Ward *et al.*, 2004; Webster *et al.*, 2004). Current diagnostic techniques can be divided into two broad categories: biological properties related to the interaction of the virus with its host and/or vector (e.g. symptomatology and transmission tests) and inherent properties of the virus itself (coat protein and nucleic acid).

### **2.4.1 Detection methods based on biological properties**

#### **2.4.1.1 Symptomatology**

Plants displaying unusual symptoms are generally the first indication of disease. Visual inspection is relatively simple when symptoms are clearly characteristic of a specific virus disease. Disease symptoms are however influenced by many factors, including the virus isolate, host plant variety, time of infection and environmental conditions (Matthews 1980). Typical virus infections on plants include distortion, mosaic patterns on the leaves, yellowing and wilting. However, plants may also exhibit virus-like

symptoms as a response to soil nutrient imbalances, damage caused by insects and mites, and pesticides. In addition, some viruses may cause symptomless infection, while different viruses can produce similar symptoms. While symptoms provide vital information on virus diseases, an accurate diagnosis cannot be made on symptomatology alone and it should be used in conjunction with laboratory tests (Bock 1982).

#### **2.4.1.2 Transmission tests**

Viruses were originally identified and detected by the mechanical, vector, and graft transmission of the specific virus to susceptible indicator plants (Jones 1993). Herbaceous indexing, which is the mechanical transmission of viruses to herbaceous plants by sap inoculation, is a method that is still widely used today. This procedure can be performed with minimal facilities and produces characteristic symptoms, which allows for the detection and identification of many viruses (Horvath 1983 and 1993). Viruses that cannot be transmitted mechanically can be diagnosed by vector transmission or grafting onto suitable indicator hosts (Fridlund 1980, Nemeth 1986, Martelli 1993). These assays are used both for diagnosis and maintenance of virus cultures but are generally time and resource consuming and therefore not practical in a diagnostic setup.

#### **2.4.1.3 Electron Microscopy**

Electron microscopy (EM) allows the assessment of virus particles based on their morphology and is commonly used for virus detection (Baker *et al.*, 1985, Milne 1993). Certain virus groups like filamentous and rod-shaped viruses can be more readily differentiated than isometric viruses. Many plant viruses produce unique intracellular inclusions and their detection by electron microscopy can provide a simple, rapid, and relatively inexpensive method to confirm viral infection (Edwardson *et al.*, 1993). As these distinctive inclusions are being produced as a result of infection by certain viruses, it is sometimes possible to identify unknown viruses to the genus level based on inclusion bodies observed using selective stains. Another method for detecting

viruses is Immunosorbent Electron Microscopy (ISEM) where virus particles are selectively trapped on antibody-coated grids with some contaminating host-plant material (Roberts and Harrison 1979). ISEM combines the specificity of serological assays with the visualisation capabilities of the EM which not only makes it more sensitive for virus detection, but useful to estimate the degree of serological relationship between viruses.

## **2.4.2 Serological testing methods**

The application of serology for detection of plant viruses is a traditional technique based on the use of antibodies. The main objective of an immunodiagnostic assay is to detect or quantify the binding of the diagnostic antibody with the target antigen. Serological diagnosis is limited to viruses for which specific antibodies are available and therefore diseases of unknown origin cannot be detected. Furthermore, as the antigenic properties reside in the coat proteins, viroids cannot be detected by this process.

### **2.4.2.1 Antibody production**

Antibodies are serum immunoglobulins (Igs) that have binding specificity for particular antigens. It is of great value in applications such as experimental biology and medicine and have been utilised extensively for plant pathogen diagnostics (Schots, 1995; Dewey *et al.*, 1997; Torrance, 1998). There are two main routes for antibody production for use in diagnostic assays namely polyclonal antibodies (PABs) and monoclonal antibodies (MAbs).

Polyclonal antibodies are made by injecting purified virus from the pathogen into a host animal. Serum is collected from the animal after a specific time period and the polyclonal antibodies are purified from the serum. As polyclonal antibodies recognise multiple epitopes of the antigen, the serum obtained will contain a heterogeneous complex mixture of antibodies of different affinities. The production of polyclonal antibodies is generally rapid and cost effective and has been used successfully for the detection of plant pathogens; especially viruses (Lipman *et al.*, 2005; Raikhy *et al.*,

2007). The disadvantages of polyclonal antibodies are that it is prone to batch to batch variability, are only generated in limited amounts and may lead to false positives due to non-specificity.

Monoclonal antibodies are prepared by fusing single antibody-forming cells called lymphocytes from the spleen of the inoculated animal with cultured myeloma cells in vitro to generate hybrid cell lines called hybridomas. Each hybridoma will produce a different monoclonal antibody. As these antibodies detect only one epitope on the antigen it is generally more specific. This method provides a consistent and unlimited supply rendering it ideal for the detection and identification of specific viral strains (Konaté *et al.*, 1995; Franz *et al.*, 1996; Naidu *et al.*, 1997). However, monoclonal antibody production is generally time consuming and costly and occasionally cell lines can expire or cease to produce the required antibody.

The critical step in the production of monoclonal and polyclonal antibodies is the availability of purified virus particles. This process is generally slow and labour intensive and delivers varying results with its own difficulties including virus concentration and purity and non-specificity amongst others (Fajardo *et al.*, 2007; Ling *et al.*, 2007). Advances in molecular biology have made it possible for structural protein genes, such as coat protein genes to be amplified, cloned and expressed in *Escherichia coli*. The purified coat protein genes can then be expressed and used in the production of polyclonal (Vaira *et al.*, 1996; Minafra *et al.*, 2000; Xu *et al.*, 2006) and monoclonal antibodies. The increasing availability of virus nucleotide sequences has made recombinant expressed coat proteins the standard strategy for the production of antibodies for the detection of plant viruses (Abou-Jawdah *et al.*, 2004, Aparicio *et al.*, 2009, Shahanavaj *et al.*, 2012).

### 2.4.2.2 Enzyme linked immunosorbent assay (ELISA)

Early serological research was of great value in classifying and identifying viruses, but lacked the sensitivity for routine diagnosis. A remarkable increase in sensitivity was achieved with the development of the enzyme-linked immunosorbent assay (ELISA), which makes use of antibodies conjugated to an enzyme to amplify and signal the presence of viral antigens (Voller *et al.*, 1976). Since its first introduction to plant virology by Clark and Adams in 1977, ELISA has become a very popular method for the detection of viruses in plant material, insect vectors and seeds. Several variants of the ELISA assay have since been developed (Clark and Bar-Joseph 1984; Cooper and Edwards 1986; Van Regenmortel and Dubs 1993) and it can be divided into two broad categories: “direct” and “indirect” ELISA procedures.

The DAS (double antibody sandwich) ELISA is one of the most commonly used for virus detection as it is a relatively easy procedure with a high sensitivity. Viral antigens in the test sample are first trapped by virus-specific antibodies bound to the surface wells of the microtitre plate and then covered by enzyme-conjugated virus antibodies. Finally, the addition of an appropriate substrate induces a colorimetric reaction in the presence of the antigen-enzyme-antibody conjugate complex (Figure 2.10). The colorimetric reaction can be measured using a spectrophotometer and the resulting colour (optical density [OD]) relates directly to the amount of antigen present within the sample. Another format of ELISA that is often used is the plate-trapped antigen (PTA) ELISA, where the microtitre plate wells are coated directly with the test sample followed by incubation with a specific antibody which binds to the target antigen. The specific antibody is either conjugated to the enzyme (direct detection) or detected by a second antibody which is conjugated to the enzyme (indirect detection).

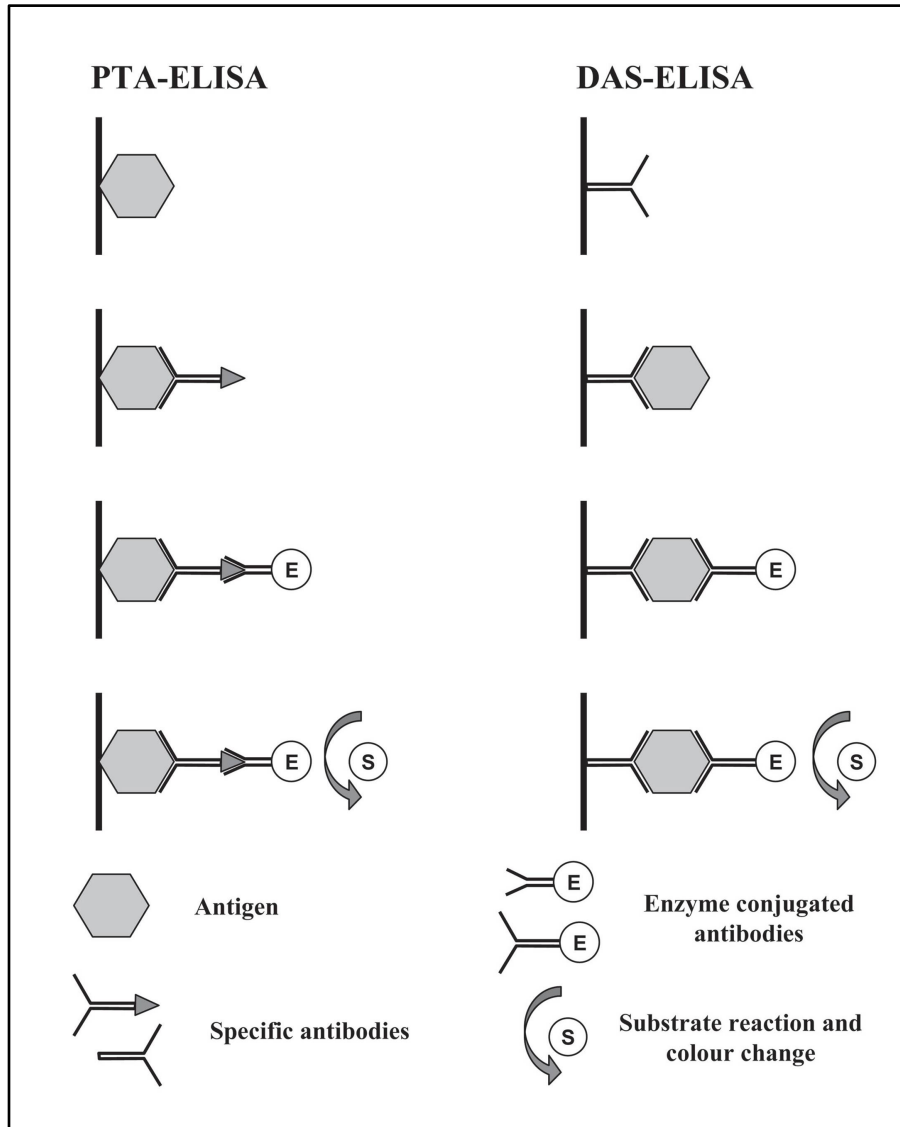


**Figure 2.10:** Schematic diagram illustrating two of the most common ELISA formats: Indirect detection system of the Plate-trapped antigen (PTA-ELISA) and the Double antibody sandwich (DAS-ELISA). Diagram from Ward *et al.*, (2004)

ELISA offers many advantages when compared with older diagnostic techniques (Clark and Bar Joseph, 1984) and remains the assay of choice for routine diagnostic assays. These advantages include among others its sensitivity to detect very little amounts of virus, specificity for differentiating serotypes and low cost and relatively long shelf life of reagents.

### **2.4.2.3 Immunoblotting**

The Dot Immunobinding assay (DIBA) has the same sensitivity as the ELISA and can be used to detect viruses in both plants and vectors (Makkouk *et al.*, 1993). In this method, plant extracts are spotted onto a nitrocellulose or polyvinylidene difluoride (PVDF) membrane and followed by colour-based immunological detection. Tissue blot immunoassay (TBIA) is a rapid technique for plant virus detection where plant pathogens are detected *in situ* by imprinting plant tissues directly onto membranes followed by immunodetection. In addition, tissue imprinting can provide data on the distribution of viruses in plant tissues (Hu *et al.*, 1997). Both DIBA and TBIA are rapid, sensitive, and cost-effective and require minimum laboratory facilities which make them useful as diagnostic techniques. The major disadvantage of immunoblotting techniques is possible interference of sap components with the subsequent diagnostic reactions which can influence quantification of results.

## **2.4.3 Nucleic-acid based detection methods**

### **2.4.3.1 Molecular hybridisation**

The use of molecular hybridisation-based assays in plant pathology was first demonstrated for the detection of *Potato spindle tuber viroid* (Owens and Diener, 1981) and adapted for the diagnosis of plant viruses (Hull, 1993). This method makes use of probes which are single stranded DNA or RNA molecules labeled with a reporter molecule and used to detect the presence of a complementary sequence on the target sample. However, several concerns including problems related with the use of radioactive probes, low sensitivity and complexity of the techniques have minimised the development of new improvements and applications. The most frequent molecular hybridisation format for the detection of viruses used nowadays is non-isotopic dot-blot hybridization using digoxigenin-labelled probes (Pallás *et al.*, 1998). The use of non-radioactive precursors to label the probes has proven to be a sensitive and more

accessible method for large-scale routine testing of plant viruses (Loconsole *et al.*, 2009; Rodriguez *et al.*, 2011).

#### **2.4.3.2 Polymerase chain reaction (PCR)**

Polymerase chain reaction (PCR) is a highly sensitive technique that transformed molecular biology and diagnostics since its invention in the 1980s (Mullis *et al.*, 1986). PCR is an *in vitro* method for rapidly amplifying millions of copies of a target nucleic acid sequence and has since become a popular method for the diagnosis of plant virus diseases (Henson and French 1993; Candresse *et al.*, 1998). The technique consists of three steps: (1) denaturation to separate the double-stranded DNA, (2) annealing of the two oligonucleotide primers to their complementary sequences of the target DNA, and (3) extension of each primer through the target region. Oligonucleotide primers are short sequences of single-stranded DNA which bind specifically to the target DNA by complementary base pairing, and are responsible for the specificity of the PCR. Each DNA strand produced will serve as template for the synthesis of a new DNA strand in the next cycle resulting in an exponential increase in PCR product as a function of cycle number.

For RNA viruses, an initial step to convert the RNA target to its complementary DNA (cDNA) is needed. This is facilitated by the enzyme reverse transcriptase (RT) and is known as RT-PCR (Veres *et al.*, 1987). Several variations of the PCR procedure have since been developed to improve the sensitivity and/or specificity of the assay. One of these is nested PCR which consists of two consecutive PCR reactions where the second reaction uses primers that recognise a region within the PCR product amplified by the first primer set (Dovas and Katis, 2003). Another method is immunocapture PCR (IC-PCR) where antibodies bound to the surface of a microtitre plate or microcentrifuge tube are used to capture the pathogen, which is then detected by PCR (Wetzel *et al.*, 1992; Mulholland 2009). In addition to its value as a detection technique, PCR can also be used in combination with techniques like restriction fragment length polymorphism (RFLP) and DNA sequencing to study the variability of viruses at molecular level (Almond *et al.*, 1992).

### **2.4.3.3 Real time PCR (qPCR)**

Real-time or quantitative PCR follows the same common principle of standard PCR – its key feature is that the amplified DNA is quantified as it accumulates while the reaction progresses, compared to standard PCR where the product is detected at the end. The two main types of qPCR detection chemistries that have been applied in recent years are: (a) using non-specific fluorescent dyes (e.g. SYBR Green) that intercalate with any double-stranded DNA and (b) using sequence-specific DNA probes consisting of oligonucleotides labeled with a fluorescent reporter that are specific to the target DNA e.g. TaqMan oligonucleotide probes (Livak *et al.*, 1995). The real-time PCR system is based on the detection of a fluorescent signal, which increases in direct proportion to the amount of PCR product in the reaction. The fluorescence amount is calculated as the cycle threshold value (Ct value), which increases with decreasing amounts of target DNA (Dorak 2006).

Reverse transcription quantitative PCR (RT-qPCR) for the detection of plant viruses have been successful using both the SYBR Green method (Varga and James, 2006; Stewart *et al.*, 2007) and TaqMan technology (Osman *et al.*, 2007; Hongyun *et al.*, 2008). Both methods have advantages with the SYBR Green method being more economical as it eliminates the use of expensive probes. In addition to simplifying quantification, qPCR has a number of other advantages over conventional PCR – higher sensitivity and specificity, provides a higher throughput, reduces the risk of cross-contamination and eliminates post processing reactions.

### **2.4.3.4 Microarrays**

The introduction of microarrays has been the most promising technology for the development of multi-pathogen detection systems. Microarrays were initially designed for the study of the gene expression (Schena *et al.*, 1995) and single-nucleotide polymorphism typing (Lareu *et al.*, 2003) but have since become an accepted tool for both molecular biology research and diagnostics. The principle of microarrays is the hybridisation of a nucleic acid sample (target) to its complementary sequence on a very

large set of oligonucleotide probes, which are attached to a solid support. Probes can either be denatured PCR amplicons or synthetic oligonucleotides (Bystricka *et al.* 2005). Many pathogens can be detected simultaneously as thousands of DNA probes can be spotted in a defined configuration onto a glass microscopic slide to form the chip. The potential of microarray technology in plant disease diagnosis is very high, due to its multiplex capabilities and the ability to couple with other systems (Van Doorn *et al.*, 2007), but its practical applications must still be developed.

#### **2.4.3.5 Next-generation sequencing**

In recent years, there have been significant advances in DNA sequencing technologies with the introduction and rapid development of next-generation sequencing (NGS), also known as parallel sequencing (Metzker, 2010). In principle, the theory behind NGS is similar to the automated Sanger method (Sanger *et al.*, 1977) – the bases of a small DNA fragment are identified sequentially from the signals emitted when each fragment is re-synthesised from a DNA template strand. NGS expands this process across millions of reactions in a parallel fashion, rather than being limited to a single or a few DNA fragments, which enables the rapid sequencing of large stretches of DNA base pairs spanning an entire genome. Different NGS platforms are available that are capable of producing millions of DNA sequencing reads in a single run, avoiding the need for prior cloning into a vector. NGS also avoids the limitations associated with Sanger sequencing, like limited scalability and the use of chain termination chemistry and electrophoresis (Mardis, 2008; Voelkerding, 2009)

In virus diagnostics, NGS can be applied for the identification of novel viral pathogens (Adams *et al.*, 2013), full-length viral genome sequencing (Adams *et al.*, 2009; Wylie *et al.*, 2014) and the analysis of virus-host interaction (Peng *et al.*, 2009) amongst others. A very interesting application of NGS-based virus identification is vector-enabled metagenomics (VEM) where insect vectors are used to identify viruses present in the environment (Ng *et al.*, 2011; Rosario *et al.*, 2013). Using this approach, insects can

effectively be used to monitor specific environments for the presence or introduction of new viruses.

**Table 2.1:** Comparison of different techniques in detection of plant viruses

Technique	Sensitivity <sup>a</sup>	Specificity <sup>b</sup>	Feasibility <sup>c</sup>	Rapidness	Cost
<b>Molecular hybridisation</b>	+ <sup>d</sup>	++++	++	+	+++
<b>Conventional PCR</b>	+++	++++	+++	+++	+++
<b>Nested PCR</b>	++++	++++	+++	++	+++
<b>Real-time PCR<sup>e</sup></b>	+++++	+++++	++++	+++++	+++
<b>Microarrays</b>	+	+++++	+	++	+

<sup>a</sup>Sensitivity: probability of detecting true positives

(adapted from Lopez *et al.*, 2009)

<sup>b</sup>Specificity: probability of detecting true negatives

<sup>c</sup>Feasibility: practicability in routine analysis, execution and interpretation

<sup>d</sup>The number of + symbols indicates how methods rate regarding each considered criterion, from acceptable (+) to optimum (+++++)

<sup>e</sup>Using TaqMan probes

It is evident that in plant disease diagnostics there is no single molecular test to rely on as various factors play a role in deciding which method to use for detection (Table 2.1). Furthermore, in many laboratories, especially in developing countries, the high cost of reagents and equipment and lack of skilled personnel makes it difficult for molecular techniques to be implemented as routine procedures. Currently, quantitative PCR provides the highest levels of sensitivity on the diagnostic scene and remains the method of choice for rapid and accurate diagnosis of plant pathogens but conventional serological methods like ELISA is still the most frequently applied method for virus detection (Boonham *et al.*, 2014).

## CHAPTER 3

---

### Development of a DAS-ELISA assay for the detection of *Tomato ringspot virus*

#### 3.1 Introduction

*Tomato ringspot virus* (ToRSV) is one of the most widespread and economically important viruses in many crops including *Vitis* spp., *Rubus* spp., *Prunus* spp., and *Fragaria* spp. The ToRSV virion is a small isometric particle, 28 nm in diameter, with an outer shell composed of multiple copies of a single coat protein with a Mr of 58 kDa (Allen and Dias, 1977). The coat protein envelops the single stranded genome consisting of two positive sense RNA segments, RNA-1 and RNA-2, which are 8124 nt and 7273 nt in length respectively.

It was once assumed that the principal role of the plant viral coat protein is to encapsidate the genomic nucleic acid. It has since been discovered that coat proteins are multifunctional proteins that are involved in almost every facet of the viral infectious cycle, including assistance in replication of the viral nucleic acid, movement between cells and organs, and transfer from infected to uninfected plants through mobile biological vectors. Plant viral coat proteins have also been acknowledged as possibly beneficial in the development of commercially useful products including enzymes, vaccines (Johnson *et al.*, 1989; Fikrig *et al.*, 1990) and pharmaceuticals (Giddings *et al.*, 2000). By using a transiently expressed GFP reporter gene, Karran and Sanfacon (2014) showed recently that the ToRSV-CP is a suppressor of RNA silencing by repressing translation.

The development of molecular techniques and the increasing availability of virus sequences have made it possible for the genes of structural proteins such as viral coat proteins to be amplified, cloned, expressed and purified. These can then be used as viral antigen for the production of monoclonal and polyclonal antibodies (Radaelli *et al.*,

2008; Aparicio *et al.*, 2009; Cerovska *et al.*, 2010). The use of recombinant DNA technology for coat protein expression generates high amounts of specific viral protein with ample antigenicity, thereby eliminating the contamination of antigens with plant proteins and other inhibitory compounds (Ling *et al.*, 2007).

There are various criteria to consider when devising a strategy for protein expression and purification, including choice of vector, reading frame and orientation of the insert, as well as choice of host cells for cloning and maintenance of the insert and for subsequent expression. Various microorganisms can act as host systems including bacteria, yeast, filamentous fungi and unicellular algae, all having their strengths and weaknesses with the protein of interest acting as the deciding factor (Demain and Vaishnav, 2009; Adrio and Demain, 2010). *Escherichia coli* is a popular host due to its many advantages including low cost, fast growth kinetics, and fast and easy transformation (Pope and Kent, 1996; Sezonov *et al.*, 2007). The expression of foreign proteins in *Escherichia coli* also presents the ability to obtain large amounts of the desired protein which can be used for a wide range of studies including molecular immunology (Toye *et al.*, 1990) and structural, biochemical and cell biology studies.

For the purification of soluble and active recombinant protein it is necessary to include either a peptide tag or a fusion protein tag *in tandem* with the desired protein. Whilst peptide tags are small and less likely to interfere when fused to the protein, the addition of a non-peptide fusion partner has been shown to enhance solubility (Hammarstrom *et al.*, 2002). One of the more widely used systems for the expression and purification of recombinant proteins is the Glutathione-S-Transferase (GST) Gene Fusion System. The GST gene fusion system provides an integrated system for the expression, purification and detection of fusion proteins produced in *Escherichia coli*. It consists of three key components, namely pGEX plasmid vectors, a variety of GST purification options and various GST detection products. The system is based on inducible, high-level expression of genes or gene fragments as fusions with *Schistosoma japonicum* GST (Smith and Johnson, 1988). In this study, the glutathione S-transferase (GST) gene

fusion system was chosen as bacterial expression system and KRX single step competent cells (Promega) as host strain for expression.

Another method of gene expression is transient expression which provides a fast and flexible platform for the functional analysis of proteins in their native, or near-native, environment (Janssen & Gardner, 1990) and can be localised to specific tissues at specific developmental stages. Transient gene expression in plants allows for the accumulation of high amounts of recombinant proteins within a very short time frame. Transient expression can be approached in various ways including biolistic transformation of naked DNA, infiltration with recombinant *Agrobacterium* (agroinfiltration) and infection with modified viral vectors. Agroinfiltration is a popular method to induce transient expression of genes in a plant or to produce a desired protein due to its speed and convenience. In this method a suspension of *Agrobacterium tumefaciens* is injected into a plant leaf, where it transfers the desired gene to plant cells. Agroinfiltration has been best used in *Nicotiana benthamiana* (Goodin *et al.*, 2008), although it has also been successfully applied to several other plant species, including *Arabidopsis thaliana* (Wroblewski *et al.*, 2005), tobacco (Sparkes *et al.*, 2006) and grapevine (Zottini *et al.*, 2008). The use of *Agrobacterium tumefaciens* to transfer recombinant plant and viral sequences into plant leaves is now routine and has been applied to promoter analysis and protein production (Kapila *et al.*, 1997; Vaquero *et al.*, 1999; Bendahmane *et al.*, 2000; Yang *et al.*, 2000 and Voinnet *et al.*, 2003).

*Agrobacterium*-mediated expression makes use of binary vectors for transformation of foreign genes into plants. A binary vector system is a two plasmid system designed to transport T-DNA (Transfer DNA) into plant cells while avoiding the formation of crown gall tumours (Hoekema *et al.*, 1983). One plasmid contains the virulence genes responsible for transfer of the T-DNA and the other the T-DNA borders, the selectable marker and the DNA to be transferred. In this study, pBIN61S, which is part of the pBIN vector series, was used as binary vector due to its proven success in expressing genes in transient assays (Ghazala *et al.*, 2008; Stephan *et al.*, 2011). pBIN61S, a derivative

of pBIN19, also prevents additional cloning steps as it contains an enhanced cauliflower mosaic virus 35S-promoter and polyA-terminator cassette (Silhavy *et al.*, 2002).

While the bacterial system using *Escherichia coli* is certainly the most widely employed method for recombinant protein expression, it can require a lot of optimisation and has certain limitations. Plants as an alternative host for recombinant proteins have important advantages over microbial or animal cell systems. Unlike bacteria, plant cells have the ability to produce proteins with post-translational modifications, as well as correctly folded and assembled multimeric proteins such as antibodies (Stoger *et al.*, 2002). For this study both systems were investigated in order to achieve optimal expression of the ToRSV coat protein gene.

The objective of this chapter was to isolate and clone the coat protein gene from the grapevine yellow vein (GYV) strain of ToRSV for subsequent expression and specific antibody production. Two expression systems were used for expression of the ToRSV-CP, the GST gene fusion system and an *Agrobacterium*-mediated expression system.

## 3.2 Materials and Methods

### 3.2.1 Plant material

As ToRSV is not present in South Africa, a source of infected research material was obtained from Dr. M. Digiario from the IAMB (Istituto Agronomico Mediterraneo di Bari) in Italy, after attending the 15<sup>th</sup> Meeting of the International Council for the study of virus and virus-like diseases of the grapevine (ICVG) in Stellenbosch in April 2006. The infected grapevine rootstocks are currently maintained under strict quarantine conditions at the Stellenbosch Quarantine station of the Department of Agriculture, Forestry and Fisheries. A lyophilized ToRSV positive control (BIOREBA AG) for use in ELISA testing, made from extracts of infected plants, was used as a reference sample.

### 3.2.2 Isolation of total RNA

RNA was isolated from leaf material using a Cetyltrimethylammonium bromide (CTAB) extraction protocol (White *et al.*, 2008). 0.5g of leaf material was placed in a sterile mortar and macerated to a fine powder using liquid nitrogen. Samples were kept frozen until addition of CTAB buffer (0.5M Tris-HCl, pH 8; 1.4M NaCl; 3% (w/v) CTAB; 20mM Ethylene diamine tetra-acetic acid di-sodium salt (EDTA); 0.5% (v/v)  $\beta$ -Mercaptoethanol). 1ml of CTAB buffer was added to the sample, homogenized, transferred to a microcentrifuge tube and incubated at 60°C for 15 minutes. 500 $\mu$ l of chloroform: isoamylalcohol (CIAA; 24:1) was added, vortexed briefly and mixed thoroughly by inverting the tube several times. The phases were separated by centrifugation at 12,000rpm for 15 minutes at 4°C. The upper aqueous layer was transferred to a new sterile centrifuge tube. One-third volume of 8M lithium chloride was added to the supernatant and incubated overnight at 4°C. The sample was centrifuged at 12 000rpm for 30 minutes at 4°C and RNA was recovered from the pellet. The pellet was washed twice with 500 $\mu$ l of 70% (v/v) ethanol to remove excess salt. The RNA was air-dried for five minutes and suspended in 50 $\mu$ l of sterile nuclease-free water. Agarose gel electrophoresis was performed according to Sambrook *et al.* (2001).

Quality of RNA was analysed by electrophoresis through a 1% (w/v) TBE (44.5mM Tris Base, 44.5mM Boric Acid, 2mM EDTA pH 8.0) agarose gel stained with ethidium bromide (EtBr) and visualised with a Geldoc UV-transilluminator (Vilber Lourmat). The RNA concentration was determined on a NanoDrop® ND-1000 spectrophotometer (NanoDrop Technologies) according to the manufacturer's instructions.

### 3.2.3 Primer design and RT-PCR

The partial ToRSV-GYV RNA2 coat protein gene sequence (Accession No. AF135411) was used for primer design using PRIMER3 software. Four primers were designed to conserved internal regions of the ToRSV coat protein - two forward primers, ToRSV-F-3 and ToRSV-F-724 and two reverse primers ToRSV-R-1038 and ToRSV-R-1687. Primers were synthesized by IDT® (Integrated DNA Technologies). Characteristics of primers used are shown in Table 3.1.

**Table 3.1:** Characteristics of primers used in this chapter

Primer	bp	Sequence 5' – 3'	T <sub>m</sub> (°C)	%GC
ToRSV-F-3	19	AGG GCC ATG GCA GGA AGG T	62.1	63.1
ToRSV-F-724	20	GGA GTG CTT CAC GGG CGT AT	59.9	60
ToRSV-R-1038	20	GCG TGG CAC TTG TTC ATC CA	58.5	55
ToRSV-R-1687	20	AGC CAC GGC CAA AGG GAT TT	60.2	55
ToRSV-SalI-F	24	GTC GACAGG AGG GCC ATG GCA GGA	66.9	66.6
ToRSV-SalI-R	23	GTC GAC TCA GCC ACG GCC AAA GG	64.5	65.2

T<sub>m</sub> – melting temperature;

Nucleotides in red represent the *SalI* recognition site. The nucleotide in blue in primer ToRSV-SalI-F represents the inserted nucleotide to maintain the CP open reading frame.

The rapid-direct-one-tube-RT-PCR is a modified protocol adapted from the method of Osman *et al.* (2007). Plant material was macerated in grinding buffer (1.59g/L Na<sub>2</sub>CO<sub>3</sub>, 2.93g/L NaHCO<sub>3</sub>, pH 9.6 containing 2% (w/v) Polyvinyl Pyrrolidone (PVP) 40, 0.2% (w/v) Bovine Serum Albumin (BSA), 0.05% (v/v) Tween-20, 1% (w/v) Sodium metabisulphide at a ratio of 1:20, and centrifuged briefly. 4µl of the plant extract was added to 25µl of

sterile 1X GES buffer (0.1M Glycine, 50mM NaCl, 1mM EDTA, 0.5% (v/v) Triton X-100, pH 9.0) and boiled at 95°C for 10 minutes. The sample was chilled on ice for five minutes, centrifuged briefly and 2µl of the supernatant was added to the RT-PCR reaction mixture (1x NH<sub>4</sub> buffer, 1.5mM MgCl<sub>2</sub>, 0.2mM dNTP mix, 0.4µM of each primer, 5mM DTT, 1U Biorline Taq DNA polymerase and 1U AMV Reverse Transcriptase) with a total volume of 25µl. This sample preparation method was used for control samples only of which limited material was available. Alternatively, RNA isolated from leaf material as described above was used as template. The PCR reaction was performed in 0.2ml thin-walled tubes in an Eppendorf® Mastercycler (Eppendorf). A Reverse Transcriptase (RT) step at 42°C for 45 minutes was followed by an initial denaturation at 94°C for three minutes. This was followed by 30 cycles of denaturation at 94°C for 30 seconds, annealing at 55°C for 30 seconds and elongation at 72°C for 90 seconds (for amplification of longer fragments an extended elongation period was used). A final elongation step of seven minutes at 72°C was included.

Primers were used in the following combinations:

- a) ToRSV-F-724 and ToRSV-R-1038, yielding a fragment of ~314bp
- b) ToRSV-F-3 and ToRSV-R-1038, yielding a fragment of ~1035bp
- c) ToRSV-F-724 and ToRSV-R-1687, yielding a fragment of ~963bp
- d) ToRSV-F-3 and ToRSV-R-1687, yielding a fragment of ~1684bp

Primers ToRSV-F-724 and ToRSV-R-1038 was used initially to determine whether ToRSV is detected in all samples. Primers ToRSV-F-3 and ToRSV-R-1687 was used to amplify the whole coat protein gene. Primers used in b and c above were included as an alternative approach for partial purification of the coat protein gene if any difficulty was experienced in amplifying the product of 1684bp.

The PCR products were analysed by electrophoresis through a 1% (w/v) TBE (44.5mM Tris Base, 44.5mM Boric Acid, 2mM EDTA pH 8.0) agarose gel stained with EtBr and visualised with a Geldoc UV-transilluminator (Vilber Lourmat).

### **3.2.4 Cloning of the ToRSV-CP gene into the pDRIVE cloning vector**

#### **3.2.4.1 Ligation**

The fragment(s) of interest was excised from the gel with minimal exposure to short wavelength UV light and the DNA eluted using the Zymoclean<sup>®</sup> Gel DNA Recovery kit (Zymo Research) according to the manufacturer's instructions. For cloning of the PCR fragments into the pDRIVE cloning vector, the Qiagen<sup>®</sup> PCR Cloning kit (Qiagen) was used according to the manufacturer's instructions. Ligation was set at 1:4 vector:insert ratio and the ligation reaction was incubated at 16°C for four hours.

#### **3.2.4.2 Transformation**

Ligated plasmids were transformed into chemically competent DH5 $\alpha$  cells as described by Sambrook *et al.* (2001). 100 $\mu$ l of competent cells were mixed with 2 $\mu$ l of each ligation reaction and the mixture was incubated on ice for five minutes and heat shocked at 42°C for 40 seconds. 900 $\mu$ l of SOC medium (0.5% [w/v] Yeast extract, 2% [w/v] Tryptone, 10mM NaCl, 2.5mM KCl, 10mM MgCl<sub>2</sub>, 10mM MgSO<sub>4</sub>, 20mM Glucose) was added to each reaction and incubated at 37°C for one hour, shaking at ~200rpm. 100 $\mu$ l of each transformation was plated onto Luria Bertani (LB) agar plates containing the antibiotic Ampicillin (Amp) to a final concentration of 100 $\mu$ g/ml. For blue-white colony selection, to identify positive clones, 40  $\mu$ g/ml 5-bromo-4-chloro-3-indolyl- $\beta$ -D-galactoside (X-Gal) (Fermentas) and 0.2 mM Isopropyl- $\beta$ -D-thiogalactoside (IPTG) (Fermentas) were added to agar plates. The plates were incubated overnight at 37°C.

#### **3.2.4.3 Screening of recombinants by PCR**

Positive recombinants were screened by direct colony PCR. Ten colonies were picked with a sterile toothpick, transferred to a LB-Amp agar plate and suspended directly into the PCR reaction mixture. The reaction mixture, with a total volume of 25 $\mu$ l, contained 1x NH<sub>4</sub> buffer, 1.5mM MgCl<sub>2</sub>, 0.2mM dNTP mix, 0.4 $\mu$ M of each primer and 1U Boline

Taq DNA polymerase. PCR primer combinations (a) and (d) as described in section 3.2.3 were used for screening. PCR was carried out as described in section 3.2.3, without the initial RT step and with an elongation period of 30 seconds. PCR products were analysed on a 1% (w/v) agarose gel as described above. Colonies from the confirmed transformants were inoculated in 5 ml LB broth containing 100µg/ml Amp and incubated overnight (37°C) with shaking (225 rpm) for subsequent isolation of plasmid DNA.

#### **3.2.4.4 Plasmid DNA isolation**

Plasmid DNA was isolated using the GeneJet<sup>®</sup> Plasmid Miniprep kit (Fermentas) according to the manufacturer's instructions. The DNA concentration was determined on a NanoDrop<sup>®</sup> ND-1000 spectrophotometer (NanoDrop Technologies) according to the manufacturer's instructions.

#### **3.2.4.5 Sequencing of recombinant DNA**

Automated sequencing was performed at Stellenbosch University's Central Analytical Facility (CAF). Results were obtained in the form of electropherograms and subsequently analysed using BioEdit Sequence Alignment Editor (version v7.0.4, Hall, 1999). The ToRSV coat protein gene sequence was analysed with NEBcutter, New England BioLabs Inc. ([www.tools.neb.com/NEBcutter2](http://www.tools.neb.com/NEBcutter2)) to determine restriction sites within the CP sequence. A restriction enzyme that did not cut within the coat protein had to be selected to facilitate cloning of the full-length CP into the pDRIVE and pGEX-6P2 vectors. PCR primers that include the *Sa*II restriction site, ToRSV-*Sa*II-F and ToRSV-*Sa*II-R, were designed. To maintain the CP open reading frame, an extra nucleotide was incorporated in the forward primer (Table 1) for cloning into the pGEX vector.

### **3.2.4.6 Cloning of the full-length ToRSV CP gene**

PCR primers ToRSV-*Sa*II-F and ToRSV-*Sa*II-R were used for amplification of the full-length ToRSV coat protein gene. A 1:10 000 dilution of the 1684bp plasmid DNA obtained in section 3.2.4.4 was used as template for PCR. In addition, the reaction mixture, with a total volume of 25µl, contained 1x NH<sub>4</sub> buffer, 1.5mM MgCl<sub>2</sub>, 0.2mM dNTP mix, 0.4µM of each primer and 1U ExTaq (Takara) DNA polymerase. PCR was carried out with an initial denaturation at 94°C for two minutes followed by five cycles of denaturation at 94°C for 30 seconds, annealing at 52°C for 30 seconds and elongation at 72°C for 90 seconds. This was followed by 25 cycles of denaturation at 94°C for 30 seconds, annealing at 55°C for 30 seconds and elongation at 72°C for 90 seconds. A final elongation step of seven minutes at 72°C was included. The 1684bp fragment was cloned into the pDRIVE cloning vector and the resultant clones were screened as described in section 3.2.4. Plasmid DNA was isolated using the GeneJet<sup>®</sup> Plasmid Miniprep kit (Fermentas) according to the manufacturer's instructions. Restriction enzyme digest using the *Sa*II restriction enzyme were performed to verify cloning. 0.5µg of plasmid DNA was digested with 1U of *Sa*II enzyme and 1X enzyme buffer, in a total reaction volume of 20µl, at 37°C for one hour. The restriction products were resolved on a 1% (w/v) agarose gel. Sequencing of the recombinants was performed at the Stellenbosch University's Central Analytical Facility.

### **3.2.5 Bacterial expression of the ToRSV-CP gene using the GST gene fusion system**

#### **3.2.5.1 Preparation of the pGEX6P2 vector**

The pGEX-6P-2 expression vector was linearized by digestion with the *Sa*II restriction enzyme (~400ng pGEX-6P-2; 1U *Sa*II enzyme; 1X buffer O, Fermentas) at 37°C for 60 minutes. The reaction was incubated at 65°C for 10 minutes to deactivate the enzyme before dephosphorylation with Shrimp Alkaline Phosphatase (SAP) (Fermentas), as suggested by the manufacturer. The linearised, SAP-treated vector was resolved on a

1% (w/v) agarose gel in 0.5X TBE buffer. The fragment was excised from the gel and the DNA eluted using the Zymoclean<sup>®</sup> Gel DNA Recovery kit (Zymo Research) according to the manufacturer's instructions.

### **3.2.5.2 Ligation and Transformation**

The pDRIVE:ToRSV-CP plasmid DNA was digested with *SalI* restriction enzyme (as described above) and separated on a 1% (w/v) agarose gel in 0.5X TBE buffer. The correctly sized fragment of ~1.7kb was excised from the gel and purified using the Zymoclean<sup>®</sup> Gel DNA Recovery kit (Zymo Research). The insert was ligated into the prepared pGEX-6P-2 vector using a vector:insert ratio of 1:5. The ligation reaction was incubated at 16°C for four hours. The ligated plasmids were transformed into chemically competent DH5 $\alpha$  cells (section 3.2.4.2) and plated onto LB agar plates containing the antibiotic Ampicillin (100 $\mu$ g/ml) for selection.

### **3.2.5.3 Screening of pGEX-6P-2: ToRSV-CP constructs**

Recombinants were initially screened with colony PCR using the primer set ToRSV *SalI*-F and ToRSV *SalI*-R, yielding a fragment of ~1.7kb (Table 3.2). The recombinants yielding the correctly sized fragment were further analysed for correct orientation by using specific primer sets. The pGEX sequencing primers bind on the following regions on the pGEX-6P-2 vector - pGEX 5': 869 – 891 & pGEX 3': 1057 – 1035. The *SalI* restriction enzyme cuts the pGEX-6P-2 vector at position 965 (Figure 3.1). Primer sets used for orientation screening are shown in Table 3.2.

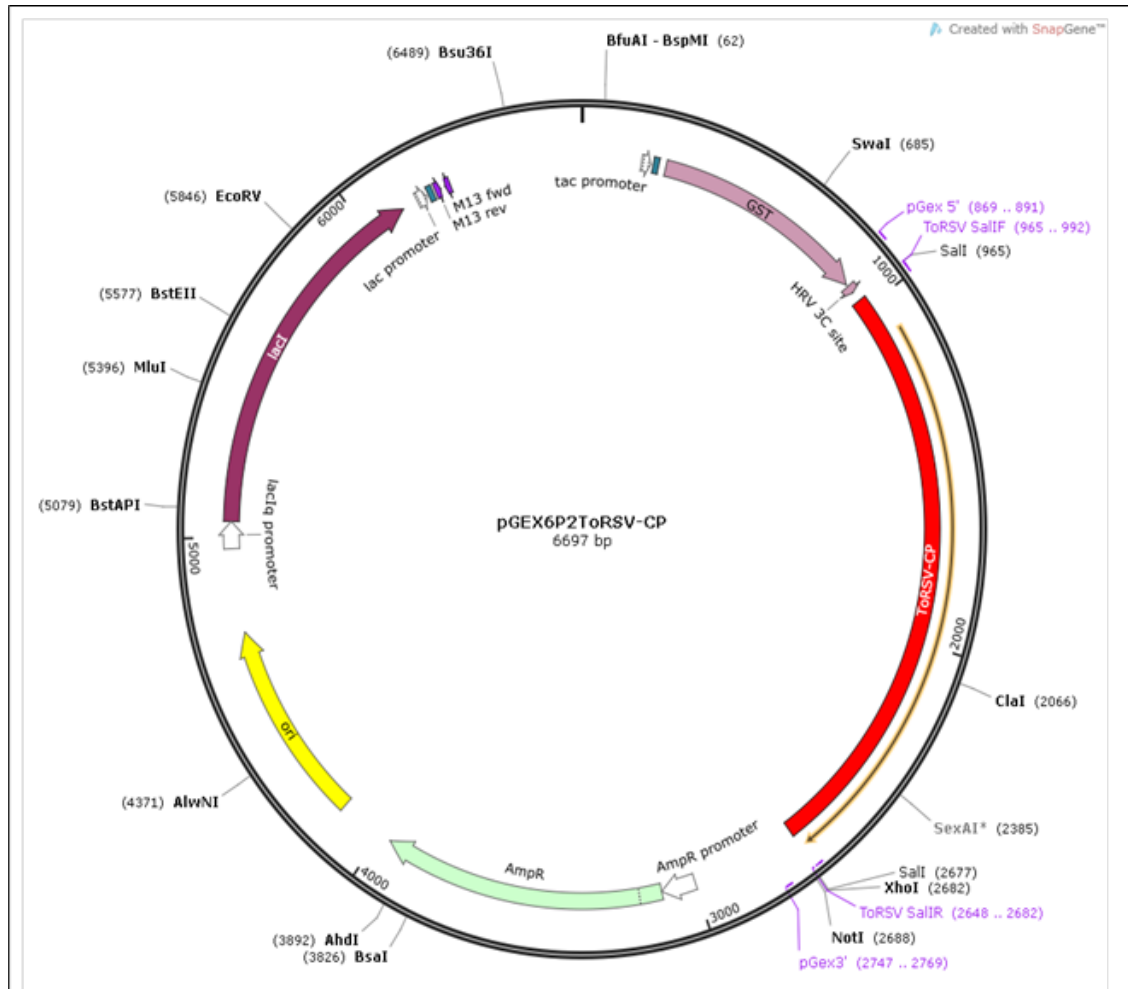


**Figure 3.1:** Plasmid map of pGEX-6P-2 showing the inserted ToRSV-CP gene at the *SalI* restriction site as well as the binding sites for the ToRSV-*SalI* and pGEX primers used. [Created using SnapGene® software from GSL Biotech; available at [snapgene.com](http://snapgene.com)]

**Table 3.2:** Primer sets used for orientation screening of the pGEX-6P-2 expression vector containing the ToRSV-CP gene

Primer set	Size of product	Orientation
pGEX 5' & ToRSV <i>SalI</i> -R	~ 1.8kb	forward
pGEX 3' & ToRSV <i>SalI</i> -F	- ~1.8kb	forward
pGEX 5' & ToRSV <i>SalI</i> -F	~ 1.8kb	reverse
pGEX 3' & ToRSV <i>SalI</i> -R	~ 1.8kb	reverse
ToRSV <i>SalI</i> -F & ToRSV <i>SalI</i> -R	~ 1.7kb	forward & reverse

Recombinants in the correct orientation were inoculated in 5ml LB broth containing 100µg/ml Amp and incubated overnight with shaking (37°C, 225rpm). Plasmid DNA was isolated using the GeneJet<sup>®</sup> Plasmid Miniprep kit (Fermentas, Thermo Scientific, USA) according to the manufacturer's instructions.

#### **3.2.5.4 Transformation of constructs into KRX competent cells**

Transformations into KRX competent cells (Promega) were performed as prescribed in the technical bulletin (Part# TB352) provided by Promega. 50ng of pGEX-6P-2:ToRSV-CP plasmid DNA was inoculated into 50µl of KRX competent cells. 100µl of each transformation was plated onto LB-agar plates containing 100µg/ml Amp and incubated overnight at 37°C. Single colonies were inoculated in 25ml LB–Amp (100µg/ml) medium and incubated overnight at 37°C. From these, freezer cultures were made using Microbank<sup>™</sup> cryovials (Pro-lab Diagnostics).

#### **3.2.5.5 Recombinant Protein Expression**

For protein expression, an adapted protocol of Mercado-Pimentel *et al.*, (2002), optimised to enhance soluble protein expression was followed. One bead was removed aseptically from the freezer culture and transferred to 25ml LB medium containing 100µg/ml Amp. The culture was incubated overnight at 37°C with shaking at 225rpm. The starter culture was diluted 1:100 in Terrific Broth (TB, 12g/L Bacto-Tryptone, 24g/L Bacto-Yeast extract, 0.4% (v/v) glycerol, 1% (w/v) glucose, 17mM KH<sub>2</sub>PO<sub>4</sub>, 72mM K<sub>2</sub>HPO<sub>4</sub>) containing 100µg/ml Amp. The culture flask was incubated at 37°C with shaking at ~225rpm and measured at regular intervals until an optical density (OD<sub>600</sub>) of 0.8-1.0 was reached. The flask was then moved to 25°C and continued shaking at ~225rpm. Once an OD<sub>600</sub> of 1.0-1.5 was reached, protein expression was induced by the addition of 0.1% (w/v) rhamnose and 0.1% (w/v) rhamnose + 1mM IPTG. A sample of the culture was kept aside as an un-induced control and was subjected to the same conditions as the rest of the culture. Cultures were grown overnight at ~25°C with shaking at ~225rpm.

The bacterial cells were harvested by centrifuging at 7000 x g for seven minutes at 4°C and the resulting pellet was resuspended in ice-cold 1X STE buffer (10mM Tris-HCl, pH 8; 150mM NaCl; 1mM EDTA; 100µg/ml Phenylmethanesulphonylfluoride [PMSF]). After resuspension, DTT (1,4-Dithiothreitol) was added to a final concentration of 5mM, followed by 0.5% (w/v) of N-Lauryl-sarcosine (Sarkosyl, MERCK). To break the bacterial cell walls, the cell suspension was treated to three freeze-thaw cycles by first incubating in liquid nitrogen for 15 minutes and then at 37°C for 10 minutes. The suspension was vortexed for about five seconds, DNase treated (50µg/ml DNase 1) for one hour at 37°C and sheared by drawing through a 12 gauge syringe needle. Once the lysate had reached a less viscous consistency, 1ml of the total cell protein was kept aside for SDS-Page analysis and the rest of the suspension was centrifuged at 10 000 x g for 25 minutes at 4°C. The clarified supernatant containing the soluble fraction was transferred to a clean tube whilst the pellet, containing the insoluble fraction, was resuspended in an equivalent volume of STE buffer. All samples were stored at -20°C.

### **3.2.5.6 SDS-Page Analysis**

The expressed protein samples were analysed on a denaturing polyacrylamide gel. A 10% (w/v) resolving gel and a 4% (w/v) stacking gel was used. The resolving gel consisted of 1X resolving gel buffer (375mM Tris-HCl, pH 8.8, 0.1% [w/v] SDS), 10% [w/v] acrylamide solution (30% stock: 29g acrylamide, 1g N,N'-methylenebisacrylamide per 100ml), 1% [w/v] ammonium persulfate (APS, 10% [w/v] stock solution, prepared fresh) and 0.13% [v/v] Tetramethylethylenediamine (TEMED). The stacking gel consisted of 1X stacking gel buffer (125mM Tris-HCl, pH 6.8, 0.1% [w/v] SDS), 4% (w/v) acrylamide solution, 0.15% (w/v) APS and 0.15% (v/v) TEMED. Samples were prepared using the Protein loading buffer pack (Fermentas) as follows: 2µl of 20X Reducing Agent; 10µl of 5X Protein loading buffer; protein sample; dH<sub>2</sub>O to 50µl; heat samples at 100°C for 3-5 minutes and apply directly to SDS-Page gel. Molecular markers used include the PageRuler™ Unstained Protein Ladder (Fermentas) and the PageRuler™ Prestained Protein Ladder Plus (Fermentas), both according to the manufacturer's instructions.

Electrophoresis was performed at 30mA per gel for approximately two hours in a Cleaver Scientific Vertical Electrophoresis System. The protein bands were visualized by using PageBlue™ Protein Staining solution (Fermentas) as follows: wash gels in dH<sub>2</sub>O for 10 minutes (X3); stain gels overnight in PageBlue™ solution with gentle agitation; destain gels in dH<sub>2</sub>O for one hour.

### **3.2.5.7 Western Blot**

Western blot analysis was performed according to the conditions as prescribed by the Amersham ECL GST Western Blotting Detection kit (GE Healthcare). In addition, the membrane was also incubated for one hour in ToRSV IgG (Bioreba) [diluted 1:1000 in TBS-Tween (TBST)] as primary antibody followed by an one hour incubation in Goat-anti-rabbit antibody (GAR-AP, Sigma-Aldrich) conjugate [diluted 1:10 000 in TBST] as secondary antibody. The membrane was briefly rinsed in two changes of TBST for 15 minutes each, and again for five minutes (X3) with fresh changes of TBST wash buffer. Detection was carried out using the ECL™ detection reagents as prescribed by the manufacturer's instructions.

## **3.2.6 Agrobacterium-mediated transient expression of the ToRSV-CP gene**

### **3.2.6.1 PCR analysis**

Primers were designed to facilitate cloning of the GST-ToRSV CP fragment into the pBIN61S binary vector - forward primer, ToRSV-CPexpress-s with a *SacI* recognition site and reverse primer ToRSV-CPexpress-as with a *XbaI* recognition site. The GST fragment was kept intact with the ToRSV-CP to assist with subsequent purification of the fusion protein from the leaf material. Primers were synthesized by IDT® (Integrated DNA Technologies). Characteristics of primers used are shown in Table 3.3.

**Table 3.3:** Characteristics of primers to facilitate pBIN61S cloning

Primer	bp	Sequence 5' – 3'	T <sub>m</sub> (°C)	%GC
ToRSV-CPexpress-s	32	AA <b>GAG CTC</b> ATG TCC CCT ATA CTA GGT TAT TGG	61.3	43.8
ToRSV-CPexpress-as	25	AA <b>TCT AGA</b> TCA GTC ACG ATG CGG CC	61.4	52.0

T<sub>m</sub> – melting temperature;

Nucleotides in red represent the *SacI* and *XbaI* recognition sites.

The pGEX-6P-2:ToRSV-CP plasmid DNA was used as template for PCR. The reaction mixture, with a total volume of 25µl, contained 1x reaction buffer, 0.2mM dNTP mix, 0.4µM of each primer and 1U ExTaq DNA polymerase. PCR was carried out with an initial denaturation at 94°C for two minutes followed by 35 cycles of denaturation at 94°C for one minute, annealing at 58°C for one minute and elongation at 72°C for two minutes. A final elongation step of seven minutes at 72°C was included. PCR products were resolved on a 1% (w/v) agarose gel in 0.5X TBE. The 2.5kb GST:ToRSV-CP fragment was excised from the gel and the DNA eluted using the Zymoclean<sup>®</sup> Gel DNA Recovery kit according to the manufacturer's instructions.

### 3.2.6.2 Cloning of GST:ToRSV-CP fragment into pDRIVE

For cloning of the PCR fragments into the pDRIVE cloning vector, the QIAGEN<sup>®</sup> PCR Cloning kit was used. Ligation and transformation was carried out as described in section 3.2.4. Recombinants were screened by direct colony PCR as described in section 3.2.4.3 and using ToRSV-CPexpress primers (Table 3.3). Plasmid DNA was isolated using the GeneJet<sup>®</sup> Plasmid Miniprep kit (Fermentas) according to the manufacturer's instructions. Restriction enzyme digests, using the *EcoRI* restriction enzyme, which cuts the recombinant clones into four fragments of 3836bp, 1213bp, 716bp and 523bp, were performed to confirm cloning. Plasmid DNA was then digested with the restriction enzymes *SacI* and *XbaI* to facilitate cloning into the pBIN61S vector (figure 3.2). Between digestions, SureClean (Bioline), which avoids additional cleaning steps, was added to the mixture according to the manufacturer's instructions.

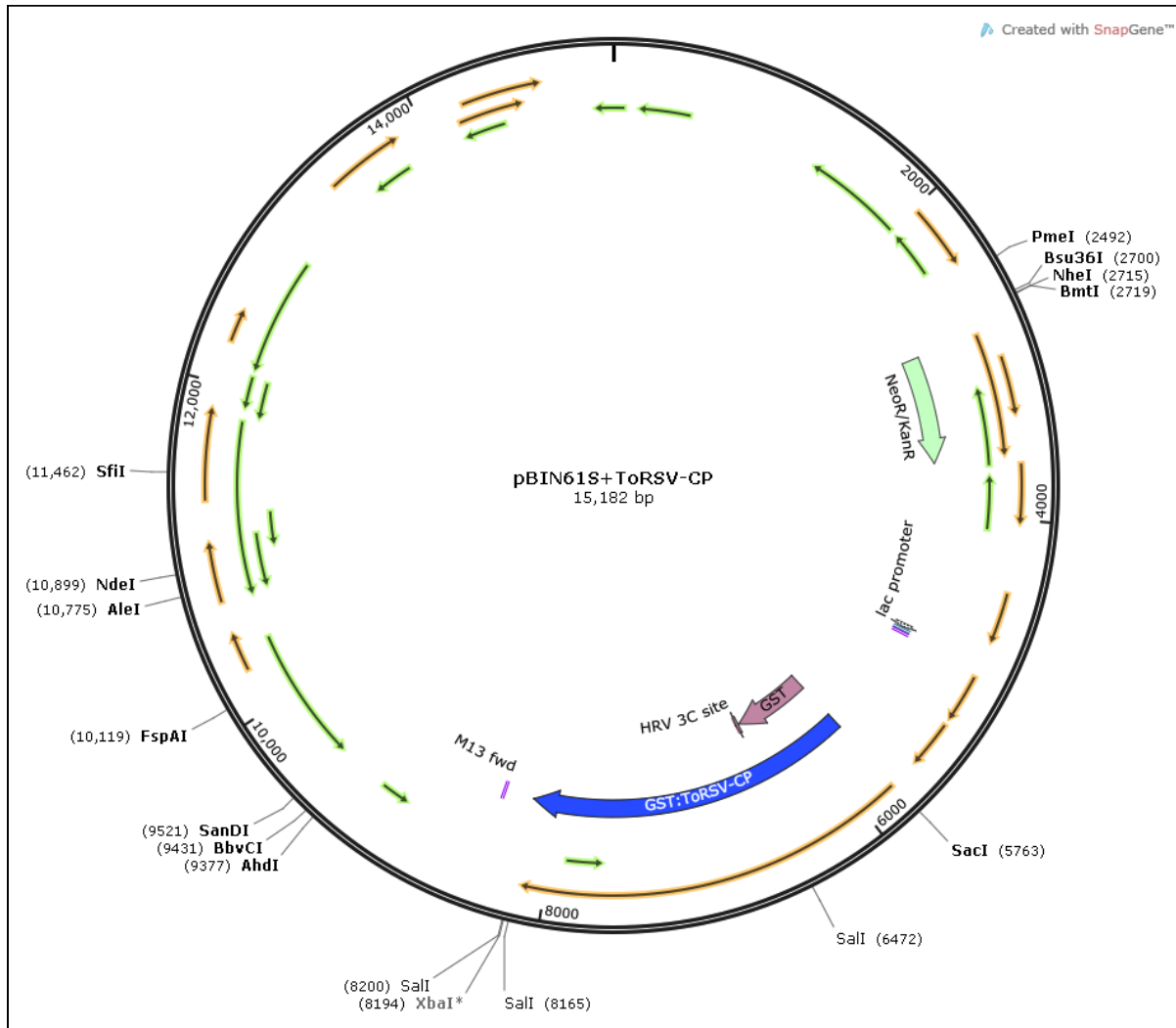


**Figure 3.2:** Plasmid map of pBIN61S indicating the inserted GST:ToRSV-CP sequence (blue arrow) at the *SacI* and *XbaI* restriction sites. [Created using SnapGene® software from GSL Biotech; available at [snapgene.com](http://snapgene.com)]

The pDRIVE:ToRSV-CP plasmid DNA was transformed into JM 110 (NEB), a non-methylating strain of *E.coli*, and recombinants were screened by direct colony PCR. Plasmid DNA was isolated using the GeneJet® Plasmid Miniprep kit (Fermentas) according to the manufacturer's instructions. pBIN61S vector DNA and pDRIVE-ToRSV-CP plasmid DNA were subjected to *SacI* and *XbaI* digestions as above to facilitate cloning into the pBIN61S vector.

### 3.2.6.3 Cloning of GST-ToRSV-CP fragment into pBIN61S

The digested plasmid DNA was separated on a 1% (w/v) agarose gel and the fragment of 2.5kb was excised from the gel and purified using the Zymoclean<sup>®</sup> Gel DNA Recovery kit. The insert was ligated into the prepared pBIN61S vector using different vector:insert ratios of 1:1, 1:2.5 and 1:5. The ligation reactions were incubated overnight at 16°C. The ligated plasmids were transformed into chemically competent DH5 $\alpha$  cells (as described previously) and plated onto LB agar plates containing the antibiotic Kanamycin (Kan) (50 $\mu$ g/ml) for selection. Positive recombinants were screened by direct colony PCR with the ToRSV-CPexpress primers as described in Table 3.3. The GeneJet<sup>®</sup> Plasmid Miniprep kit (Fermentas) was used to isolate plasmid DNA, according to the manufacturer's instructions. Successful cloning was further confirmed by digesting the plasmid DNA with the restriction enzymes *Eco*RI and *Sal*I (as described previously) and observing the fragment patterns.

### 3.2.6.4 Transformation into *Agrobacterium* via electroporation

Electrocompetent *Agrobacterium tumefaciens* strain C58 cells were used for agroinfiltrations (provided by the Vitis lab, Department of Genetics, Stellenbosch University). Electroporation was performed on a Bio-Rad Gene Pulser<sup>®</sup> II and Bio-Rad Pulse Controller Plus. All cuvettes and media used for electroporation were pre-chilled at 4°C and kept on ice during the procedure. A 40 $\mu$ l aliquot of competent cells was thawed on ice and 1 $\mu$ l of plasmid DNA was added and mixed gently. The mixture was incubated on ice for one minute, transferred to a pre-chilled 0.1cm cuvette, and electroporated under the following conditions: capacitance of 25 $\mu$ F, resistance of 200 Ohm, voltage of 1.5kV and for a pulse length of 4.5ms. The cuvette was removed immediately after electroporation, and 800 $\mu$ l of cold sterile SOC medium was added to the mixture. The bacterial suspension was subsequently transferred to a sterile 1.5ml microcentrifuge tube and incubated at 28°C shaking at 225rpm for approximately 3.5 hours. 100 $\mu$ l of each transformation was then plated out on LB-Kan plates and incubated at 28°C for three days. Recombinants were screened with colony PCR to

verify transformation using the ToRSV-CP express primer set which yields a fragment of ~2.5kb.

### **3.2.6.5 *Agrobacterium*-infiltration of *Nicotiana benthamiana* plants**

*N. benthamiana* plants were propagated from seed under controlled conditions in a growth room with temperatures of 22-28°C, a relative humidity of 70%, and with a 16/8hour light/dark cycle. Recombinant *Agrobacterium tumefaciens* containing the pBIN61S-GST-ToRSV-CP constructs were streaked onto fresh LB-Kan agar plates and grown for two days at 28°C. A single colony of each construct was inoculated in 50ml LB medium with 50µg/ml Kanamycin and incubated overnight at 28°C shaking at 225rpm. A volume of 2ml of the overnight culture was re-inoculated into 20ml LB medium containing 50µg/ml Kanamycin, 10mM 2-[Morpholino]ethanesulfonic acid (MES) and 20µM acetosyringone, and incubated overnight at 28°C, whilst shaking at 225rpm. The saturated bacterial culture was centrifuged for five minutes at 4000Xg and suspended in re-suspension solution (10mM MES, 100µM acetosyringone, 10mM MgCl<sub>2</sub>) to an OD<sub>600</sub> of 1. The resuspended solutions were incubated at room temperature for approximately three hours before infiltrations were performed. Top leaves of *N. benthamiana* plants were infiltrated with ~1ml of bacterial culture per leaf. As a negative control, leaves were infiltrated with re-suspension solution only and kept under the same conditions as test plants. The plants were kept in a growth room under the conditions described above and monitored over a period of seven days.

### **3.2.6.6 Tissue-print Immuno Assay**

Tissue-print Immuno assay (TPIA), adapted from the protocol of Franco-Lara *et al.*, 1999, was performed to detect the presence of the GST-ToRSV-CP fragment in *N. benthamiana* plants at seven days post inoculation (dpi). A Hybond PVDF membrane was pre-wetted in methanol and immediately rinsed in water for 15 minutes. The membrane was then equilibrated in 1X Phosphate-buffered Saline (PBS) [3.2mM Na<sub>2</sub>HPO<sub>4</sub>, 0.5mM KH<sub>2</sub>PO<sub>4</sub>, 1.3mM KCl, 135mM NaCl, pH 7.4] buffer for 15 minutes and

air-dried on filter paper before blotting the leaf tissue. A segment of the epidermis of infiltrated leaves was carefully removed with tweezers to expose the mesophyll tissue which was then pressed firmly onto the Hybond PVDF membrane for two seconds. The membrane was incubated for one hour whilst gently shaking in a blocking solution of 4.5% (w/v) milk powder dissolved in 1X PBS buffer. The blocking solution was discarded and the membrane washed for 3X five minutes in PBS-Tween buffer (1X PBS buffer, 0.1% (v/v) Tween 20). The membrane was then incubated in the primary antibody solution of a 1:200 dilution of ToRSV-ch-IgG (Bioreba) in PBS-TPO buffer (0.2% [w/v] Ovalbumin, 2% [w/v] Polyvinylpyrrolidone 40, PBS-Tween pH7.4) for 2h while shaking gently. The antibody solution was collected and stored at 4°C and the membrane washed in PBS-Tween for 3X five minutes. This was followed by incubation of the membrane in the secondary antibody of a 1:10 000 dilution of Goat-anti-rabbit antibody (GAR-AP, Sigma) in PBS-Tween for one hour on a shaker. The conjugate solution was collected and stored at 4°C and the membrane subjected to 3X five minute washes in PBS-Tween. The membrane was then incubated in the substrate colour reaction solution of AP-BCIP-NBT (10ml AP buffer [100mM Tris HCl, 100mM NaCl, 5mM MgCl<sub>2</sub>, 0.05% (v/v) Tween 20, pH 9.5], 33µl 5-bromo-4-chloro-3-indolyl phosphate (BCIP) stock solution [50mg/ml in 100% DMF]), 66µl Nitro Blue Tetrazolium (NBT) stock solution [75mg/ml in 70% DMF]) for 30 minutes in the dark, rinsed thoroughly in water and dried overnight at room temperature between filter paper.

### **3.2.6.7 SDS Page analysis & Western Blot**

SDS-Page analysis was performed as described in section 3.2.5. After 7 days post infiltration, sections of *N. benthamiana* leaves showing definite areas of infiltration were macerated in a 1:4 ratio with Sample Extraction buffer (50mM Tris, pH 7.5, 150mM NaCl, 0.1% [v/v] Tween-20, 0.1% [v/v] β-mercaptoethanol). Plant extracts were clarified by centrifuging at 13 000xg for 15 minutes. Leaves from control plants (infiltrated with buffer only and subjected to the same conditions as *Agrobacterium*-infiltrated plants) were macerated in the same manner. Samples were prepared using the Protein loading

buffer pack (Fermentas), as described in section 3.2.5 and analysed on 8% (w/v), 10% (w/v) and 12% (w/v) SDS-Page gels respectively.

Western blot analysis was performed according to the conditions as prescribed by the Amersham GST Western Blotting Detection kit (GE Healthcare) with an additional incubation step in ToRSV-IgG as described in 3.2.5.7. The substrate solution AP-BCIP-NBT was used as detection method as described above.

### 3.3 Results

#### 3.3.1 Isolation and cloning of the ToRSV-CP gene

A total RNA yield of approximately 1.8µg/µl was obtained from 0.5g of leaf material. The quality of the RNA was analysed by agarose gel electrophoresis and ethidium bromide staining. Three distinct bands were visible representing the ribosomal 28s, 18s and 16s RNA subunits (Figure 3.3).

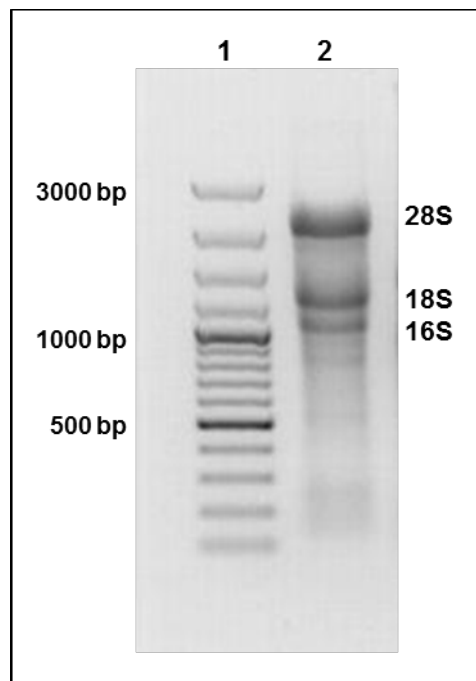


**Figure 3.3:** Total RNA isolated from ToRSV-infected leaf material. Lane 1:100bp plus DNA marker; Lane 2: Total RNA isolated from infected grapevine material

Direct one-tube RT-PCR was performed with primers ToRSV-F-3 & ToRSV-R-1687 to amplify the partial ToRSV-CP fragment of 1684bp (Figure 3.4). The 1684bp PCR product was purified and cloned into the pDRIVE cloning vector. Recombinant clones were screened with colony PCR and positive clones were selected for sequencing.

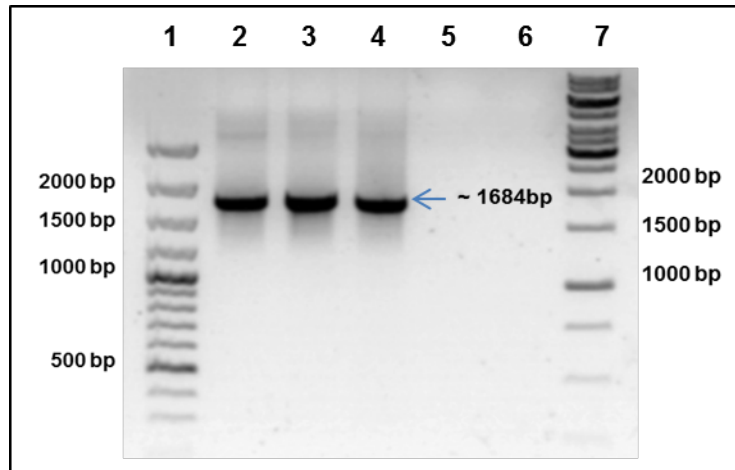


**Figure 3.4:** One-step RT-PCR to amplify partial ToRSV-CP fragment. Lane 1: 100bp+ DNA marker; Lanes 2: ToRSV positive control; Lane 3-4: 1684bp fragment amplified from ToRSV positive sources. Lane 5: Negative control; Lane 6: No template control; Lane 7: 1kb DNA ladder

Sequence results were subjected to BLAST (**B**asic **L**ocal **A**lignment **S**earch **T**ool; <http://blast.ncbi.nlm.nih.gov/Blast.cgi>) analysis to determine its homology to the ToRSV coat protein. The isolated sequence showed 98% homology to the coat protein gene of the grape yellow vein strain of ToRSV (Accession No. AF135411). Plasmid DNA containing the 1684bp CP fragment was used as template for PCR amplification of the full-length coat protein. A fragment of 1702bp was amplified comprising the ToRSV CP of 1689bp, the *Sa*I recognition sites of 12bp and the extra nucleotide incorporated into the forward primer to maintain the frame (Figure 3.5). The faint bands noted in lanes 3, 5 and 7 are probably due to product overflow as a result of the intensity of the amplified fragments.

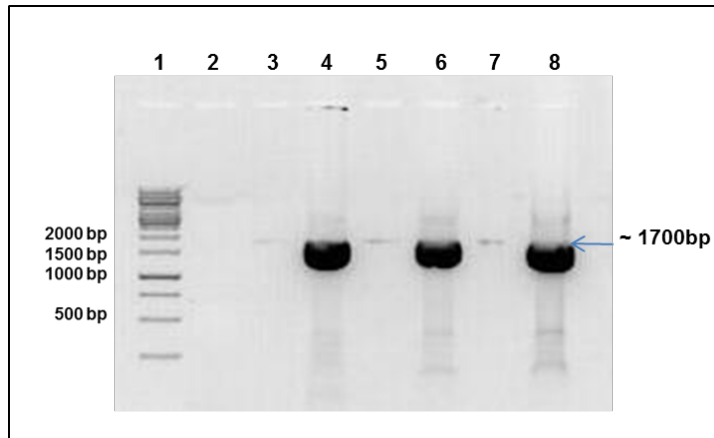


**Figure 3.5:** Amplification of the full-length ToRSV-CP. Lane 1: 1kb DNA marker; Lane 2: No template control; Lanes 3, 5 & 7: left blank; Lanes 4, 6 & 8: 1702bp fragment amplified

The 1702bp fragment was excised from the agarose gel, purified and cloned into the pDRIVE cloning vector. pDRIVE:ToRSV-CP constructs were digested with the *Sa*I restriction enzyme to further confirm the positive transformation. Eight of the ten plasmids digested, confirmed a positive cloning result, with the pDRIVE vector at ~4kb and the ToRSV insert at ~ 1.7kb (Figure 3.6). Positive clones were subsequently used for cloning into the pGEX-6P2 vector for expression studies.

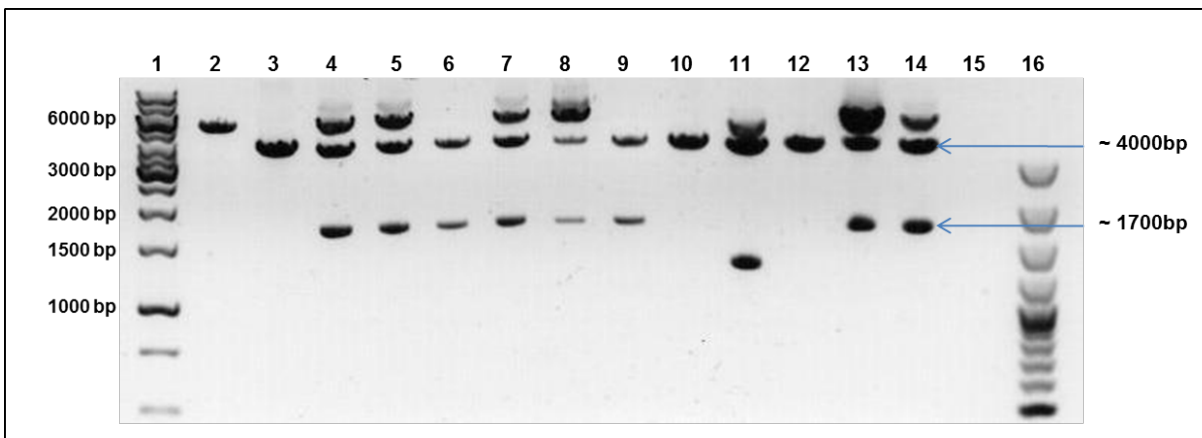


**Figure 3.6:** Restriction digest of pDRIVE:ToRSV-CP construct with *Sa*I enzyme. Lane 1: 1kb DNA marker; Lane 2: pDRIVE vector, uncut; Lane 3: pDRIVE vector, digested; Lanes 4-9 & 11-14: pDRIVE-ToRSVcp constructs, digested; Lane 10: Negative control; Lane 15: blank; Lane 16: 100bp+ DNA marker

Sequencing results also confirmed that the coat protein was cloned correctly with the *SalI* restriction enzyme and the extra nucleotide inserted at the 5' end (Figure 3.7).

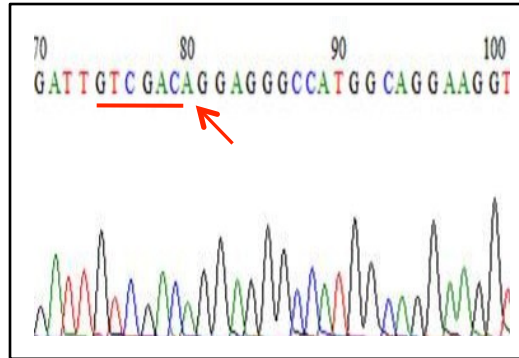


**Figure 3.7:** Sequencing result of the pDRIVE:ToRSV-CP construct showing the *SalI* sequence (underlined) and the extra 'A' nucleotide that was inserted to maintain the reading frame.

### 3.3.2 Expression of the ToRSV-CP gene using the GST gene fusion system

The ToRSV CP gene was cloned into pGEX-6-P2 by *SalI* digestion. The sub-cloning into pGEX6P2 was non-directional and orientation was confirmed with restriction digests and PCR using pGEX and ToRSV-*SalI* primers. Two of the six clones analysed tested positive consistently for the forward orientation with the different primer combinations used (Figure 3.8). Orientation was further confirmed by sequencing and these plasmids were transformed into KRX cells for recombinant protein expression.

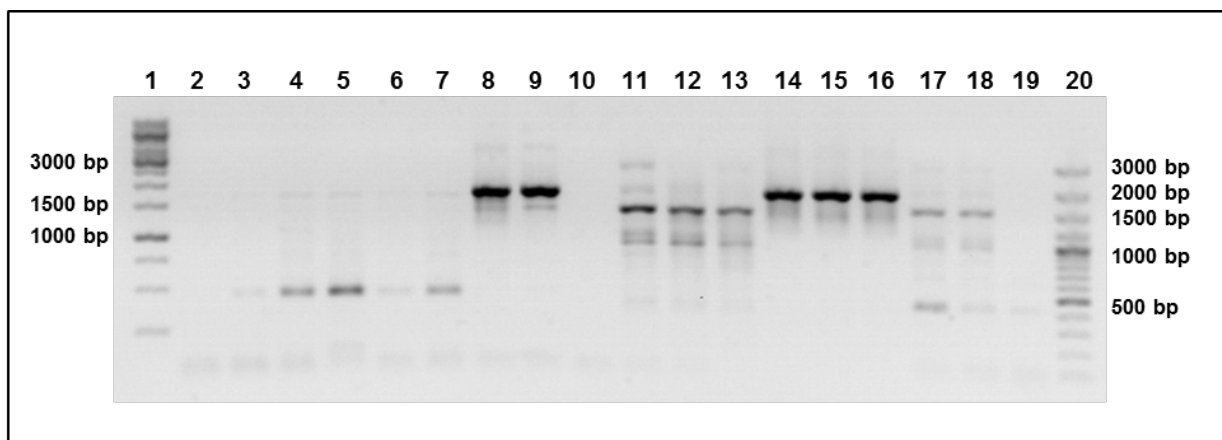


**Figure 3.8:** Orientation screening of recombinant clones by PCR using primers pGEX-F and ToRSV-*SalI*-R (lanes 2-10) and primers pGEX-F and ToRSV-*SalI*-F (lanes 11-19). Lane 1: 100bp plus DNA marker. Lanes 2-19: Recombinant clones. Lane 20: 1kb DNA marker. Clones in the correct orientation should yield a band of ~1800bp with the first primer set (as seen in lanes 8 and 9) and not with the second primer set (as seen in lanes 17 and 18).

The size of the GST:ToRSV-CP fusion protein was estimated to be 85kDa, with the GST tag being 26kDa and the ToRSV-CP predicted to be 59kDa in size. KRX competent cells were used for protein expression. This cell line, prepared from the KRX strain according to a modified procedure (Hanahan, 1985), is an *E. coli* K12 derivative that has engineered attributes to optimise controlled protein expression. KRX incorporates a chromosomal copy of the T7 RNA polymerase gene driven by the rhamnose promoter ( $rhaP_{BAD}$ ) to provide robust control of recombinant protein expression (Figure 3.9).

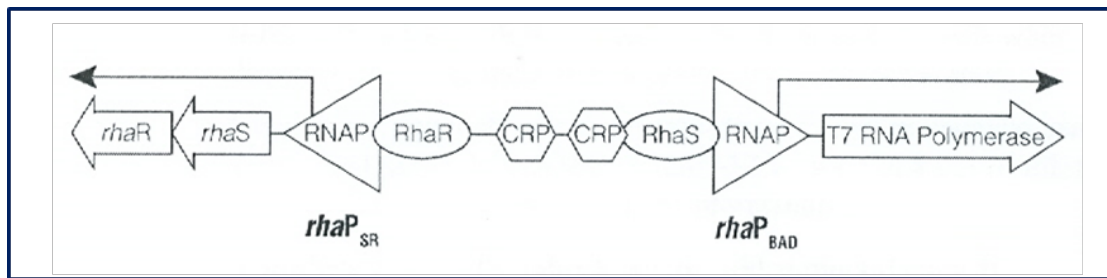


**Figure 3.9:** Rhamnose control of T7 RNA Polymerase in KRX cells. Expression of T7 RNA polymerase is controlled by the  $rhaP_{BAD}$  promoter. This promoter undergoes catabolite repression by glucose and is activated by the addition of rhamnose. In addition, rhamnose induces the activator RhaR, resulting in the production of active RhaS. In turn, RhaS bind to rhamnose activating transcription from  $rhaP_{BAD}$ . [from Promega Technical Bulletin, Part# TB352]

Initially expression was performed by inducing cultures overnight with 0.1% (w/v) rhamnose, but no expression was noted in the induced cultures in lanes 7 or 8 below (Figure 3.10).

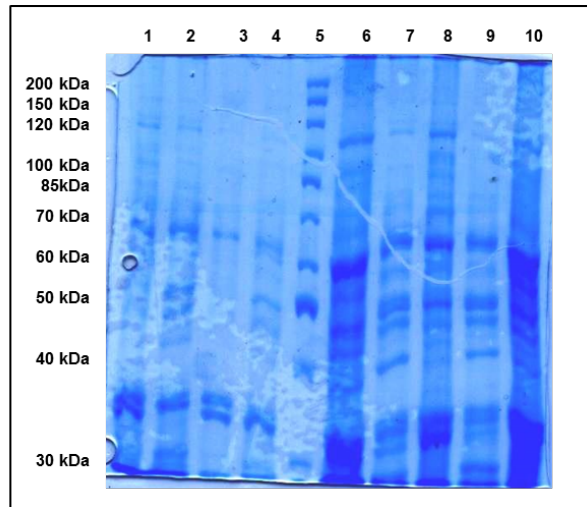


**Figure 3.10:** SDS-Page analysis of GST:ToRSV-CP fusion protein. Lane 5: Unstained protein ladder. Lanes 1-4: Uninduced insoluble (1) and soluble (2) fractions of pGEX-6P-2 without the fusion protein and uninduced insoluble (3) and soluble (4) fractions of the expressed GST:ToRSV-CP. Lane 6: Total cell protein. Lanes 7-10: Induced insoluble (10) and soluble (9) fractions of vector and soluble (7) and insoluble (8) fractions of the expressed fusion protein.

The protocol was then adjusted as follows: a) induce with 0.1% (w/v) rhamnose, (b) induce with 0.1% (w/v) rhamnose + 1mM IPTG, and (c) induce with no sarkosyl, sarkosyl at 0.5% (w/v) and sarkosyl at 1% (w/v) (Figures 3.11 and 3.12). It made no difference whether rhamnose was used alone or in conjunction with IPTG and the different sarkosyl concentrations also showed to have no real impact. It was noted however that protein was mostly expressed in insoluble form.

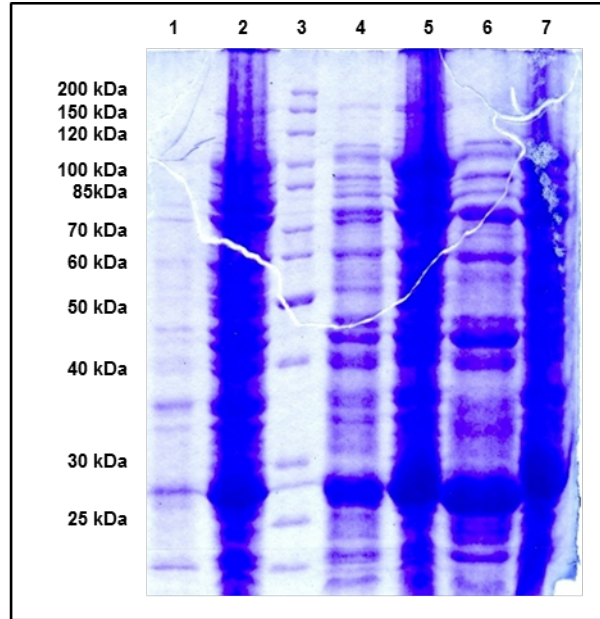


**Figure 3.11:** SDS-Page analysis of GST:ToRSV-CP fusion protein with different parameters. Lane 1: Uninduced fusion protein, soluble. Lane 2: Uninduced fusion protein, insoluble. Lane 3: Unstained protein ladder. Lane 4: Induced fusion protein (+ rhamnose, + IPTG, no sarkosyl), soluble. Lane 5: Induced fusion protein (+ rhamnose, + IPTG, no sarkosyl), insoluble. Lane 6: Induced fusion protein (+ rhamnose, + IPTG, 0.5% sarkosyl), soluble. Lane 7: Induced fusion protein (+ rhamnose, + IPTG, 0.5% sarkosyl), insoluble.

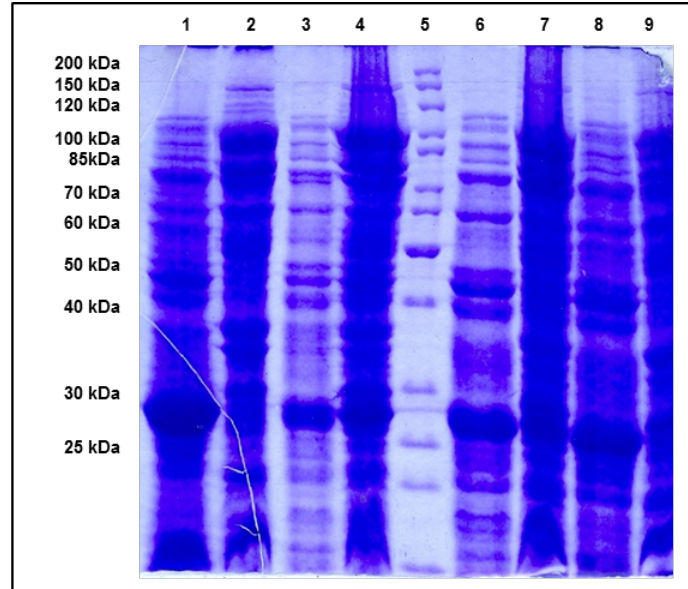


**Figure 3.12:** SDS-Page analysis of GST:ToRSV-CP fusion protein with different parameters. Lane 1: Induced fusion protein (+ rhamnose, + IPTG, 1% sarkosyl), soluble. Lane 2: Induced fusion protein (+ rhamnose, + IPTG, 1% sarkosyl), insoluble. Lane 3: Induced fusion protein (+ rhamnose, no sarkosyl), soluble. Lane 4: Induced fusion protein (+ rhamnose, no sarkosyl), insoluble. Lane 5: Unstained protein ladder. Lane 6: Induced fusion protein (+ rhamnose, 0.5% sarkosyl), soluble. Lane 7: Induced fusion protein (+ rhamnose, 0.5% sarkosyl), insoluble. Lane 8: Induced fusion protein (+ rhamnose, 1% sarkosyl), soluble. Lane 9: Induced fusion protein (+ rhamnose, 1% sarkosyl), insoluble.

Other parameters tested were a) increase rhamnose concentration to 0.25% (w/v), (b) induce with 0.25% (w/v) rhamnose + 1mM IPTG, (c) remove 10ml of culture hourly for four hours and leave rest of culture overnight. Again, no noticeable difference was seen between uninduced and induced cultures with any of the implemented changes (results not shown) and it was decided to proceed with 0.1% (w/v) rhamnose only.

It was then decided to adapt the lysis buffer (1X STE buffer) by the addition of 0.2mg/ml of lysozyme. Lysozyme is an enzyme with the ability to break down bacterial cell walls to improve protein or nucleic acid extraction efficiency. For purification of inclusion bodies, lysozyme is added to digest cell debris and release the inclusion bodies. The enzyme is easily eliminated with other proteins during fusion tag-specific affinity purification of the target recombinant protein.

The addition of lysozyme to the buffer resulted in a sharper gel with more defined bands – however, no distinction was noted between the uninduced and induced cultures (Figure 3.13).

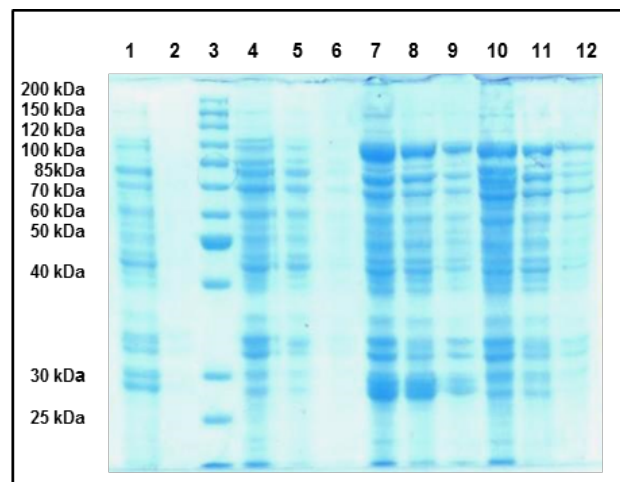


**Figure 3.13:** SDS-Page analysis of GST:ToRSV-CP fusion protein with lysozyme added to lysis buffer. Lane 3: Unstained protein ladder. Lanes 1-2: Uninduced soluble and insoluble fractions of pGEX-6P2. Lanes 4-6: Uninduced TCP, soluble and insoluble fractions of the fusion protein. Lanes 7-9: Induced TCP, soluble and insoluble fractions of pGEX-6P-2. Lanes 10-12: Induced TCP, soluble and insoluble fractions of the fusion protein.

As a final attempt, a protease inhibitor was added to the lysis buffer. Protease inhibitors acts by blocking or inactivating endogenous proteolytic enzymes that are released from subcellular compartments and would otherwise degrade proteins of interest and their activation states. SDS-Page analysis was performed using lysis buffer containing lysozyme and protease inhibitor cocktail. Western Blot analysis was performed but after 30 minutes of exposure no signal was visible on the blot. Western Blot analysis was performed using both the anti-GST antibody and ToRSV-specific IgG (obtained from the Bioreba ELISA kit) as primary antibody but no signal was detected (data not shown).

### **3.3.3 Agrobacterium-mediated transient expression of the ToRSV-CP gene**

To enable cloning into the pBIN61S vector the GST-ToRSV-CP fragment of 2.5kb was firstly cloned into pDRIVE. The plasmid DNA was digested with the restriction enzymes *Xba*I and *Sac*I to facilitate cloning into the pBIN61S vector.

The experiment was repeated various times with different DNA concentrations and using different conditions, but no digestion occurred. We then examined the pDRIVE:GST-ToRSV-CP sequence and discovered that the GST-ToRSV-CP fragment was cloned in the reverse orientation into the pDRIVE vector – this rendered the *Xba*I restriction endonuclease sensitive to *E.coli* K-12 Dam methylation. The methylase encoded by the *dam* gene (Dam methylase) transfers a methyl group from S-adenosylmethionine to the N<sup>6</sup> position of the adenine residues in the sequence GATC. Certain sites for restriction endonucleases may be resistant to cleavage when isolated from strains expressing the Dam methylases, which is the case with *Xba*I.

The plasmid DNA was subsequently transformed into a non-methylated strain of *E.coli* where after the 2.5kb fragment was digested with *Sac*I/*Xba*I digestion (Figure 3.14) and excised from the gel to be cloned into pBIN61S.

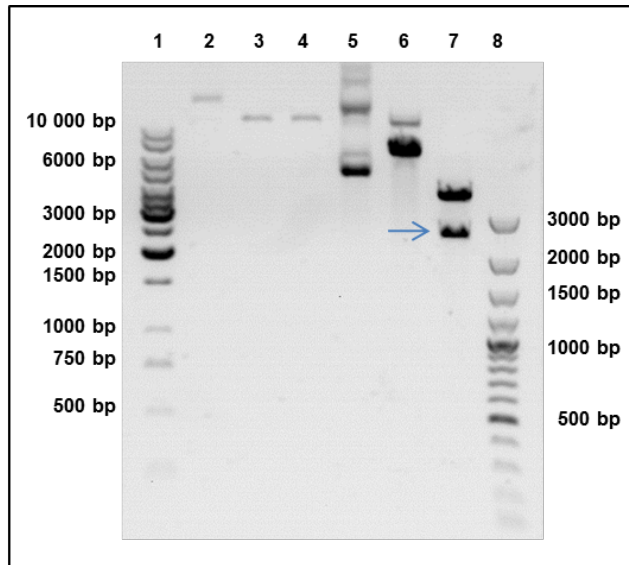


**Figure 3.14:** Restriction digest of the pDRIVE:GST-ToRSV-CP fragment with *SacI* and *XbaI* enzymes to facilitate cloning into pBIN61S vector. Lane 1: 1kb DNA ladder. Lane 2: pBIN61S vector uncut. Lane 3: Vector DNA, digested with *SacI*. Lane 4: Vector DNA, digested with *XbaI*. Lane 5: Insert DNA, uncut. Lane 6: Insert DNA digested with *SacI*. Lane 7: Insert DNA digested with *XbaI* showing 2.5kb fragment (indicated by arrow).

The successful cloning of the 2.5kb GST-ToRSV-CP fragment into the pBIN61S vector was confirmed with colony PCR and restriction digests. For restriction digests, the pBIN61S:GST-ToRSV-CP-*SacI/XbaI* sequence was loaded into NEBcutter for restriction enzyme selection and *EcoRI* and *Sall* were chosen. *EcoRI* should yield a band pattern of 523bp, 1421bp and 12984bp after digestion and *Sall* a pattern of 35bp, 1693bp and 13200bp (Figure 3.15).

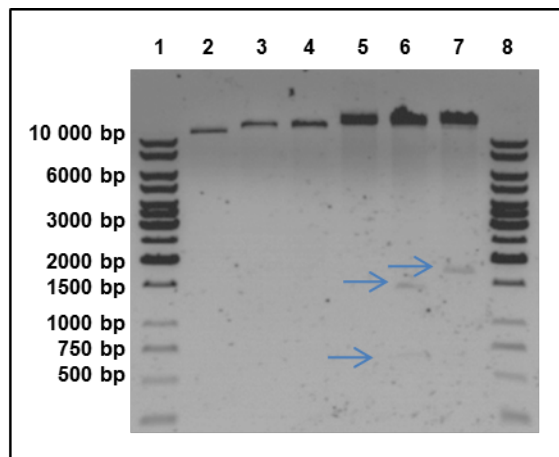


**Figure 3.15:** Restriction digest of the pBIN61S:GST-ToRSV-CP fragment with *EcoRI* and *Sall* enzymes to confirm successful cloning. Lanes 1 & 8: 1kb DNA ladder. Lane 2: pBIN61S uncut. Lanes 3-4: pBIN61S digested with *EcoRI* and *Sall*. Lane 5: pBIN61S:GST:ToRSV-CP uncut. Lane 6: Construct digested with *EcoRI* showing the expected bands at ~523bp and ~1423bp (indicated with arrows). Lane 7: Construct digested with *Sall* with the arrow indicating the band at ~1693. The band of 35kb is too small to be seen on the gel.

The pBIN61S:GST-ToRSV-CP constructs were subsequently transformed into *Agrobacterium* using electroporation and tobacco leaves were infiltrated with the bacterial culture. After 3-5dpi definite areas of chlorosis (infiltration) could be seen in the infiltrated plants (A-C) whilst the control plants (D-E) showed no change (Figure 3.16). At 7dpi, leaves with areas of definite infiltration were removed and subjected to TPIA and SDS-page analysis to determine if expression occurred.

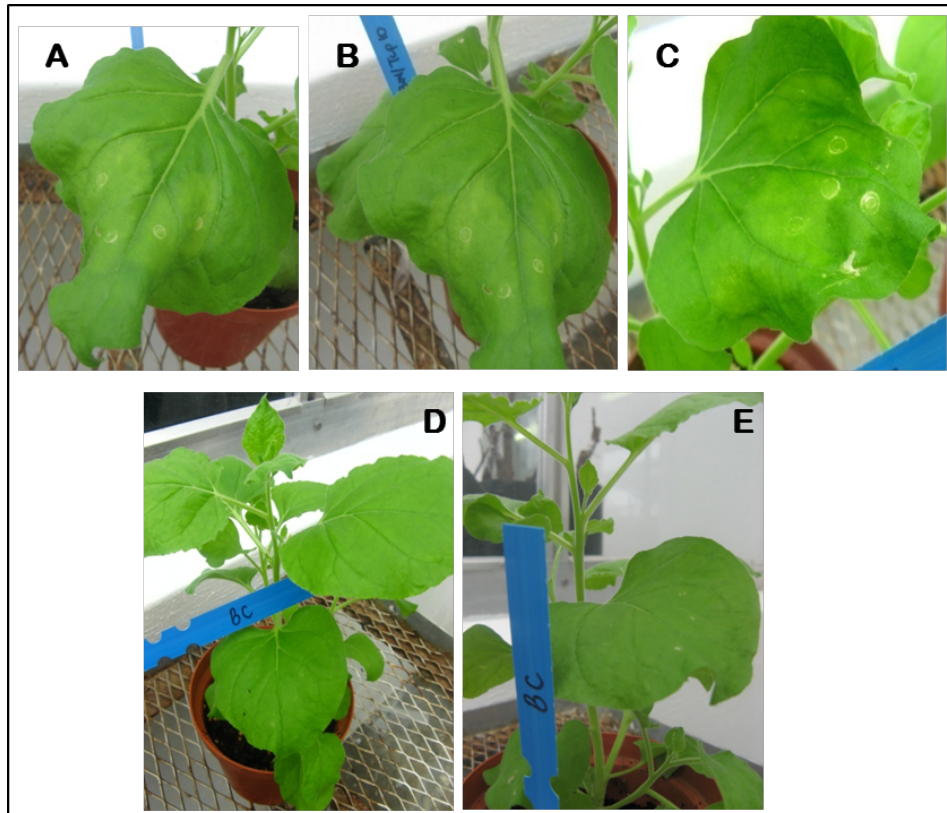


**Figure 3.16:** *N. benthamiana* plants infiltrated with *Agrobacterium* transformed with the pBIN61S:GST-ToRSV-CP construct. **A-C:** Leaves infiltrated with transformed *Agrobacterium* culture. **D-E:** Negative control – leaves infiltrated with re-suspension solution.

Transient expression was determined at 7dpi with a tissue-print immune assay that detects the presence of ToRSV. The epidermis of the abaxial side of the leaf was removed and the exposed mesophyll tissue was incubated with ToRSV-ch (*Tomato ringspot virus*-Chickadee strain) antibodies which react specifically with the grape yellow vein strain of ToRSV. Plants infiltrated with the *Agrobacterium* culture containing the

pBIN61S:GST-ToRSV-CP construct showed a definite reaction which means that ToRSV was detected and expression was possibly successful (Figure 3.17; 2&3). Negative control plants showed no reaction to the ToRSV antibodies (Figure 3.17; 1).

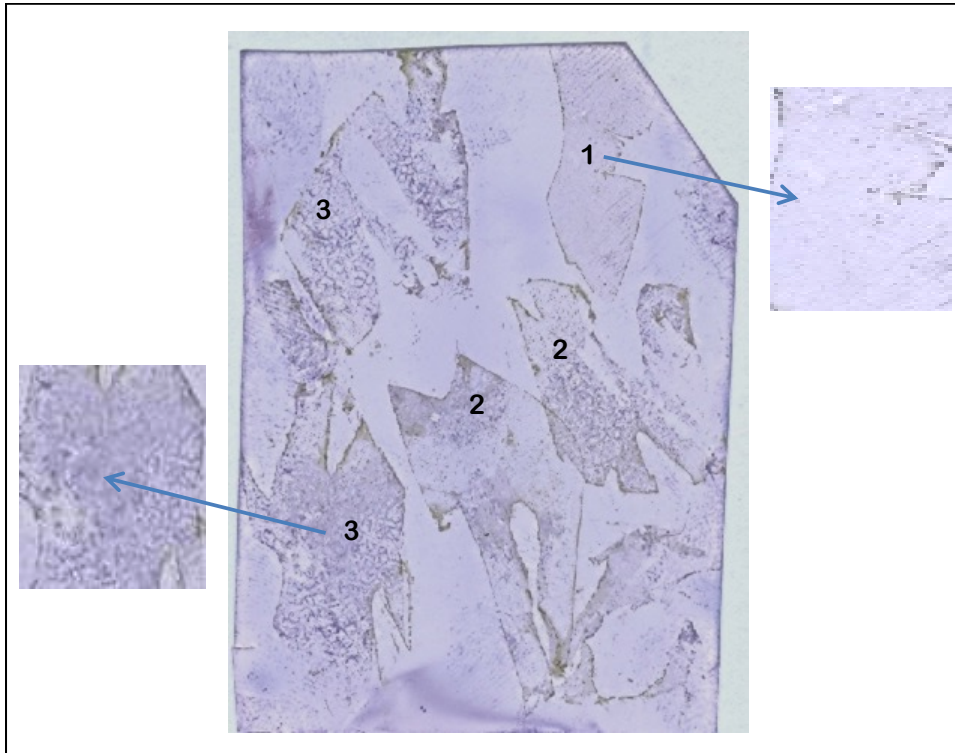


**Figure 3.17:** TPIA results for the mesophyll tissue of *N.benthamiana* after agroinfiltration. **1:** Negative control shows no reaction to the ToRSV antibodies. **2-3:** Leaves infiltrated with *Agrobacterium* containing the pBIN61S:GST-ToRSV-CP construct shows a definite reaction to the antibodies, indicating the presence of ToRSV.

Transient expression was further confirmed with SDS-Page analysis. Infiltrated leaf samples were macerated in a sample extraction buffer and analysed on a 10% polyacrylamide gel. The GST-ToRSV-CP fragment should yield a band of approximately 85kDa. In the gel below (Figure 3.18), a band in the region of 85kDa is seen in three of the four infiltrated leaf samples. In the negative control samples, no band of 85kDa is noted.

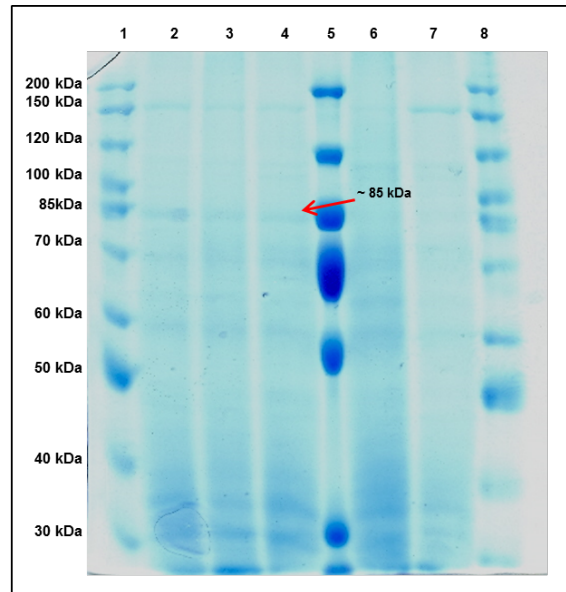


**Figure 3.18:** SDS-Page analysis of *N.benthamiana* after agroinfiltration on a 10% polyacrylamide gel.. Lanes **1 & 8**: Unstained Protein ladder. Lanes **2-4, 6**: Leaves infiltrated with *Agrobacterium* containing the pBIN61S:GST-ToRSV-CP construct. Lane **5**: Prestained Protein ladder Lane **7**: Negative control – leaves infiltrated with buffer only.

The samples were also analysed on an 8% (w/v) polyacrylamide gel and a ToRSV positive control (ToRSV-ch positive control, Bioreba) was included (Figure 3.19A). Very faint bands in the region of 85kDa was noted on the gel but when analysed with Western Blot no signal was detected even after six hours incubation - instead a multiple band pattern was observed (Figure 3.19B).

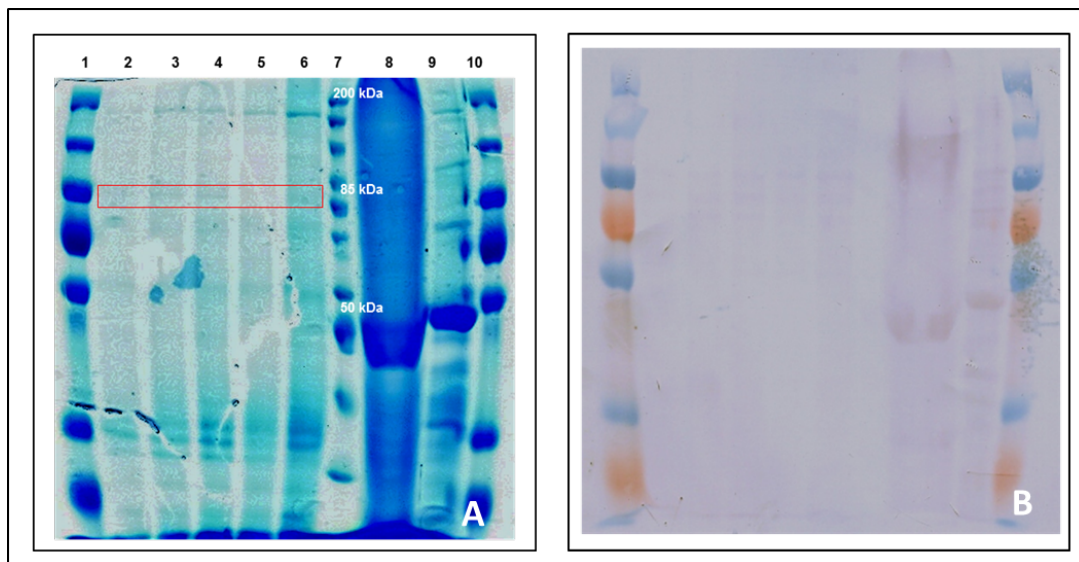


**Figure 3.19:** (A) SDS-Page analysis of *N.benthamiana* after agroinfiltration on a 8% polyacrylamide gel. Lanes 1 & 10: Prestained protein ladder. Lanes 2 – 6: Leaves infiltrated with *Agrobacterium* containing the pBIN61S:GST-ToRSV-CP construct. Lane 7: Unstained Protein ladder. Lane 8: ToRSV-ch positive control. Lane 9: Negative control, crude leaf extract of *N. benthamiana*. (B) Western Blot analysis of 8% polyacrylamide gel

Further analysis on a 10% (w/v) polyacrylamide gel to detect the GST fragment of the fusion protein was also unsuccessful (Figure 3.20).

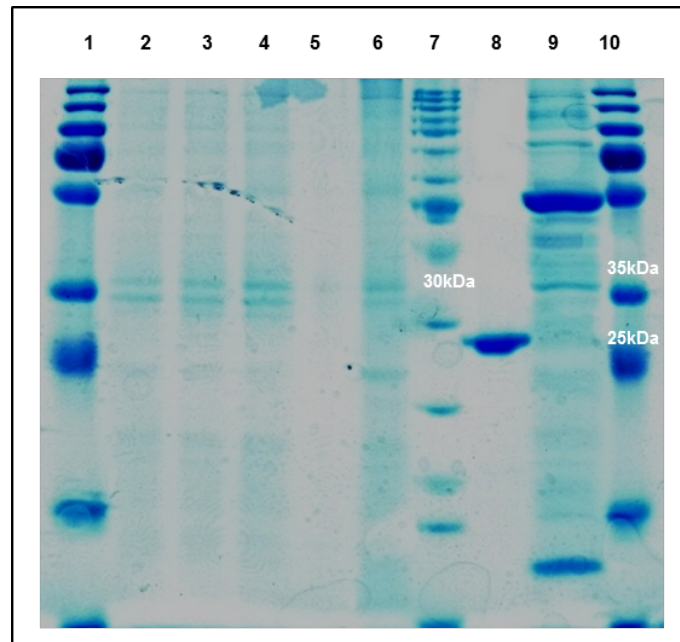


**Figure 3.20:** 10% polyacrylamide gel to detect the GST fragment of the fusion protein. Lanes 1 & 10: Prestained protein ladder. Lanes 2 – 6: Leaves infiltrated with *Agrobacterium* containing the pBIN61S:GST-ToRSV-CP construct. Lane 7: Unstained Protein ladder. Lane 8: rGST positive control (supplied with detection kit). Lane 9: Negative control, *N. benthamiana*.

### 3.4 Discussion

The Grape yellow vein (GYV) strain of ToRSV occurs naturally in grape and is typically found in the western region of the United States of America (USA). Since the ToRSV-infected material received originated from the USA the GYV strain sequence was used for primer design and as a result the ToRSV-CP was amplified successfully. It has been shown that the sequence of the GYV strain differs significantly from the other strains of ToRSV and when aligned almost no homology existed between base pairs 1 to about 70. Wang and Sanfaçon (2000) showed that the GYV strain shared 78 to 81% sequence similarity with raspberry and peach isolates and presented the first molecular data suggesting that GYV is a unique strain that differs from ToRSV strains from other hosts. This is consistent with serological data from Bitterlin and Gonsalves (1988) which classified a peach and raspberry isolate into the same serogroup (serogroup c) whereas GYV was classified in a distinct serogroup (serogroup b). ELISA assay tests between the two serogroups showed little or no cross reactivity.

The expression of the ToRSV coat protein was investigated using two systems – the GST Gene Fusion system and agroinfiltration. The GST gene fusion expression was not successful as inadequate soluble protein expression prevented the completion of the assay. Several factors known to improve protein expression were tested including the use of IPTG in addition to rhamnose but was not successful. Although a difference was noted between uninduced and induced cultures of the fusion protein no definite expression of the 85kDa fusion protein was obtained despite numerous parameters being investigated.

For the initial confirmation of transient expression, tissue print immunoassay (TPIA) using ToRSV-ch antibody was used for the detection of ToRSV gene expression and a clear difference was noted between areas infiltrated with pBIN61S:GST-ToRSV-CP and negative control areas. SDS-Page analysis was used for further confirmation of transient expression. Infiltrated patches of tobacco leaves were analysed on a 10% SDS-Page gel and a band of 85kDa, which is the size of the GST-ToRSV-CP construct

were obtained. However, this band was very faint and other non-specific bands were also visible on the gel. Further SDS-Page and Western Blot analysis gave inconclusive results and it cannot be confirmed with certainty that the GST-ToRSV-CP was successfully expressed.

As the ToRSV-CP gene could not be expressed using the GST gene fusion system and only at very low levels using Agroinfiltration it may be possible that the fusion protein was toxic and interfered with cellular proliferation and differentiation of the host cells. The expression of recombinant proteins induces a metabolic burden on the host cells causing cellular stress and a considerable decrease in generation time (Bentley *et al.*, 1990; Carneiro *et al.*, 2013).

Another possible reason for the low levels of expression of the ToRSV-CP gene could be due to the protein being expressed in insoluble form. Insoluble protein expression can be due to various reasons, including rapid overexpression of the protein under the control of strong bacterial promoters (Weickert *et al.*, 1996; Lilie *et al.*, 1998) and the absence of certain posttranslational modifications such as phosphorylation (Lee *et al.*, 2004). One of the major problems during protein overexpression in *E. coli* that results in the formation of inclusion bodies is protein misfolding. Different methods have been used to solve this, such as refolding of proteins after dissolving inclusion bodies in denaturing reagents (Guise *et al.*, 1996) and enhancing protein folding by culturing cells at low temperature (Mukhopadhyay 1997). Chen *et al.*, (2002) described a method where the cell culture is simply heat-shocked prior to protein induction, which results in the enhancement of the solubility and yield of the overexpressed protein in *E. coli*.

It has also been shown that expressing proteins with a non-peptide fusion tag can increase solubility (Dyson *et al.*, 2004; Chen *et al.*, 2005), prevent proteolysis (Tang *et al.*, 1997) and improve protein yield (Sun *et al.*, 2005). The reason for this however remains unclear and several hypotheses have been proposed (Raran-Kurussi and Waugh, 2012). In this study, glutathione S-transferase (GST) was used as affinity tag as part of the GST gene fusion system mainly because it provided a complete and simple approach for expression, purification and detection of the fusion protein. The expression

of foreign proteins fused to GST is a popular system and have been used successfully in the past (Smith and Johnson, 1988). In spite of this, the GST fusion proteins are at times expressed at low levels and may also be insoluble and difficult to purify (Frangioni and Neel, 1993; Park *et al.*, 2009). The protocol of Mercado-Pimentel *et al.* (2002) used in this study suggests the use of sarkosyl in the lysis buffer to increase solubilisation when using GST as affinity tag. Sarkosyl is thought to help solubilise the protein by partially denaturing it (Frankel *et al.*, 1991) – different sarkosyl concentrations were tested to determine which gave the best solubility but again it made no difference to the expression of the fusion protein. This may indicate that solubilisation of the fusion problem was not the reason for no expression.

The stability of a particular fusion protein can also show large differences among different strain backgrounds as different laboratory strains of *E. coli* differ a good deal in the levels and types of proteases that are produced. Although a wide variety of *E. coli* host strains are available for cloning and expression with the pGEX vectors, there are specially engineered strains which are more suitable that may increase expression of full-length fusion proteins. Strains such as Lon, OmpT, DegP or HtpR, which are deficient in known cytoplasmic protease gene products, may aid in the expression of fusion proteins by minimizing the effects of proteolytic degradation by the host (Baker *et al.*, 1984; Grodberg & Dunn, 1988). In this study, single step KRX competent cells prepared from the KRX strain, an *E.coli* K12 derivative was used. KRX strains have several attributes that makes it a good expression strain including the ompT- and ompP- mutations that eliminates proteolysis of overexpressed protein.

Transient expression of the GST-ToRSV-CP fusion seems to have been more successful as a positive result was obtained with TPIA. However, when SDS page analysis was conducted, only a faint band was observed which was not detected with Western Blot analysis. So although it seems that expression did occur, it was at a very low level, which indicates that the protocol should be upscaled and optimized to increase expression - due to time constraints this could not be attempted with this study. The success of a transient assay is dependent on various factors including the the physiological condition of the plants and the stress incurred on the plant as a result of

infiltration and all of these have to be considered when optimising an transient expression strategy. The virulence factor of a specific *A. tumefaciens* strain was also shown to have an influence on the transformation and efficiency of foreign gene expression (Santos-Rosa *et al.*, 2008) and it may be feasible to test a different strain in order to increase expression. Agrobacterium can also be applied using vacuum infiltration where whole leaves or the entire plant can be infiltrated at once. Arzola *et al.* (2011) applied vacuum-infiltration to transiently transform the leaves of *Nicotiana benthamiana* plants and successfully expressed a novel antrax receptor decoy protein in these plants. Their study also demonstrated that the co-expression of certain suppressor proteins effectively increased the expression level of the recombinant protein by suppressing the post-transcriptional gene silencing mechanism of *N. benthamiana*.

In theory, the process for obtaining a recombinant protein seems simple and straightforward but in practice a myriad of things can go wrong making it evident that protein expression is challenging with each approach presenting its own obstacles and limitations.

## CHAPTER 4

---

### Diagnostic assay for the detection of *Grapevine fanleaf virus*

#### 4.1 Introduction

*Grapevine fanleaf virus* (GFLV) is the causal agent of grapevine fanleaf degeneration which is one of the most widespread and damaging viral diseases of grapevine affecting the production of grapes worldwide (Andret-Link *et al.*, 2004). Discovered in 1960 by Cadman *et al.*, the virus causes a wide range of symptoms resulting in a general decline of vines with reduced yields as high as 80% being reported (Bovey, 1973; Martelli and Savino, 1990).

GFLV is a member of the genus *Nepovirus* in the family *Secoviridae* and is at present the only nepovirus that is known to occur in South Africa. GFLV is not yet a major threat to the South African wine industry as the virus is mostly confined to the Breede River Valley region in the Western Cape, due to the presence of its ectoparasitic nematode vector, *Xiphinema index*. The implementation of accurate certification schemes and quarantine procedures has led to a considerable reduction in the distribution of the virus among propagation material but effective strategies are still necessary for GFLV control in naturally infected vineyards.

The bipartite genome of GFLV is composed of two single-stranded, positive-sense RNAs, named RNA-1 and RNA-2 (Pinck *et al.*, 1988). Due to the absence of proof-reading ability associated with the RNA-dependent RNA polymerase (RdRp), encoded in the RNA 1, there is great potential for genetic variability within the GFLV genome. The genetic diversity of the GFLV genome has been studied extensively (Naraghi-Arani *et al.* 2001; Vigne *et al.*, 2004; Pompe-Noak *et al.*, 2007), thereby verifying the quasi-species nature of the virus. To date, the full genome sequence of RNA-1 and RNA-2 are only available for five GFLV strains in the Genbank database, with two of these being

South African isolates namely GFLV-SACPS3 (Lamprecht *et al.*, 2012) and GFLV-SACH44 (Lamprecht *et al.*, 2013).

Diagnostic techniques for the detection of GFLV have evolved throughout the years. These methods include biological indexing (Habibi *et al.*, 1992), ELISA (Huss *et al.*, 1986; Walter and Etienne, 1987), RT-PCR (Fattouch *et al.*, 2001; Wetzel *et al.*, 2002) and microarrays (Engel *et al.*, 2010). While biological indexing and ELISA are still being used mainly in research environments, more commercial laboratories are moving toward molecular methods for grapevine virus detection. Molecular methods proved to be more sensitive than biological assays and serology and the introduction of quantitative (real-time) PCR (qPCR) assays have made further progress in the rapid and specific detection of viruses (Osman *et al.*, 2008). The combination of speed, sensitivity and specificity has established the popularity of qPCR in grapevine virus diagnostics (Bertolini *et al.*, 2010; Cepin *et al.*, 2010; Pacifico *et al.*, 2011; Osman *et al.*, 2013) in recent years.

The objective of this chapter was to develop a qPCR assay based on SYBR green technology for the rapid and reliable detection and relative quantification of GFLV. The assay was based on a conserved region of the RNA-2 genome and in order to achieve this, the complete sequence of the RNA-2 of a South African grapevine isolate was generated.

## 4.2 Materials and Methods

### 4.2.1 Cloning and sequencing of the RNA2 from a South African isolate of GFLV

#### 4.2.1.1 RNA isolation

GFLV-Vak7 was sampled from a grapevine plant (*Vitis vinifera* cv Chenin blanc) established at the Plant Quarantine facility of DAFF in Stellenbosch. Total RNA was isolated from leaf material using a CTAB extraction protocol (White *et al.*, 2008) as described in Chapter 3, section 3.2.2. The concentration and purity of the extracted RNA was verified with a NanoDrop® ND-1000 spectrophotometer and the quality analysed on a 1% (w/v) TBE agarose gel stained with EtBr. The RNA samples were stored at -80 °C.

#### 4.2.1.2 Primer design and RT-PCR

A multiple sequence alignment was constructed from the 82 available full-length GFLV RNA2 sequences retrieved from GenBank using CLC Genomics Workbench 6.7.1 (<http://www.clcbio.com>). From the alignment a consensus sequence of 3529bp was generated. Primers for sequencing were designed to generate amplicons of approximately 1kb with a 200bp overlap, using OligoExplorer software. This strategy allows for the overlapping fragments to be assembled into one contiguous sequence covering the entire genome. Four sets of primers were generated starting from base pairs 117 to 3481 (Table 4.1). The program could not design primers that met the specified criteria in the regions spanning base pairs 1-116 and 3482-3529, and these regions were therefore omitted.

**Table 4.1:** Characteristics of primers used for sequencing

Primer	Sequence 5' – 3'	T <sub>m</sub> (°C)	%GC	Region (bp)
Seq_1-fwd	CCG CCA AAC TGT TAA GGA G	53.6	52.6	117-1119
Seq_1-rev	AGT CGG AAT ACC ATT GAG C	52.0	47.3	
Seq_2-fwd	AGG GTC AGC ACA TCA GTA G	53.9	52.6	835-1836
Seq_2-rev	TCC TCT ACC AGC TAA TCC TC	52.7	50	
Seq_3-fwd	TAC TGG AAC CCC TGA AGC AAG	56.8	52.3	1623-2691
Seq_3-rev	AGG CGT TCG GTG ATA TGG AG	56.9	55	
Seq_4-fwd	AAT GGT TGG CAC TAC TAA GG	52.2	45	2442-3481
Seq_4-rev	CCA AAG GAC AAA CAA CAC AC	52.4	45	

T<sub>m</sub> – melting temperature

The four primers sets were initially tested with one-step reverse transcription PCR (RT-PCR) using a gradient of annealing temperatures ranging from 45°C to 58°C, to determine the best temperature for amplification. One-step RT-PCR was performed using 400ng of isolated RNA as template. The standard reaction mixture, with a total volume of 20µl, contained 1X reaction buffer, 0.2mM dNTP mix, 0.4µM of each primer, 0.1U/µl of AMV RT and 0.05 U/µl of KAPA DNA polymerase. cDNA synthesis was carried out at 48°C for 30 minutes followed by one cycle of three minutes at 94°C, 35 cycles of 30 seconds at 94°C, 30 seconds at X°C and two minutes at 72°C, with a final elongation step of 10 minutes at 72°C. The PCR products were analysed by electrophoresis through 1% (w/v) TBE agarose gels stained with EtBr. The correct sized fragments were excised from the gel and the DNA recovered using the Zymoclean® Gel DNA Recovery kit according to the manufacturer's instructions.

#### 4.2.1.3 Cloning and plasmid DNA isolation

The purified PCR products were ligated into the pGEM<sup>®</sup>-T easy Vector with T4 DNA ligase (Promega). 2µl of the ligation mix was added to 50µl of chemically competent JM109 *E.coli* cells. The transformation reaction was incubated on ice for 20 minutes, heat shocked at 42°C for 45 seconds and transferred to ice for a further two minutes. 950µl of SOC medium was added to each reaction and incubated at 37°C for two hours, shaking at ~175rpm. 100µl of each transformation was plated onto LB agar plates containing Ampicillin (100µg/ml), IPTG (0.2mM) and X-gal (40µg/ml) for blue-white colony selection.

Recombinant colonies were screened by direct colony PCR using the relevant sequencing primers (Table 4.1) and M13 primers. Colonies that were confirmed positive were inoculated in 5ml LB broth containing 100µg/ml Amp and incubated overnight (37°C) with shaking (225 rpm) for subsequent isolation of plasmid DNA. Plasmid DNA was isolated using the GeneJet<sup>®</sup> Plasmid Miniprep kit (Fermentas) according to the manufacturer's instructions.

#### 4.2.1.4 Sequencing and Analysis

The purified fragments were quantified with a NanoDrop<sup>®</sup> ND-1000 spectrophotometer and sent for sequencing to the Central Analytical Facility (CAF) at Stellenbosch University (SU). Sequencing data were analysed using Geneious 6.1.6 (Biomatter; <http://www.geneious.com>). The South African GFLV isolates GFLV-SACH44 and GFLV-SAPCS3 were used for comparative analysis. Phylogenetic trees were constructed with MEGA5 analysis software (Tamura *et al.*, 2011) to determine if the generated sequence was related to known GFLV sequences from South Africa.

## **4.2.2 Relative quantification of GFLV by real-time PCR**

### **4.2.2.1 Sample collection and RNA isolation**

Grapevine leaf material was collected during November 2012 to April 2013 from infected vineyards in Robertson, infected plants in the SU Genetics department greenhouse and from the field and greenhouse at the DAFF Quarantine facility. Mostly young grapevine leaves displaying typical GFLV symptoms were chosen although in the infected Robertson vineyards, not all of the vines displayed symptoms. Fresh plant material was macerated with liquid nitrogen and stored at -80°C. Total RNA was isolated as described in Chapter 3 section 3.2.2. The assay was performed using 17 GFLV infected samples as well as a healthy grapevine sample which was also used as a negative control.

### **4.2.2.2 DNase treatment of RNA and cDNA synthesis**

After isolation, RNA samples were treated with RQ1 DNase (Promega) in the supplied buffer to avoid residual DNA contamination, followed by a phenol/chloroform extraction. An equal volume of elution buffer (10mM Tris-HCl, pH8.5) and phenol:chloroform (1:1) was added to each sample. Samples were mixed gently, centrifuged (16000g; 10 minutes; 4°C) and the top aqueous phase transferred to a new sterile centrifuge tube. To this, 2.5 volumes of absolute ethanol and 0.1 volumes of NaOAc (3M, pH 5.2) was added and incubated at -20°C for one hour. The sample was centrifuged at 16000g for 30 minutes at 4°C and the supernatant was removed. The pellet was washed with 1ml of 70% (v/v) ethanol to remove excess salt, air-dried on ice for 20 minutes and re-suspended in 15µl of DEPC-treated water.

DNase-treated RNA was converted to cDNA using AMV Reverse Transcriptase (Thermo Scientific). RNA (1µg) and random primers (Promega) were incubated in a 2720 Thermal Cycler (Applied Biosystems) for five minutes at 65°C and immediately placed on ice for two minutes. To this, 5X AMV RT buffer, 10mM dNTPs, 10U AMV Reverse Transcriptase and nuclease-free water were added to a final volume of 30µl. The reaction was then incubated at 48°C for one hour in a 2720 Thermal Cycler (Applied Biosystems). cDNA samples were stored at -20°C.

#### **4.2.2.3 Design of GFLV primers for real-time PCR analysis**

Primers were designed from the conserved coat protein region on the RNA-2 of the GFLV genome. A multiple sequence alignment was generated using 12 partial South African GFLV isolates (EU702440.1-EU702451.1), two full-length South African GFLV isolates (JF968121.1 & KC900163.1) and the partial South African GFLV isolate sequenced in 4.1.1 (GFLV-V7 RNA2). The resulting primer pair (Table 4.2) was subjected to a BLAST analysis against all the available GFLV sequences in Genbank to ensure its specificity.

**Table 4.2:** Characteristics of primers used for real-time PCR

Set	Primer	Sequence 5' – 3'	T <sub>m</sub> (°C)	%GC	Genomic position
1	GFLVq C-fwd	TGA CGG GTA ACA ACA AAG AG	52.5	45.0	2522-2541; CP gene
	GFLVq C-rev	CTG GGT CGA AAA CCA AAG T	52.9	47.3	2635-2617; CP gene
2*	Actin-fwd	CTT GCA TCC CTC AGC ACC TT	61.5	55	n/a
	Actin-rev	TCC TGT GGA CAA TGG ATG GA	61.1	50	n/a
3*	UBC-fwd	GAG GGT CGT CAG GAT TTG GA	61.2	55	n/a
	UBC-rev	GCC CTG CAC TTA CCA TCT TTA AG	60.3	48	n/a
4*	GAPDH-fwd	TTC TCG TTG AGG GCT ATT CCA	60.9	48	n/a
	GAPDH-rev	CCA CAG ACT TCA TCG GTG ACA	60.9	52	n/a

T<sub>m</sub> – melting temperature; \* Primer sequences obtained from Reid *et al.*,(2006)

#### 4.2.2.4 Optimisation of the real-time PCR assay

cDNA samples were amplified by real-time PCR using the SensiFAST SYBR No-ROX Kit (Bioline). All experiments were performed on the Qiagen Rotor-Gene Q thermal cycler. Each reaction was performed in triplicate and consisted of 1X SensiFast mastermix, forward and reverse primers at a final concentration of 0.4µM, 100ng of cDNA and DEPC-treated water to a final volume of 20µl. Real-time PCR cycling conditions were as follows for all genes tested: initial denaturation for two minutes at 95°C; 40 cycles of five seconds at 95°C, annealing for 10 seconds at 60°C and elongation for 15 seconds at 72°C. Acquisition on the green channel was recorded at the end of the extension step. A melt curve analysis of the PCR amplicons was included from 65°C to 95°C with a 0.1°C increase in temperature every two seconds. A non-template control was included in each run to eliminate potential contamination and false positives.

#### 4.2.2.5 Relative quantification of GFLV

To ensure the validity and repeatability of a real-time PCR assay it is necessary to include the appropriate reference genes for normalisation (Hugget *et al.*, 2005). The expression stability of several reference genes were evaluated on *Vitis vinifera* by Reid *et.al.* (2006). From that study, four reference genes were selected for the real-time PCR assay: Actin, EF-1 $\alpha$  (Elongation factor 1-alpha), UBC (Ubiquitin-conjugating enzyme) and GAPDH (glyceraldehyde 3-phosphate dehydrogenase).

Standard curves were constructed for each reference gene as well as the gene of interest (GFLV) using a calibrator sample to which the data of the other samples can be normalised. The calibrator sample consisted of a pooled reaction of all 18 grapevine samples to be tested. Standard curves were based on a five-fold serial dilution of cDNA in water, ranging from undiluted cDNA to a 1:625 ( $5^{-4}$ ) dilution, with each dilution being tested in triplicate. The calibrator sample was included in every run to ensure that the relevant standard curve could be imported and relative comparisons could be made.

Relative quantification was performed using the standard curve method in which variations in transcript expression is determined relative to the calibrator and then normalised to reference gene expression levels. All grapevine samples were diluted to 1:5 to ensure that their expression levels fell within the limits of the generated standard curves. The samples were tested with the four primer sets representing the three reference genes and GFLV – with each reaction being done in triplicate. The geometric mean of the calculated concentration values (ng/reaction) of the triplicates were calculated for the reference genes and the gene of interest. The geometric mean of the three reference genes values was then calculated. Relative quantification of GFLV was expressed as the ratio of the GFLV concentration to the reference gene concentration in each sample.

MIQE (Minimum Information for Publication of Quantitative Real-Time PCR Experiments) guidelines were taken into consideration throughout the execution of this assay to ensure the precision and reproducibility of the experiment (Bustin *et al.*, 2009).

## 4.3 Results

### 4.3.1 Cloning of the GFLV-V7 RNA-2 isolate

Four primer sets were designed in order to clone the complete RNA-2 genome of GFLV by overlapping the resulting fragments into one contiguous sequence. One-step RT-PCR was performed at a gradient annealing temperature to determine optimum amplification. Primer set Seq\_1 amplified the expected 1003bp fragment at an annealing temperature of 58°C and primer set Seq\_4 amplified the expected 1040bp fragment at a temperature of 47°C. However, no amplification was obtained with primer sets Seq\_2 and Seq\_3. Various parameters were modified in an attempt to amplify the two fragments but with no success. It was decided to combine Seq\_2-fwd and Seq\_3-rev in an attempt to amplify a fragment of 1856bp. Again the one-step RT-PCR was tested at a gradient annealing temperature and the correct fragment was amplified at a temperature of 50°C. The standard RT-PCR protocol was modified by using a final primer concentration of 0.2µM to eliminate primer dimers. All three fragments were cloned and sequenced successfully.

### 4.3.2 Sequence analysis and phylogeny

The generated sequence data for the GFLV-Vak7 RNA-2 genome was constructed using CLC Main Workbench and analysis was performed using Geneious 6.1.6 and MEGA5 software. From the 3529bp consensus sequence, 3318bp were sequenced, which amounts to 94%. When aligned to GFLV-SAPCS3 RNA-2 it shows that a large section of the ORF, including the complete 2C<sup>CP</sup>, and part of the 3'UTR was sequenced successfully (Figure 4.1).

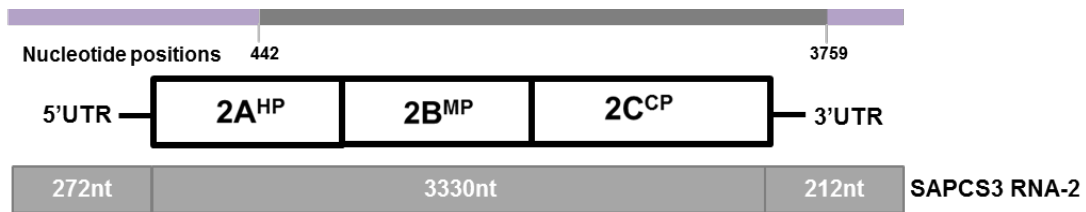


**Figure 4.1:** Regions of the sequenced GFLV-Vak 7 RNA-2 genome compared to GFLV-SAPCS3 RNA-2. The region of the Vak7 RNA-2 that was successfully sequenced is indicated in grey and the nucleotide positions of where it aligns to SAPCS3 are indicated below. Regions not sequenced are indicated in purple. The SAPCS3 RNA-2 genome is shown with the sizes of the ORF, 5'UTR and 3'UTR indicated inside the blocks

Multiple nucleotide sequence alignments of GFLV-Vak7 RNA-2 and other available full-length GFLV RNA-2 isolates were performed. It was shown that GFLV-Vak7 RNA-2 grouped together with GFLV-SACH44 and GFLV-SAPCS3 - the only two full-length GFLV isolates from South Africa (Figure 4.2).

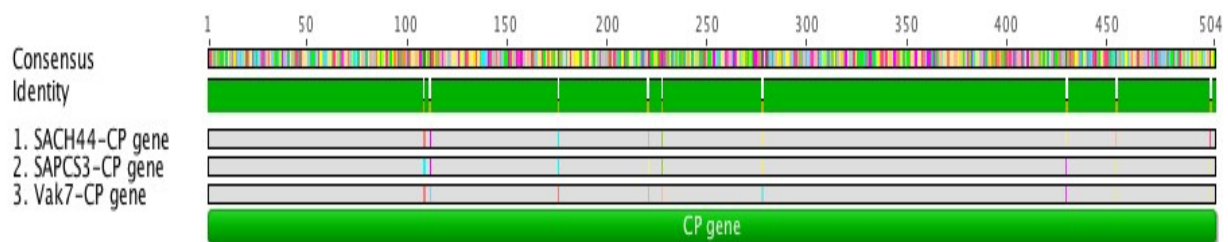


**Figure 4.2:** Alignment of the 2C<sup>CP</sup> of the two South African isolates GFLV-SACH44 and GFLV-SAPCS3 with GFLV-Vak7 showing nucleotide differences between the three sequences. Each coloured line is a SNP representing a different nucleotide. The alignment was performed using Geneious 6.1.6 software.

The degree of sequence variation was determined by generating pair wise comparisons and Neighbor-joining phylogenetic trees with MEGA5 software. Phylogenetic trees were constructed based on the 2C<sup>CP</sup> of nepovirus isolates (Figure 4.3) due to the higher number of coat protein sequences available compared to other genes. It showed that isolate Vak7 clusters together with South African isolates SACH44 and SAPCS3 along with other members of the subgroup A nepoviruses.

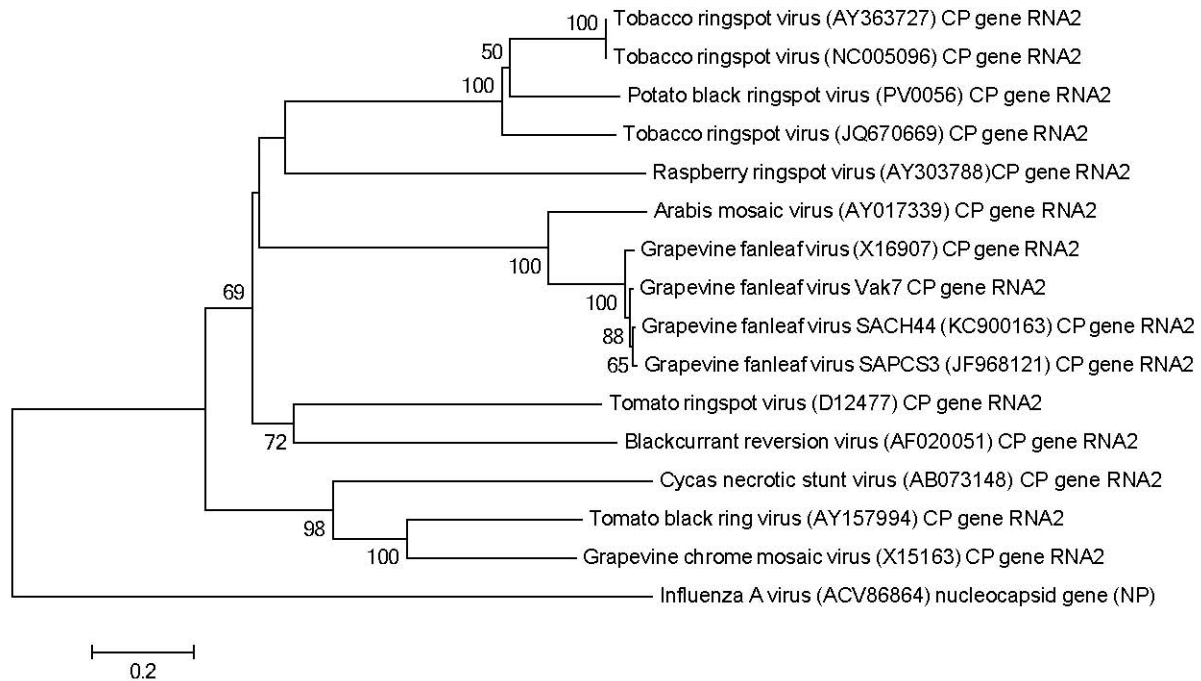


**Figure 4.3:** Phylogenetic tree based on the  $2C^{CP}$  of isolates from the genus *Nepovirus* (Richards *et al.*, 2014). Analysis was conducted using the Neighbour-joining method. The percentage of replicate trees in which the sequences clustered together in the bootstrap test (1000 replicates) is indicated next to the branches. Influenza A virus was used as an outgroup. Phylogenetic analysis was conducted in MEGA5 (Tamura *et al.*, 2011)

#### 4.3.3 Development of the real-time PCR assay

GFLV specific primers were designed from a conserved  $2C^{CP}$  region of the RNA2 genome. The samples to be used for the assay was tested with RT-PCR to confirm their status (results not shown) – 17 samples tested positive for GFLV and one sample tested negative and was used as the negative control for the assay.

The integrity of the extracted RNA samples was confirmed with gel electrophoresis and on the Nanodrop spectrophotometer. RNA samples were intact with both the 18s and 28s rRNA bands visible on the gel. The average RNA concentration of the samples was 431ng/ $\mu$ l and the  $A_{260:280}$  and  $A_{260:230}$  ratios were within the expected range, indicating RNA of suitable quality for downstream applications.

A standard curve was constructed for GFLV using a five-fold serial dilution series from 100ng to 0.16ng of the calibrator sample. The standard curve was constructed by correlating the Ct values against the logarithm of the relative concentrations for each dilution. The PCR products were run on a 2% agarose gel to confirm that the correct product was amplified and that no amplification occurred in the NTC (Figure 4.4).

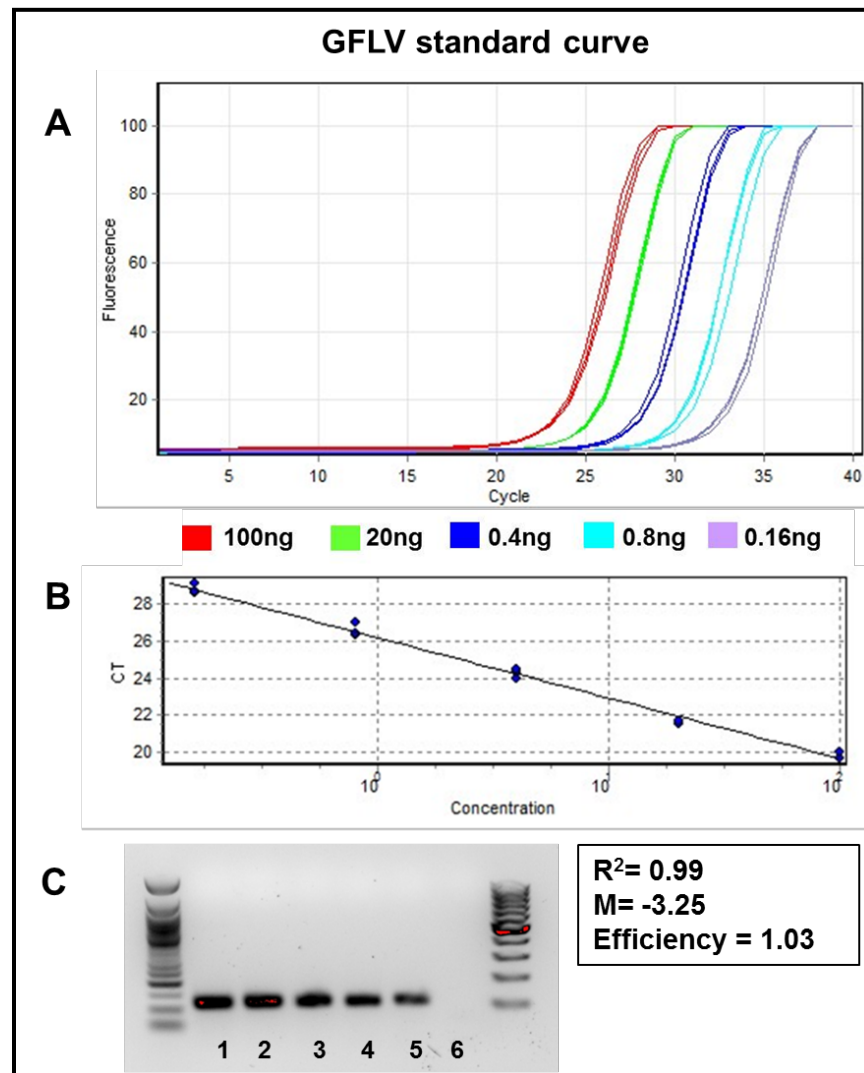


**Figure 4.4:** Standard curve using primers to amplify the GFLV gene. (A) Amplification profile of the five-fold dilution series of the calibrator sample (B) Standard curve of the Ct values of each triplicate plotted against the logarithm of the relative concentration of the sample (C) 2% agarose gel of the five –fold dilution series (lanes 1-5) and the NTC (lane 6)

The amplification efficiency of the standard curve was 1.03 and the slope of the trendline was -3.25, which indicates effective doubling of the PCR product with each cycle. The  $R^2$  value for the standard curve was 0.99.

Standard curves for Actin, UBC and GAPDH were constructed in the same manner as for GFLV (Figures 4.5, 4.6 and 4.7). EF1  $\alpha$  was initially selected as a reference gene but it gave inconsistent results. The replicates of the dilution series were not overlapped and the amplification curves were unevenly spaced - it was therefore decided not to continue with this reference gene as a linear standard curve could not be generated.

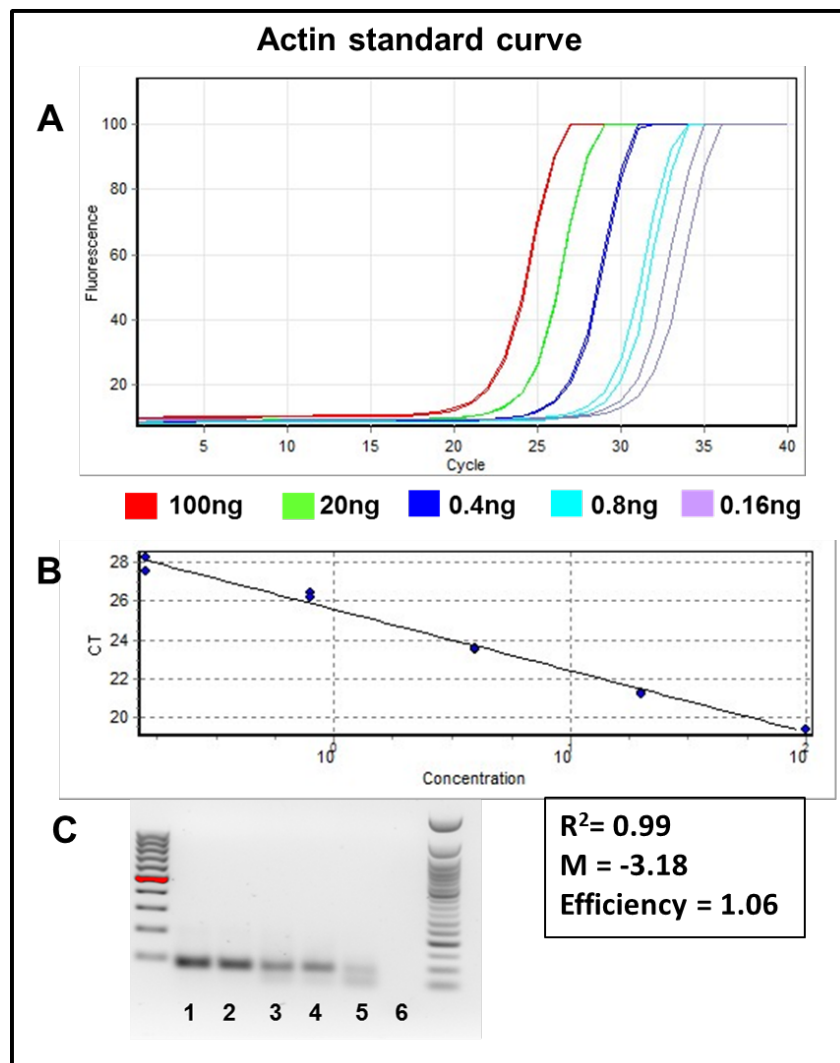


**Figure 4.5:** Standard curve using primers to amplify the Actin gene. (A) Amplification profile of the five-fold dilution series of the calibrator sample (B) Standard curve of the Ct values of each triplicate plotted against the logarithm of the relative concentration of the sample (C) 2% agarose gel of the five -fold dilution series (lanes 1-5) and the NTC (lane 6)

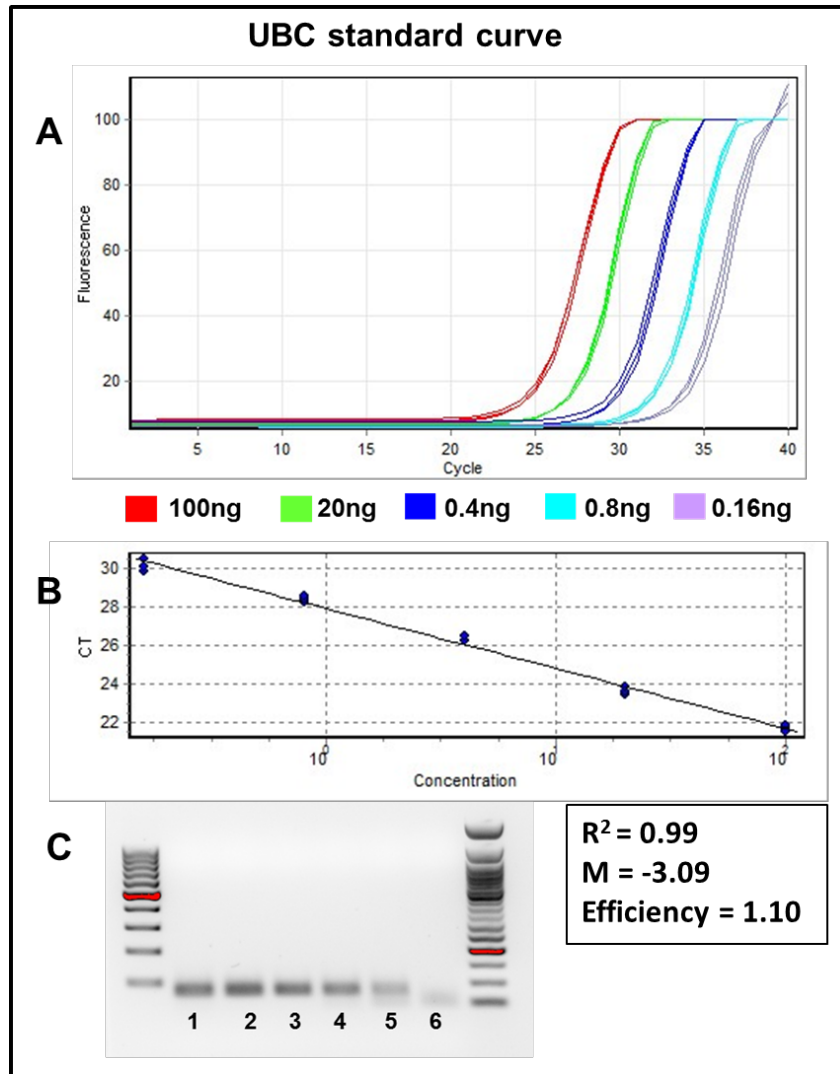


**Figure 4.6:** Standard curve using primers to amplify the UBC gene. (A) Amplification profile of the five-fold dilution series of the calibrator sample (B) Standard curve of the Ct values of each triplicate plotted against the logarithm of the relative concentration of the sample (C) 2% agarose gel of the five –fold dilution series (lanes 1-5) and the NTC (lane 6)

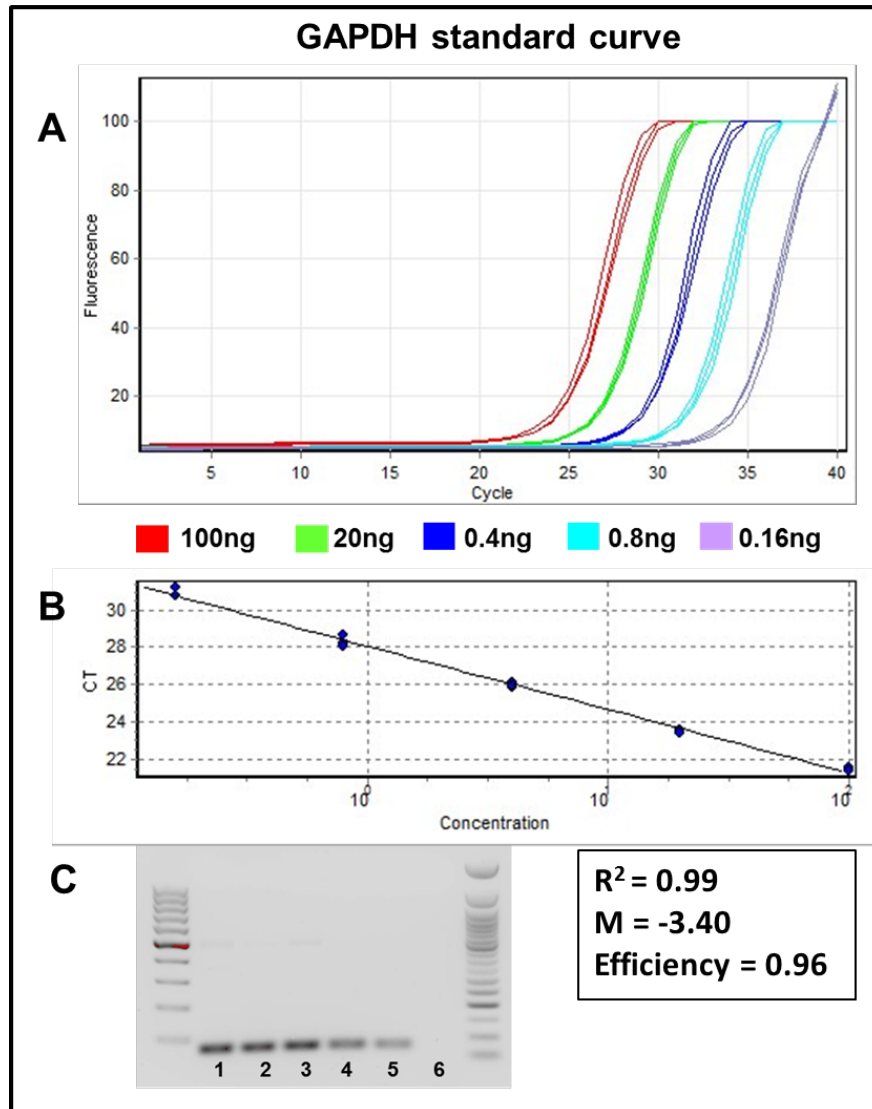


**Figure 4.7:** Standard curve using primers to amplify the GAPDH gene. (A) Amplification profile of the five-fold dilution series of the calibrator sample (B) Standard curve of the Ct values of each triplicate plotted against the logarithm of the relative concentration of the sample (C) 2% agarose gel of the five –fold dilution series (lanes 1-5) and the NTC (lane 6)

The  $R^2$  value of the standard curves for all three reference genes was 0.99 which indicates a good correlation coefficient. The amplification efficiency was 1.06 for Actin, 1.10 for UBC and 0.96 for GAPDH indicating effective doubling of the PCR product with all the reference genes.

#### **4.3.4 Relative quantification of GFLV**

For the relative quantification of GFLV and for accurate normalisation of the data, all grapevine samples were amplified with the primers for the gene of interest and the three reference genes. The samples to be tested were diluted 1:5 to ensure that the values would fall within the standard curve range. Melting curve analysis of the amplified PCR products showed melting temperatures of between 85.3°C and 85.5°C for GFLV. The Ct values of the amplified samples were within the Ct range of the standard curve and were therefore well aligned with the standard curve (Figure 4.8).

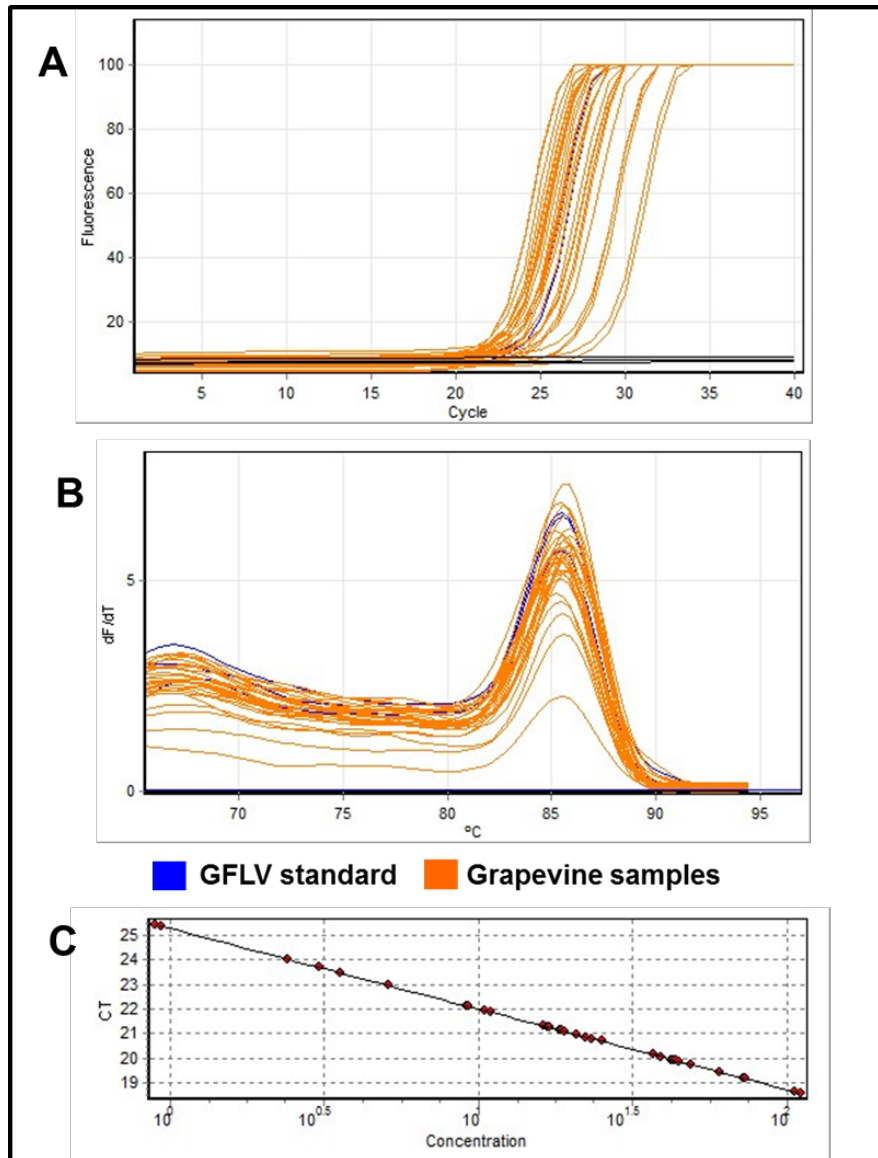


**Figure 4.8:** Grapevine samples tested with GFLV primers. (A) Amplification curves of the grapevine samples diluted 1:5 (B) Melting curve analysis confirming amplification of the correct amplicon with melting peaks of between 85.3 – 85.5 $^{\circ}C$  (C) Ct values of amplified samples imported onto the GFLV standard curve.

The samples were tested in triplicate and the geometric mean of the calculated concentration (ng/reaction) for each sample and each gene amplified are shown in Table 4.3. Relative expression of GFLV was calculated as the ratio of the GFLV concentration to the reference gene concentration in each sample.

**Table 4.3:** Calculated concentration values of the grapevine samples in ng/reaction. Column 7 represents the geometric mean value for the three reference genes: Actin, GAPDH and UBC.

Sample nr	Sample ID	GFLV	Actin	GAPDH	UBC	Ref genes	Relative expression of GFLV
1	CH 41	2.94	20.60	21.82	22.39	21.59	<b>0.14</b>
2	CB3	10.20	10.48	3.70	5.05	5.81	<b>1.76</b>
3	RPV236	0.77	1.78	1.00	1.20	1.29	<b>0.60</b>
4	V4	1.93	19.10	17.43	16.98	17.81	<b>0.11</b>
5	V5	20.81	14.55	12.44	14.61	13.83	<b>1.50</b>
6	FP1	108.79	19.30	15.75	9.98	14.48	<b>7.52</b>
7	FP2	66.57	7.22	6.41	6.80	6.80	<b>9.79</b>
8	CM9	18.02	1.69	1.60	2.22	1.82	<b>9.92</b>
9	CH30	37.59	16.03	14.21	18.69	16.21	<b>2.32</b>
10	CK3	43.76	12.60	11.65	23.20	15.05	<b>2.91</b>
11	SACPS3	47.24	36.48	34.61	18.81	28.74	<b>1.64</b>
12	Vak7	4.50	40.70	42.67	24.02	34.68	<b>0.13</b>
13	R99	1.72	30.15	39.16	40.84	36.40	<b>0.05</b>
14	CH44	0.11	15.71	26.36	19.70	20.13	<b>0.01</b>
15	CH46	55.11	62.64	83.45	43.53	61.05	<b>0.90</b>
16	CH47	1.03	24.55	55.44	43.72	39.04	<b>0.03</b>
17	V10	1.67	25.89	28.35	24.53	26.21	<b>0.06</b>
18	I3798 (NC)	0.00	N/A	N/A	N/A	N/A	<b>0.00</b>

qPCR was able to detect GFLV in all samples with values ranging between 0.11 and 108.79ng/reaction. No amplification occurred in the negative sample (I3798) as expected.

For the relative quantification of GFLV values ranged between 0.01 to 9.92ng/reaction (Figure 4.9). Of the 18 samples tested, 11 were collected from the greenhouse (including the negative control sample) and seven were collected from the field. Overall greenhouse samples showed higher concentrations of GFLV infection.

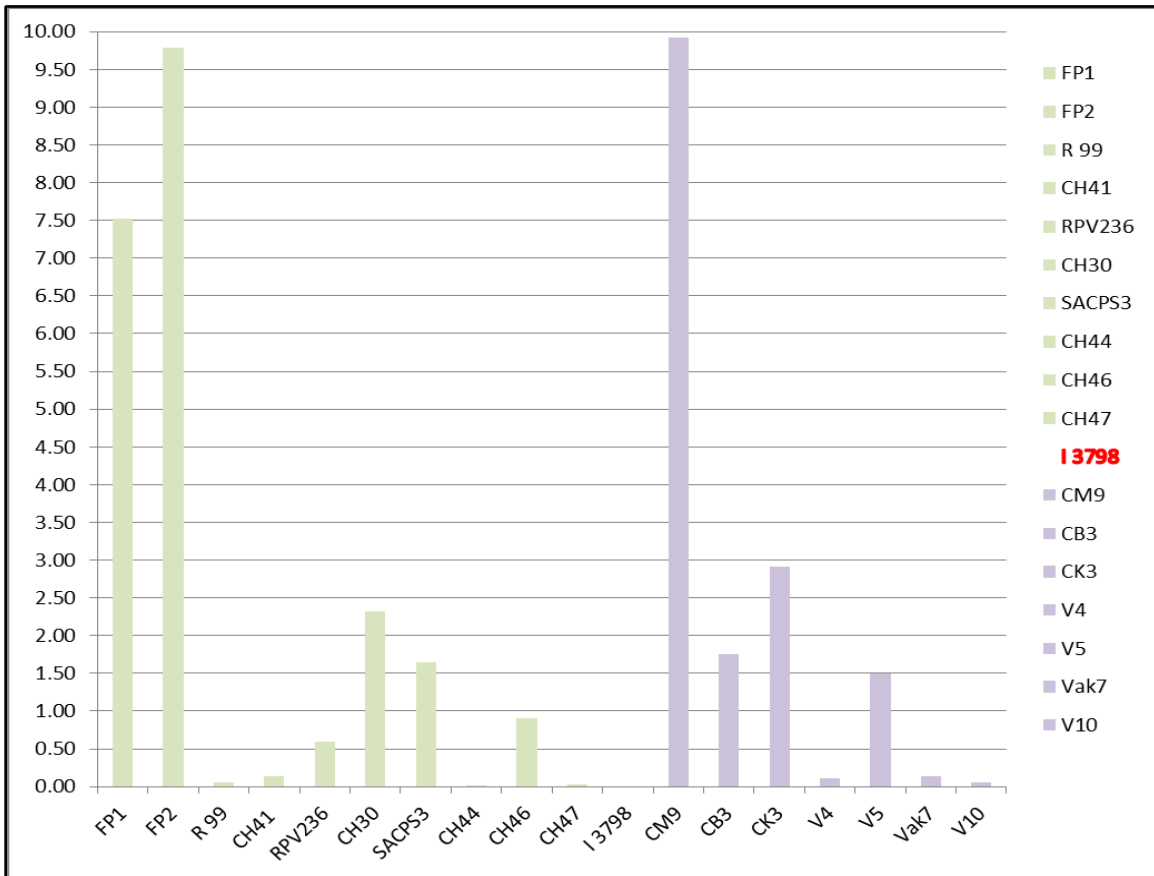


**Figure 4.9:** Bar chart representing the relative expression of GFLV in each sample. Values on the y-axis indicate ng/reaction. The different samples are indicated on the x-axis. Samples in green represents greenhouse samples and samples in purple represents field samples. I 3798 represent the negative sample.

## 4.4 Discussion

Phylogenetic analysis of the partial GFLV-Vak7 RNA-2 isolate sequenced in this study clusters it together with South African isolates GFLV-SAPCS3 and GFLV-SACH44 and other nepoviruses of subgroup A. Genbank BLAST analysis of the partial GFLV-Vak7 RNA-2 isolate shows 97% nucleotide identity to SAPCS-3 and SACH44 and between 89-90% identity to other full-length GFLV-RNA2 sequences in the database. In their study, Lamprecht *et al.*, (2012 and 2013) showed that GFLV-SAPCS3 has the highest nucleotide identity to French isolate GFLV-F13 and that GFLV-SACH44 is associated with a satellite RNA. Since the complete genome sequence of GFLV-Vak7 is not available it is not possible to make any further conclusions regarding its relationship to other GFLV isolates and nepoviruses. During primer design it was difficult to design primers within the first 116 base pairs of the RNA-2 consensus sequence which forms part of the 2A<sup>HP</sup> of the RNA-2 genome. Various studies have proven the variability of the GFLV RNA-2 genome and have indicated that the 2A<sup>HP</sup> is not as genetically conserved as the 2B<sup>MP</sup> and 2C<sup>CP</sup> regions (Elbeaino *et al.*, 2014; Naraghi-Arani *et al.*, 2001). Sequence comparisons have indicated that the 2A<sup>HP</sup> varies in length between GFLV isolates and has a high amino acid diversity of up to 15% (Pompe-Novak *et al.*, 2007; Vigne and Fuchs, 2008).

A quantitative real-time PCR assay based on SYBR green technology for the detection of GFLV was developed. Dye-based chemistry and probe-based chemistry are the two main types of qPCR detection chemistries that have been applied in recent years, with SYBR-Green dye and TaqMan probes being the most commonly used (Mackay and Landt, 2007; Gasparic *et al.*, 2010; Cao and Shockey, 2012). Although probe-based assays are highly specific, research suggests that SYBR green assays allows for more variability within the target sequence, are more economical and produce fewer false negatives (Papin *et al.*, 2004 & 2010). As research on the direct comparison of both methods using the same primers and biological samples is still limited it is not possible to claim which chemistry is superior as both has its advantages and disadvantages. For this study SYBR green technology was selected due to simpler assay optimisation and

being less costly than TaqMan probes making it more suitable for a routine diagnostic setup.

Three different dye-based assays were tested during this study – SYTO 9 (Invitrogen), the KAPA SYBR fast qPCR kit (KAPA Biosystems) and the SensiFAST SYBR No-ROX Kit (Bioline). Both SYTO9 and the KAPA kit did not amplify all the reference genes correctly and if amplification occurred there was little uniformity between sample replicates and dilutions. It was evident that testing with SYTO9 and the KAPA kit would not yield reproducible results and it was therefore decided to optimise the assay using the SensiFAST kit as it gave consistent results from the start with no irregularities being experienced. The SensiFAST kit contains an antibody-mediated hot-start Taq polymerase that eliminates non-specific amplification, which is not offered in the KAPA kit. According to the manufacturers the Sensifast kit also contains a unique buffer chemistry allowing for the highest specificity and sensitivity. Several comparison studies with multiple dyes have been conducted to investigate the effects of dye concentration and sequence composition on qPCR amplification and melting curve analysis (Monis *et al.*, 2005; Gudnason *et al.*, 2007; Eischeid, 2011). Although SYBR green emits a very strong fluorescent signal and is widely used commercially, it has been shown to inhibit the PCR reaction and has a lower reproducibility rate than other detection chemistries (Gasparic *et al.*, 2010). In general it was found that EvaGreen and certain SYTO dyes generated highly reproducible melting curves over a broader dye concentration range and may be the desired alternatives to the commonly used SYBR Green dye. In this study however, SYBR green was superior and generated better results than SYTO 9, which may be contributed to the unique buffer composition of the SensiFAST kit.

A prerequisite for an accurate RT-qPCR is RNA of a high quality that is not degraded and free of residual DNA (Swift *et al.*, 2000). For the qPCR assay, 17 positive samples were used. Originally, 40+ samples were selected for the assay mostly from infected vineyards in Robertson in the Breede River valley. Samples were macerated on the day of collection and stored at -80°C until RNA isolation. However, after RNA extraction of the samples using the CTAB method, most of the samples were degraded and/or

showed poor yields of RNA. The same samples were also extracted using a different method (Bioline RNA extraction kit) to see if this improved the yield and quality, but this was not successful either (results not shown). This can probably be attributed to reasons like low viral titre, and age and quality of the leaf material. In the end, good quality RNA could only be obtained from 18 of the samples and it was decided to continue with this number only, as the season for GFLV symptom expression has passed by then. The presence of genomic DNA in RNA samples can also adversely affect the RT-qPCR assay by causing false positive results and background. A study conducted in 2012 by Osman *et al.* on grapevine tissues indicated that DNase digestion of the purified RNA prior to cDNA synthesis improved virus detection and yielded the lowest quantitation cycle values in RT-qPCR. After DNase treatment of the RNA, samples were subjected to phenol and chloroform extractions but this resulted in significantly lower yield and poor quality RNA. This problem was eventually solved by using a one-step phenol:chloroform extraction which yielded better quality and quantity of RNA.

The reverse transcription (RT) step is believed to be the principal source of variability in a RT-qPCR experiment and an optimal reverse transcription is therefore crucial for a successful and reliable RT-qPCR assay (Freeman *et al.*, 1999). A RT-qPCR can be carried out using either a one-step or a two-step reaction and both have its advantages (Wacker and Godard, 2005). The main advantages of a two-step method are reduced primer dimer formation and reduced variability between reactions (Vandesompele *et al.*, 2002). For this study, a two-step approach was chosen using random primers for cDNA synthesis as this allows for the same calibrator sample to be used for testing of all the genes.

After optimisation of the qPCR assay, standard curves were constructed for the three reference genes and the gene of interest. The standard curves for all four genes showed adequate amplification efficiencies and linearity and was therefore suitable for gene quantification. The qPCR assay for the detection of GFLV proved to be highly sensitive as an infection rate of 0.11ng/reaction could be detected. Melting curve

analysis of GFLV-infected samples showed a clearly defined peak at 85.3°C – 85.5 °C. Samples from both the greenhouse and field were tested and overall greenhouse samples showed a higher level of infection than field samples. It was noted during field sampling that not all of the infected vines displayed symptoms whereas greenhouse samples showed distinct symptoms. It is known that accurate field diagnosis of grapevine virus diseases can be difficult as symptoms displayed are rarely unique to a particular disease and can be influenced by the virus strain, plant variety and the environment (Martelli, 1993).

Relative quantification showed that GFLV expression levels as low as 0.01ng/reaction could be successfully detected. The main objective of this study was to develop a quantitative qPCR assay for the detection of GFLV that was accurate, sensitive and reproducible. The developed qPCR assay proved to be sensitive enough to detect very low levels of GFLV infection and can be used effectively as a high throughput diagnostic tool for virus detection in grapevine material.

## CHAPTER 5

---

### Conclusion

One of the most devastating viral disease complexes that affects grapevine worldwide is fanleaf degeneration/decline disease which is caused by several different virus species from the genus *Nepovirus*, including GFLV and ToRSV. ToRSV is a broad host range nepovirus infecting numerous berry and fruit crops, including grapevine. It is transmitted by nematode species of the *Xiphinema americanum* group which are endemic to certain regions of the USA and Canada where the virus is widespread, but has also been reported from ornamentals and berry crops in other parts of the world. GFLV is currently the only nepovirus known to occur in South Africa and is limited to the Breede River valley in the Western Cape. As grapevine is one of South Africa's most important commodities, it is imperative that the entry of foreign viruses is prohibited and that the spread of existing viruses is adequately controlled. All grapevine material imported into South Africa is routinely tested by DAFF: Inspection Services for various nepoviruses, including ToRSV and GFLV. The aim of this project was to develop a diagnostic assay for the detection of nepoviruses in grapevine by developing an ELISA kit for the detection of ToRSV and designing a qPCR assay for the detection of GFLV.

The first aim of this study was to produce specific and sensitive antibodies against the ToRSV coat protein using recombinant DNA technology for subsequent development of an ELISA kit. The ToRSV CP was successfully isolated from imported ToRSV infected grapevine and cloned into the pGEX6P2 expression vector. Expression of the fusion protein was however not achieved despite several strategies being attempted to improve soluble protein expression. In a further attempt to achieve expression of the ToRSV coat protein, transient expression via agroinfiltration of *N. benthamiana* leaves was performed. The GST-ToRSV-CP fusion was successfully cloned into the pBIN61S binary vector and transformed into *A.tumefaciens* via electroporation. After transformation, young top leaves of tobacco plants were infiltrated with the bacterial

suspension and patches of infiltration could be seen after 3 days. These leaves were subjected to Tissue print immunoassay and SDS-Page analysis to determine if the GST-ToRSV-CP fusion was expressed - and both showed positive results – however at very low levels. So, although transient expression proved to be successful the protocol will have to be optimised to determine if sufficient amounts of purified protein can be obtained.

The second aim of this study was to develop a qPCR assay for the detection of GFLV. A partial GFLV RNA-2 sequence of a South African grapevine isolate was generated to facilitate the design of GFLV-specific primers and a quantitative real-time PCR assay based on SYBR green technology was subsequently developed. Relative quantification showed that GFLV expression levels as low as 0.01ng/reaction could be successfully detected with this assay. The assay therefore proved to be accurate, sensitive and reproducible and can be used effectively as a high-throughput diagnostic tool for GFLV detection in grapevine material.

Most of the viruses being tested at DAFF, for both grapevine and deciduous crops, belong to the genus *Nepovirus*, so it would be sensible to have a testing method that is able to detect the virus group instead of testing for each virus separately. Previous research has however proved that it is difficult to design a nepovirus group-specific primer set because of the wide sequence divergence among grapevine nepovirus genomes. Instead, primers were designed to detect the three different subgroups of the genus (Digiario *et. al.*, 2007; Wei and Clover, 2008).

In recent years, the number of imported material received at DAFF for screening has increased tremendously. It has become increasingly clear that the current methods used for detection are unsuitable and that faster and more reliable testing methods are needed. In a diagnostic setup, real-time PCR seems to be the answer as it is a highly sensitive and reliable screening method for the detection of nucleic acids which can be easily implemented and would eventually minimise cost, effort and time.

## CHAPTER 6

---

### References

Abou-Jawdah, Y., Sobh, H., Cordahi, N., Kawtharani, H., Nemer, G., Maxwell, D.P. and Nakhla, M.K. 2004. Immunodiagnosis of *Prune dwarf virus* using antiserum produced to its recombinant coat protein. *Journal of Virological Methods*. 121: 31–38.

Adams, I. P., Miano, D. W., Kinyua, Z. M., Wangai, A., Kimani, E., Phiri, N., Reeder, R., Harju, V., Glover, R., Hany, U., Souza-Richards, R., Deb Nath, P., Nixon, T., Fox, A., Barnes, A., Smith, J., Skelton, A., Thwaites, R., Mumford, R. and Boonham, N. 2013. Use of next-generation sequencing for the identification and characterization of *Maize chlorotic mottle virus* and *Sugarcane mosaic virus* causing maize lethal necrosis in Kenya. *Plant Pathology*. 62: 741–749.

Adams, I.P., Glover, R.H., Monger, W.A., Mumford, R., Jackeviciene, E., Navalinskiene, M., Samuitiene, M. and Boonham, N. 2009. Next-generation sequencing and metagenomic analysis: a universal diagnostic tool in plant virology. *Molecular Plant Pathology*. 10(4): 537–545.

Adrio, J.L. and Demain, A.L. 2010. Recombinant organisms for production of industrial products. *Bioengineered Bugs*. 1: 116–131.

Agricultural Pests Act 1983 (Act No. 36 of 1983). [http://www.nda.agric.za/docs/NPPOZA/Agricultural\\_Pests\\_Act.pdf](http://www.nda.agric.za/docs/NPPOZA/Agricultural_Pests_Act.pdf) (Accessed 01 November 2014)

Allen, W. R. and Dias, H. F. 1977. Properties of the single protein and two nucleic acids of tomato ring-spot virus. *Canadian Journal of Botany*. 55: 1028-1037.

Almond, N., Jones, S., Heath, A.B. and Kitchin, P.A. 1992. The assessment of nucleotide sequence diversity by the polymerase chain reaction is highly reproducible. *Journal of Virological Methods*. 40: 37–44.

Andret-Link, P., Laporte, C., Valat, L., Laval, L., Ritzenthaler, C., Demangeat, G., Vigne, E., Pfeiffer, P., Stussi-Garaud, C. and Fuchs, M. 2004. *Grapevine fanleaf virus*: Still a major threat to the grapevine industry. *Journal of Plant Pathology*. 86(3): 183-195.

Aparicio, F., Aramburu, J., Soler, S., Galipienso, L., Nuez, F., Pallás, V. and López, C. 2009. Immunodiagnosis of *Parietaria mottle virus* in tomato crops using a polyclonal antiserum against its coat protein expressed in a bacterial system. *Journal of Phytopathology*. 157(7-8): 511-513.

Arzola, L., Chen, J., Rattanaorn, K., Maclean, J.M. and McDonald, K.A. 2011. Transient co-expression of post-transcriptional gene silencing suppressors for increased *in planta* expression of a recombinant anthrax receptor fusion protein. *International Journal of Molecular Sciences*. 12(8): 4975-4990.

Baker, K.K., Ramsdell, D.C. and Gillett, J.M. 1985. Electron microscopy: current applications to plant virology. *Plant Disease*. 69: 85–90.

Baker, T.A., Grossman, A.D. and Gross, C.A. 1984. A gene regulating the heat shock response in *E.coli* also causes a defect in proteolysis. *Proceedings of the National Academy of Sciences of the United States of America*. 81: 6779-6783.

Bendahmane, A., Querci, M., Kanyuka, K. and Baulcombe, D.C. 2000. Agrobacterium transient expression system as a tool for the isolation of disease resistance genes: application to the Rx2 locus in potato. *Plant Journal*. 21(1): 73-81.

Bentley, W. E., Mirjalili, N., Andersen, D. C., Davis, R. H. and Kompala, D. S. 1990. Plasmid-encoded protein: the principal factor in the “metabolic burden” associated with recombinant bacteria. *Biotechnology and Bioengineering*. 35: 668–681.

Bertolini, E., Garcia, J., Yuste, A. and Olmos, A. 2010. High prevalence of viruses in table grape from Spain detected by real-time RT-PCR. *European Journal of Plant Pathology*. 128: 283–287.

Bitterlin, M.W. and Gonsalves, D. 1988. Serological grouping of *Tomato ringspot virus* isolates: implications for diagnosis and cross-protection. *Phytopathology*. 78(3): 278-285.

Bock, K.R. 1982. The identification and partial characterization of plant viruses in the tropics. *Tropical Pest Management*. 28: 399–411.

Boonham, N., Kreuze, J., Winter S., Van der Vlugt, R., Bergervoet, J., Tomlinson, J. and Mumford, R. 2014. Methods in virus diagnostics: From ELISA to next generation sequencing. *Virus Research*. 186: 20–31.

Bouquet, A. 2011. Grapevines and viticulture. In: Adam-Blondon, A-F., Martinez-Zapater, J.M. and Kole, C. (eds.), *Genetics, genomics, and breeding of grapes*. 1-29. Science publishers, Jersey, USA.

Bovey, R. 1973. Maladies a virus et a mycoplasmes de la vigne. *Station Federale de Recherches Agronomiques de Changins*. 76 pp. Suisse.

Bovey, R., Gärtel, W., Hewitt, W.B., Martelli, G.P. and Vuittenez, A. 1990. Soil-borne viruses transmitted by nematodes. In: Bovey, R., Gärtel, W., Hewitt, W.B., Martelli, G.P. and Vuittenez, A. (eds.), *Virus and virus-like diseases of grapevines*. 46-50. Editions Payot, Lausanne, Switzerland.

Brown, D.J.F., Halbrecht, J.M., Robbins, R.T., and Vrain, T.C. 1993. Transmission of nepoviruses by *Xiphinema americanum* group nematodes. *Journal of Nematology*. 25: 349-354.

Bustin, S.A., Benes, V., Garson, J.A., Hellemans, J., Huggett, J., Kubista, M., Mueller, R., Nolan, T., Pfaffl, M.W., Shipley, G.L., Vandesompele, J. and Wittwer, C.T. 2009. The MIQE Guidelines: Minimum Information for Publication of Quantitative Real-Time PCR Experiments. *Clinical Chemistry*. 55(4): 611-622.

Bystricka, D., Lenz, O., Mraz, I., Piherova, L., Kmoch, S. and Sip, M. 2005. Oligonucleotide-based microarray: a new improvement in microarray detection of plant viruses. *Journal of Virological Methods*. 128: 176–182.

Cadman, C.H. and Lister, R.M. 1961. Relationship between tomato ringspot and peach yellow bud mosaic viruses. *Phytopathology*. 51: 29-31.

Cadman, C.H., Dias, H.F., Harrison, B.D. 1960. Sap-transmissible viruses associated with disease of grape vines in Europe and North America. *Nature*. 187: 577-579.

Candresse, T., Hammond, R.W. and Hadidi, A. 1998. Detection and identification of plant viruses and viroids using polymerase chain reaction (PCR). In: Hadidi, A., Khetarpal, R.K. and Koganezawa, K. (eds.), *Control of plant virus diseases*. 399-416. APS Press, Minnesota, USA.

Cao, H. and Shockey, J.M. 2012. Comparison of TaqMan and SYBR Green qPCR methods for quantitative gene expression in tung tree tissues. *Journal of Agricultural and Food Chemistry*. 60: 12296-12303.

Carneiro S., Ferreira, E.C. and Rocha, I. 2013. Metabolic responses to recombinant bioprocesses in *Escherichia coli*. *Journal of Biotechnology*. 164(3): 396-408.

Carrier, K., Xiang, Y. and Sanfacon, H. 2001. Genomic organization of RNA2 of *Tomato ringspot virus*: processing at a third cleavage site in the N-terminal region of the polyprotein *in vitro*. *Journal of General Virology*. 82: 1785 – 1790.

Čepin, U., Gutiérrez-Aguirre, I., Balažic, L., Pompe-Novak, M., Gruden, K. and Ravnikar, M. 2010. A one-step reverse transcription real-time PCR assay for the detection and quantitation of *Grapevine fanleaf virus*. *Journal of Virological Methods*. 170: 47–56.

Cerovska, N., Moravec, T., Plchova, H., Hoffmeisterova, H., Folwarczna, J. and Dedic, P. 2010. Production of polyclonal antibodies to *Potato virus X* using recombinant coat protein. *Journal of Phytopathology*. 158(1): 66-68.

Chen, H., Xu, Z., Xu, N., Cen, P. 2005. Efficient production of a soluble fusion protein containing human beta-defensin-2 in *E. coli* cell-free system. *Journal of Biotechnology*. 115: 307–315.

Chen, J., Acton, T.B., Basu, S.K., Montelione, G.T. and Inouye, M. 2002. Enhancement of the solubility of proteins overexpressed in *Escherichia coli* by heat shock. *Journal of Molecular Microbiology and Biotechnology*. 4(6): 519-524.

Clark, M.F. and Adams, A.N. 1977. Characteristics of the microplate method of enzyme-linked immunosorbent assay for the detection of plant viruses. *Journal of General Virology*. 34: 475–483.

Clark, M.F. and Bar-Joseph, M. 1984. Enzyme immunosorbent assays in plant virology. In: Maramorosch, K. and Koprowski, H. (eds.), *Methods in virology*. 51–85. Academic Press, New York, USA.

Cooper, J.I. and Edwards, M.L. 1986. Variations and limitations of enzyme-amplified immunoassays. In: Jones, R.A.C. and Torrance, L. (eds.), *Developments and applications in virus testing*. 139–154. Association of Applied Biologists, Wellesbourne, UK.

Demain, A.L. and Vaishnav, P. 2009. Production of recombinant proteins by microbes and higher organisms. *Biotechnology Advances*. 27: 297–306.

Demangeat, G., Voisin, R., Minot, J.C., Bosselut, N., Fuchs, M. and Esmenjaud, D. 2005. Survival of *Xiphinema index* in vineyard soil and retention of Grapevine fanleaf virus over extended time in the absence of host plants. *Phytopathology*. 95(10): 1151-1156.

Description of Plant Viruses. <http://www.dpvweb.net> (Accessed 05 October 2013)

Dewey, F.M., Thornton, C.R. and Gilligan, C.A. 1997. The use of monoclonal antibodies to detect, quantify and visualise fungi in soils. *Advances in Botanical Research*. 24: 275-308.

Digiario, M., Elbeaino, T. and Martelli, G.P. 2007. Development of degenerate and species-specific primers for the differential and simultaneous RT-PCR detection of grapevine infecting nepoviruses of subgroups A, B and C. *Journal of Virological Methods*. 141: 34–40.

Dorak, M.T. 2006. Real-Time PCR (Advanced Methods Series). <http://www.dorak.info/genetics/realtime.html>.

Dovas, C.I. and Katis, N.I. 2003. A spot multiplex nested RT-PCR for the simultaneous and generic detection of viruses involved in the aetiology of grapevine leafroll and rugose wood of grapevine. *Journal of Virological Methods*. 109: 217-226.

Dyson, M.R., Shadbolt, S.P., Vincent, K.J., Perera, R.L. and McCaVerty, J. 2004. Production of soluble mammalian proteins in *Escherichia coli*: identification of protein features that correlate with successful expression. *BMC Biotechnology*. 4: 32.

Edwardson, J.R. and Christie, R.G. 1997. *Viruses infecting peppers and other Solanaceous crops*. 2: 337–390. University of Florida, Gainesville, USA.

Edwardson, J.R., Christie, R.G., Purcifull, D.E. and Petersen, M.A. 1993. Inclusions in diagnosing plant virus diseases. In: Matthews, R.E.F. (ed.), *Diagnosis of plant virus diseases*. 101–128. CRC Press, Florida, USA.

Eisheid, A.C. 2011. SYTO dyes and EvaGreen outperform SYBR Green in real-time PCR. *BMC Research Notes*. 4: 263.

Elbeaino, T., Kiyi, H., Boutarfa, R., Minafra, A., Martelli, G.P., Digiario, M. 2014. Phylogenetic and recombination analysis of the homing protein domain of *Grapevine fanleaf virus* isolates associated with 'yellow mosaic' and 'infectious malformation' syndromes in grapevine. *Archives of Virology*. 159(10): 2757-64.

Engel, E.A., Escobar, P.F., Rojas, L.A., Rivera, P.A., Fiore, N. and Valenzuela, P.D. 2010. A diagnostic oligonucleotide microarray for simultaneous detection of grapevine viruses. *Journal of Virological Methods*. 163(2): 445-51.

Fajardo, T.V.M., Barros, D.R., Nickel, O., Kuhn, G.B. and Zerbini, F.M. 2007. Expression of *Grapevine leafroll-associated virus 3* coat protein gene in *Escherichia coli* and production of polyclonal antibodies. *Fitopatologia Brasileira*. 32: 496-500.

Fattouch, S., M'hirsi, S., Acheche, H., Marrakchi, M., Marzouki, N., 2001. RNA oligoprobe capture RT-PCR, a sensitive method for the detection of grapevine fanleaf virus in Tunisian grapevines. *Plant Molecular Biology Reporter*. 19: 235–244.

Fauquet, C.M., Mayo, M.A., Maniloff, J., Desselberger, U. and Ball, L.A. 2005. *Virus Taxonomy, Eighth Report of the International Committee on Taxonomy of Viruses*. Elsevier Academic Press, California, USA.

Fikrig, E., Barthold, S.W., Kantor, F.S. and Flavell, R.A. 1990. Protection of mice against the Lyme disease agent by immunizing with recombinant OspA. *Science*. 250(4980): 553-556.

Franco-Lara, L.F., Mcgeachy, K.D., Commandeur, U., Martin, R.R., Mayo, M.A. and Barker, H. 1999. Transformation of tobacco and potato with cDNA encoding the full-length genome of potato-leafroll virus: evidence for a novel distribution and host effects on virus multiplication. *Journal of General Virology*. 80: 2813-28122.

Frangioni, J.V. and Neel, B.G. 1993. Solubilization and purification of enzymatically active glutathione S-transferase (pGEX) fusion proteins. *Analytical Biochemistry*. 210: 179-187.

Frankel, S., Sohn, R. and Leinwand, L. 1991. The use of sarkosyl in generating soluble protein after bacterial expression. *Proceedings of the National Academy of Sciences of the United States of America*. 88(4): 1192-1196.

Franz, A., Makkouk, K.M., Katul, L. and Vetten, H.J. 1996. Monoclonal antibodies for the detection and differentiation of *Faba bean necrotic yellows* virus isolates. *Annals of Applied Biology*. 128: 255–268.

- Freeman, W.M., Walker, S.J. and Vrana, K.E. 1999. Quantitative RT-PCR: pitfalls and potential. *Biotechniques*. 26(1): 112-125.
- Fridlund, P.R. 1980. Glasshouse indexing for fruit tree viruses. *Acta Horticulturae*. 94: 153–158.
- Gasparic, M.B., Tengs, T., La Paz, J.L., Holst-Jensen, A., Pla, M., Esteve, T., Zel, J. and Gruden, K. 2010. Comparison of nine different real-time PCR detection chemistries for qualitative and quantitative applications in GMO detection. *Analytical and Bioanalytical Chemistry*. 396: 2023-2029.
- Ghazala, W., Waltermann, A., Pilot, R., Winter, S. and Varrelmann, M. 2008. Functional characterization and subcellular localization of the 16K cysteine-rich suppressor of gene silencing protein of tobacco rattle virus. *Journal of General Virology*. 89(7): 1748-1758.
- Giddings, G., Allison, G., Brooks, D., and Carter, A. 2000. Transgenic plants as factories for biopharmaceuticals. *Nature Biotechnology*. 18: 1151-1155.
- Goodin, M.M., Zaitlin, D., Naidu, R.A., Lommel, S.A. 2008. *Nicotiana benthamiana*: Its history and future as a model for plant-pathogen interactions. *Molecular Plant-Microbe Interactions*. 21: 1015–1026.
- Gottula, J.W., Lapato, D., Cantilina, K.K., Saito, S., Bartlett, B. and Fuchs, M. 2013. Genetic variability, evolution and biological effects of *Grapevine fanleaf virus* satellite RNAs. *Phytopathology*. 103(11): 1180-1187.
- Grodberg, J. and Dunn, J.J. 1988. *ompT* encodes the *Escherichia coli* outer membrane protease that cleaves T7 RNA polymerase during purification. *Journal of Bacteriology*. 170: 1245-1253.
- Gudnason, H., Dufva, M., Bang, D.D. and Wolff, A. 2007. Comparison of multiple dyes for real-time PCR: effects of dye concentration and sequence composition on DNA amplification and melting temperature. *Nucleic Acids Research*. 35(19):127.

- Guise, A.D., West, S.M. and Chaudhuri, J.B. 1996. Protein folding in vivo and renaturation of recombinant proteins from inclusion bodies. *Molecular Biotechnology*. 6(1): 53-64.
- Habili, N., Krake, L.R., Barlass, M. and Rezaian, M.A. 1992. Evaluation of biological indexing and dsRNA analysis in grapevine virus elimination. *Annals of Applied Biology*. 121: 277–283.
- Hammarström, M., Hellgren, N., Van Den Berg, S., Berglund, H. and Hard, T. 2002. Rapid screening for improved solubility of small human proteins produced as fusion proteins in *Escherichia coli*. *Protein Science*. 11: 313–321.
- Hanahan, D. 1985. Techniques for transformation of *E. coli*. In: Glover, D.M. (ed.), *DNA cloning: a practical approach, volume 1*. 109-135. IRL Press, Oxford, UK.
- Hans, F., and Sanfaçon, H. 1995. Tomato ringspot nepovirus protease: characterization and cleavage site specificity. *Journal of General Virology*. 76(4): 917-927.
- Henson, J.M. and French, R. 1993. The polymerase chain reaction and plant disease diagnosis. *Annual Review of Phytopathology*. 31: 81–109.
- Hewitt, W.B., Raski, D.J. and Goheen, A.C. 1958. Nematode vector of soil-borne fanleaf virus of grapevines. *Phytopathology*. 48: 586-595.
- Hoekema, A., Hirsch, P.R., Hooykaas, P.J.J. and Schilperoort, R.A. 1983. A binary plant vector strategy based on separation of *vir*- and T-region of the *Agrobacterium tumefaciens* Ti plasmid. *Nature*. 303: 179-180.
- Hongyun, C., Wenjun, Z., Qinsheng, G., Qing, C., Shiming, L. and Shuifang, Z. 2008. Real time TaqMan RT-PCR assay for the detection of *Cucumber green mottle mosaic virus*. *Journal of Virological Methods*. 149(2): 326-329.

- Horvath, J. 1983. New artificial hosts and nonhosts of plant viruses and their role in the identification and separation of viruses. XVIII. Concluding remarks. *Acta Phytopathologica Hungarica*. 18: 121–161.
- Horvath, J. 1993. Host plants in diagnosis. In: Matthews, R.E.F. (ed.), *Diagnosis of plant virus diseases*. 15-48. CRC Press, Florida, USA.
- Horvath, J., Tobias, I., Hunyadi, K. 1994. New natural herbaceous hosts of grapevine fanleaf nepovirus. *Horticultural Science*. 26: 31-32.
- Hoy, J.W., Mircetich, S.M. and Lownsbery, B.R 1984. Differential transmission of prunus tomato ringspot virus strains by *Xiphinema californicum*. *Phytopathology*. 74: 332-335.
- Hu, J.S., Sether, D.M. Liu, X.P. and Wang, M. 1997. Use of tissue blotting immunoassay to examine the distribution of *Pineapple closterovirus* in Hawaii. *Plant Disease*. 81: 1150–1154.
- Huggett, J., Dheda, K., Bustin, S. and Zumla, A. 2005. Real-time RT-PCR normalisation; strategies and considerations. *Genes and Immunity*. 6: 279–284.
- Hull, R. 1993. Nucleic acid hybridization procedures. In: Matthews, R.E.F. (ed.), *Diagnosis of plant virus diseases*. 253-271. CRC Press, Florida, USA.
- Huss, B., Walter, B., Etienne, L. and Van Regenmortel, M.H.V. 1986. *Grapevine fanleaf virus* detection in various organs using polyclonal and monoclonal antibodies. *Vitis*. 25: 178–188.
- Izadpanah, K., Zaki-Aghl, M., Zhang, Y.P., Daubert, S.D. and Rowhani, A. 2003. Bermuda grass as a potential reservoir host for *Grapevine fanleaf virus*. *Plant Disease*. 87: 1179-1182.
- Janssen, B.J. and Gardner, R.C. 1990. Localized transient expression of GUS in leaf discs following cocultivation with *Agrobacterium*. *Plant Molecular Biology*. 14(1): 61-72.

Johnson, K.S., Harrison, G.B.L., Lightowlers, M.W., O'Hoy, K.L., Cogle, W.G., Dempster, R.P., Lawrence, S.B., Vinton, J.G., Heath, D. D. and Rickard, M.D. 1989. Vaccination against ovine cysticercosis using a defined recombinant antigen. *Nature*. 338: 585–587.

Jones, A.T. 1993. Experimental transmission of viruses in diagnosis. In: Matthews, R.E.F. (ed.), *Diagnosis of plant virus diseases*. 49-72. CRC Press, Florida, USA.

Kapila, J., De Rycke, R., Van Montagu, M. and Angenon, G. 1997. An Agrobacterium-mediated transient gene expression system for intact leaves. *Plant Science*. 122: 101-108.

Kapust, R. B. and Waugh, D. S. 1999. *Escherichia coli* maltose-binding protein is uncommonly effective at promoting the solubility of polypeptides to which it is fused. *Protein Science*. 8: 1668–1674.

Karran, R.A. and Sanfaçon, H. 2014. *Tomato ringspot virus* coat protein binds to ARGONAUTE 1 and suppresses the translation repression of a reporter gene. *Molecular Plant-Microbe Interactions*. 27(9): 933-943.

Khan, S., Jan, A.T., Mandal, B. and Haq, Q.M.R. 2012. Immunodiagnosics of *Cucumber mosaic virus* using antisera developed against recombinant coat protein. *Archives of Phytopathology and Plant Protection*. 45: 561-569.

Konaté, G., Barro, N., Fargette, D., Swanson, M.M. and Harrison, B.D. 1995. Occurrence of whitefly-transmitted geminiviruses in crops in Burkina Faso, and their serological detection and differentiation. *Annals of Applied Biology*. 126: 121–129.

Lamberti, F., Taylor, C.E. and Seinhorst, J.W. 1975. *Nematode Vectors of Plant Viruses*. 460 pp. Plenum Press.

Lamprecht, R.L., Maree, H.J., Stephan, D. and Burger, J.T. 2012. Complete nucleotide sequence of a South African isolate of *Grapevine fanleaf virus*. *Virus Genes*. 45: 406–410.

Lamprecht, R.L., Spaltman, M., Stephan, D., Wentzel, T. and Burger, J.T. 2013. Complete nucleotide sequence of a South African isolate of *Grapevine fanleaf virus* and its associated satellite RNA. *Viruses*. 5: 1815-1823.

Lareu, M., Phillips, C., Torres, M., Brion, M. and Carracedo, A. 2003. Typing Y-chromosome single nucleotide polymorphisms with DNA microarray technology. *International Congress Series*. 1239: 21–25.

Le Gall, O., Iwanami, T., Karasev, A.V., Jones, A.T., Lehto, K., Sanfaçon, H., Wellink, J., Wetzel, T. and Yoshikawa, N. 2005. Family *Comoviridae*. In: Fauquet, C. M., Mayo, M.A., Maniloff, J., Desselberger, U. and Ball, L.A. (eds.), *Virus Taxonomy: The classification and nomenclature of viruses. The eight report of the International Committee on Taxonomy of Viruses (ICTV)*. 807-818. Academic Press, San Diego, USA.

Lee, G., Tanaka, M., Park, K., Lee, S.S., Kim, Y.M., Junn, E., Lee, S.H. and Mouradian, M.M. 2004. Casein kinase II-mediated phosphorylation regulates alpha-synuclein/synphilin-1 interaction and inclusion body formation. *Journal of Biological Chemistry*. 279(8): 6834-6839.

Liebenberg, A., Freeborough, M-J., Visser, C.J., Bellstedt, D.U. and Burger, J.T. 2009. Genetic variability within the coat protein gene of *Grapevine fanleaf virus* isolates from South Africa and the evaluation of RT-PCR, DAS-ELISA and ImmunoStrips as virus diagnostic assays. *Virus Research*. 142: 28–35.

Lillie, H., Schwarz, E. and Rudolph, R. 1998. Advances in refolding of proteins produced in *E. coli*. *Current Opinion in Biotechnology*. 9: 497–501.

Ling, K.S., Zhu, H.Y., Petrovic, N. and Gonsalves, D. 2007. Serological detection of *Grapevine leafroll virus 2* using an antiserum developed against the recombinant coat protein. *Journal of Phytopathology*. 155: 65-69.

Lipman, N.S., Jackson, L.R., Trudel, L.J. and Weis-Garcia, F. 2005. Monoclonal versus polyclonal antibodies: Distinguishing characteristics, applications, and information sources. *ILAR Journal*. 46:258–268.

Livak, K.J., Flood, S.J.A., Marmero, J., Giusti, W. and Deetz, K. 1995. Oligonucleotides with fluorescent dyes at opposite ends provide a quenched probe system useful for detecting PCR products and nucleic acid hybridization. *PCR Methods and Applications*. 4: 357-362.

Loconsole, G., Fatone, M.T. and Savino, V. 2009. Specific digoxigenin-labelled riboprobes for detection of *Citrus psorosis virus* and *Citrus variegation virus* by molecular hybridization. *Journal of Plant Pathology*. 91(2): 311-319.

López, M.M., Llop, P., Olmos, A., Marco-Noales, E., Cambra, M. and Bertolini, E. 2009. Are Molecular Tools Solving the Challenges Posed by Detection of Plant Pathogenic Bacteria and Viruses? *Current Issues in Molecular Biology*. 11: 13-46

Mackay, J. and Landt, O. 2007. Real-time PCR fluorescent chemistries. *Methods in Molecular Biology*. 353: 237-61.

Makkouk, K.M., Hsu, H.T. and Kumari, S.G. 1993. Detection of three plant viruses by dot-blot and tissue-blot immunoassays using chemiluminescent and chromogenic substrates. *Journal of Phytopathology*. 139: 97–102.

Malan, A.P. and Hugo, H.J. 2003. Present status of grapevine nepoviruses and their vectors in South Africa. *Wineland*. 14: 120-123.

Mardis, E.R. 2008. The impact of next-generation sequencing technology on genetics. *Trends in Genetics*. 24(3): 133-141.

Margis, R., Ritzenthaler, C., Reinbolt, J., Pinck, M. and Pinck, L. 1993. Genome organisation of grapevine fanleaf nepovirus RNA2 deduced from the 122K polyprotein P2 *in vitro* cleavage products. *Journal of General Virology*. 74: 1919-1926.

Margis, R., Viry, M., Pinck, M., Bardonnet, N. and Pinck, L. 1994. Differential proteolytic activities of precursor and mature forms of the 24K proteinase of grapevine fanleaf nepovirus. *Virology*. 200: 79-86.

Martelli G.P. 1993. Graft-transmissible Diseases of Grapevines. *Handbook for Detection and Diagnosis*. 263 pp. ICVG, FAO Publication Division, Rome.

Martelli, G.P. and Boudon-Padieu, E. 2006. *Directory of infectious diseases of grapevines and viruses and viruslike diseases of the grapevine: bibliographic report 1998– 2004. Options Méditerranéennes, Ser. B, N. 55*. Mediterranean Agronomic Institute of Valenzano, Bari, Italy.

Martelli, G.P. and Savino, V. 1990. Fanleaf degeneration. In: Pearson, R.C. and Goheen, A. (eds.), *Compendium of Grape diseases*. 48-49. APS Press, Minnesota, USA

Martelli, G.P., Walter, B. and Pinck, L. 2001. Grapevine fanleaf virus. Descriptions of Plant Viruses. <http://www.dpvweb.net/dpv/showdpv.php?dpvno=385> (Accessed 01 September 2013).

Mayo, M.A. and Robinson, D.J. 1996. Nepoviruses: molecular biology and replication. In: Harrison, B.D. and Murrant, A.F. (eds.), *The Plant Viruses: Polyedral Virions and Bipartite RNA Genomes, volume 5*. 139-185. Plenum Press, New York, USA.

Mekuria, T.A., Gutha, L.R., Martin, R.R. and Naidu, R.A. 2009. Genome diversity and intra- and interspecies recombination events in *Grapevine fanleaf virus*. *Phytopathology*. 99: 1394–1402.

Mercado-Pimentel, M.E., Jordan, N.C. and Aisemberg, G.O. 2002. Affinity purification of GST fusion proteins for immunohistochemical studies of gene expression. *Protein Expression and Purification*. 26: 260-265.

Metzker, M.L. 2010. Sequencing technologies – the next generation. *Nature Reviews Genetics*. 11(1): 31–46

Milne, R.G. 1993. Electron microscopy of in vitro preparations. In: Matthews, R.E.F. (ed.), *Diagnosis of plant virus diseases*. 215-251. CRC Press, Florida, USA.

Minafra, A., Casati, P., Elicio, V., Rowhani, A.; Saldarelli, P.; Savino, V. and Martelli, G.P. 2000. Serological detection of Grapevine rupestris stem pitting-associated virus (GRSPaV) by a polyclonal antiserum to recombinant virus coat protein. *Vitis*. 39: 115–118.

Monis, P.T., Giglio, S. and Saint, C.P. 2005. Comparison of SYTO9 and SYBR Green I for real-time polymerase chain reaction and investigation of the effect of dye concentration on amplification and DNA melting curve analysis. *Analytical Biochemistry*. 340: 24–34

Mukhopadhyay, A. 1997. Inclusion bodies and purification of proteins in biologically active forms. *Advances in Biochemical Engineering/Biotechnology*. 56:61–109.

Mulholland, V. 2009. Immunocapture-PCR for plant virus detection. *Methods in Molecular Biology*. 508:183-192

Mullis, K.F., Faloona, F., Scharf, S., Saiki, R., Horn, G. and Erlich, H. 1986. Specific enzymatic amplification of DNA in vitro: the polymerase chain reaction. *Cold Spring Harbor Symposia on Quantitative Biology*. 51: 263-273.

Murant, A.F and Mayo, M.A. 1982. Satellites of plant viruses. *Annual Review of Phytopathology*. 20: 49-70.

Naidu, R.A., Mayo, M.A., Reddy, S.V., Jolly, C.A. and Torrance, L. 1997. Diversity among the coat proteins of luteoviruses associated with chickpea stunt disease in India. *Annals of Applied Biology*. 130: 37–47.

Naraghi-Arani, P., Daubert, S. and Rowhani, A. 2001. Quasispecies nature of the genome of *Grapevine fanleaf virus*. *Journal of General Virology*. 82: 1791–1795.

- Nemeth, G. 1986. *Virus, mycoplasma, and rickettsia diseases of fruit trees*. 840 pp. Akademiai Kiado, Budapest, Hungary.
- Ng, T.F.F., Duffy, S., Polston, J.E., Bixby, E., Vallad, G.E. and Breitbart, M. 2011. Exploring the diversity of plant DNA viruses and their satellites using vector-enabled metagenomics on whiteflies. *PLOS One*. 6(4): e19050.
- Oliver, J.E., Vigne, E. and Fuchs, M. 2010. Genetic structure and molecular variability of *Grapevine fanleaf virus* populations. *Virus Research*. 152:30–40
- Osman, F., Hodzic, E., Omanska-Klusek, A., Olineka, T. and Rowhani, A. 2013. Development and validation of a multiplex quantitative PCR assay for the rapid detection of Grapevine virus A, B and D. *Journal of Virological Methods*. 194(1-2):138-45.
- Osman, F., Leutenegger, C., Golino, D. and Rowhani, A. 2007. Real-time RT-PCR (TaqMan®) assays for the detection of Grapevine Leafroll associated viruses 1–5 and 9. *Journal of Virological Methods*. 141: 22-29.
- Osman, F., Leutenegger, C., Golino, D. and Rowhani, A. 2008. Comparison of low-density arrays, RT-PCR and real-time TaqMan RT-PCR in detection of grapevine viruses. *Journal of Virological Methods*. 149: 292–299.
- Osman, F., Olinekab, T., Hodzicb, E., Golinoa, D., and Rowhani, A. 2012. Comparative procedures for sample processing and quantitative PCR detection of grapevine viruses. *Journal of Virological Methods*. 179: 303– 310.
- Owens, R.A. and Diener, T.O. 1984. Spot hybridization for the detection of viroids and viruses. In: Maramorosch, K. and Koprowski, H. (eds.), *Methods in Virology Volume VII*. 173–189. Academic Press, New York, USA.

Pacifico, D., Caciagli, P., Palmano, S., Mannini, F. and Marzachi, C. 2011. Quantitation of grapevine leafroll associated virus-1 and -3, grapevine virus A, grapevine fanleaf virus and grapevine fleck virus in field-collected *Vitis vinifera* L. 'Nebbiolo' by real-time reverse transcription-PCR. *Journal of Virological Methods*. 172: 1–7.

Pallás, V., Más, P., and Sanchez-Navarro, J.A. 1998. Detection of plant RNA viruses by nonisotopic dotblot hybridisation. *Methods in Molecular Biology*. 81: 461–468.

Papin, J.F., Vahrson, W. and Dittmer, D.P. 2004. SYBR green-based real-time quantitative PCR assay for detection of West Nile Virus circumvents false-negative results due to strain variability. *Journal of Clinical Microbiology*. 42:1511–1518.

Papin, J.F., Vahrson, W., Larson, L. and Dittmer, D.P. 2010. Genome-wide real-time PCR for West Nile virus reduces the false negative rate and facilitates new strain discovery. *Journal of Virological Methods*. 169(1): 103–111.

Park, H.M., Kim, G.Y., Nam, M.K., Seong, G.H., Han, C., Chung, K.C., Kang, S. and Rhim, H. 2009. The serine protease HtrA2/Omi cleaves Parkin and irreversibly inactivates its E3 ubiquitin ligase activity. *Biochemical and Biophysical Research Communications*. 387: 537-542.

Peng, X., Chan, E.Y., Li, Y., Diamond, D.L., Korth, M.J. and Katze, M.G. 2009. Virus–host interactions: from systems biology to translational research. *Current Opinion in Microbiology*. 12(4): 432-438.

Pinck, L., Fuchs, M., Pinck, M., Ravelonandro, M. and Walter, B. 1988. A satellite RNA in grapevine fanleaf virus strain F13. *Journal of General Virology*. 69: 233-239.

Pinck, M., Reinbolt, J., Loudes, A.M., Le Ret, M. and Pinck, L. 1991. Primary structure and location of the genome linked protein (VPg) of *Grapevine Fanleaf Nepovirus*. *FEBS Letters* 284: 117-119.

Pompe-Novak, M., Gutiérrez-Aguirre, I., Vojvoda, J., Blas, M., Tomažič, I., Vigne, E., Fuchs, M., Ravnikar, M. and Petrovič, N. 2007. Genetic variability within RNA2 of Grapevine fanleaf virus. *European Journal of Plant Pathology*. 117: 307-312.

Pope, B. and Kent, H.M. 1996. High efficiency 5 min transformation of *Escherichia coli*. *Nucleic Acids Research*. 24: 536–537.

Pourrahim, R., Rakhshandehro, F., Farzadfar, Sh. and Golnaraghi, A.R. 2004. Natural occurrence of *Tomato ringspot virus* on grapevines in Iran. *Plant Pathology*. 53: 237

Quacquarelli, A., Gallitelli, D., Savino, V. and Martelli, G.P. 1976. Properties of Grapevine fanleaf virus. *Journal of General Virology*. 32: 349-360.

Radaelli, P., Fajardo, T.V.M., Nickel, O., Eiras, M. and Pio-Ribeiro, G. 2008. Production of polyclonal antisera using recombinant coat proteins of Grapevine leafroll associated virus 2 and Grapevine virus B. *Pesquisa Agropecuária Brasileira*. 43(10): 1405-1411.

Raikhy, G., Hallan, V., Kulshrestha, S. and Zaidi, A. 2007. Polyclonal antibodies to the coat protein of *Carnation etched ring virus* expressed in bacterial system: Production and use in Immunodiagnosis. *Journal of Phytopathology*. 155(10): 616-622.

Raran-Kurussi, S. and Waugh, D.S. 2012. The ability to enhance the solubility of its fusion partners is an intrinsic property of maltose-binding protein but their folding is either spontaneous or chaperone-mediated. *PLOS One*. 7(11): e49589

Raski, D.J., Goheen, A.C., Lider, L.A. and Meredith C.P. 1983. Strategies against *Grapevine fanleaf virus* and its nematode vector. *Plant Disease*. 67: 335-339.

Reid, K.E., Olsson, N., Schlosser, J., Peng, F. and Lund, S.T. 2006. An optimized grapevine RNA isolation procedure and statistical determination of reference genes for real-time RT-PCR during berry development. *BMC Plant Biology*. 6: 27.

Richards, R.S., Adams, I.P., Kreuze, J.F., De Souza, J., Cuellar, W., Dullemans, A.M., Van Der Vlugt, R.A., Glover, R., Hany, U., Dickinson, M. and Boonham, N. 2014. The complete genome sequences of two isolates of *Potato black ringspot virus* and their relationship to other isolates and nepoviruses. *Archives of Virology*. 159(4): 811-815.

Ritzenthaler, C., Viry, M., Pinck, M., Margis, R., Fuchs, M. and Pinck, L. 1991. Complete nucleotide sequence and genetic organization of *Grapevine fanleaf nepovirus* RNA1. *Journal of General Virology*. 72: 2357-2365.

Roberts, I.M. and Harrison, B.D. 1979. Detection of Potato leafroll and Potato mop-top viruses by immunosorbent electron microscopy. *Annals of Applied Biology*. 93: 289–297.

Rodríguez-Pardina, P.E., Hanada, K., Laguna, I.G., Zerbini, F.M. and Ducasse, D.A. 2011. Molecular characterisation and relative incidence of bean-and soybean-infecting begomoviruses in northwestern Argentina. *Annals of Applied Biology*. 158(1): 69-78.

Roossinck, M.J. 1997. Mechanism of plant virus evolution. *Annual Review of Phytopathology*. 35: 191-209.

Roossinck, M.J. 2003. Plant RNA virus evolution. *Current Opinion in Microbiology*. 6(4): 406-409.

Rosario, K., Padilla-Rodriguez, M., Kraberger, S., Stainton, D., Martin, D.P., Breitbart, M. and Varsani, A. 2013. Discovery of a novel mastrevirus and alpha satellite-like circular DNA in dragonflies (Eiprocta) from Puerto Rico. *Virus Research*. 171: 231–237.

Rosenberger, D., Harrison, M. and Gosalves, D. 1983. Incidence of apple union necrosis and decline, tomato ringspot virus, and *Xiphinema* vector species in Hudson Valley orchards. *Plant Disease*. 67: 356-360.

Rott, M.E., Gilchrist, A., Lee, L. and Rochon, D. 1995. Nucleotide sequence of *Tomato ringspot virus* RNA1. *Journal of General Virology*. 76(2): 465-473.

Saldarelli, P., Minafra, A. and Walter, B. 1993. A survey of *Grapevine fanleaf nepovirus* isolates for the presence of satellite RNA. *Vitis*. 32: 99-102.

Sambrook, J., Russel, D.W., Irwin, N. and Jansen, K.A. 2001. *Molecular cloning: a laboratory manual, volume 1*. Cold Spring Harbor Laboratory Press, New York.

Sanfaçon, H., Wellink, J., Le Gall, O., Karasev, A., Van der Vlugt, R. and Wetzels, T. 2009. *Secoviridae*: a proposed family of plant viruses within the order Picornavirales that combines the families Sequiviridae and Comoviridae, the unassigned genera *Cheravirus* and *Sadwavirus*, and the proposed genus *Torradovirus*. *Archives of Virology*. 154: 899–907.

Sanger, F., Nicklen, S. and Coulson, A.R. 1977. DNA sequencing with chain-terminating inhibitors. *Proceedings of the National Academy of Sciences of the United States of America*. 74(12): 5463-5467.

Santos-Rosa, M., Poutaraud, A., Merdinoglu, D. and Mestre, P. 2008. Development of a transient expression system in grapevine via agro-infiltration. *Plant Cell Reports*. 27: 1053-1063.

Schena, M., Shalon, D., Davis, R.W. and Brown, P.O. 1995. Quantitative monitoring of gene expression patterns with a complementary DNA microarray. *Science*. 270(20): 467–470.

Schneider, I.R., White, R.M. and Clverolo, E.L. 1974. Two nucleic acid-containing components of *Tomato ringspot virus*. *Virology*. 57: 139-146.

Schneider, W.L. and Roossinck, M.J. 2001. Genetic diversity in RNA virus quasispecies is controlled by host-virus interactions. *Journal of Virology*. 75(14): 6566-71.

Schots, A. 1995. Monoclonal antibody technology. In: Skerritt, J.H. and Appels, R. (eds.), *New Diagnostics in Crop Sciences, Biotechnology in Agriculture*. 13: 65-86. CAB International, Wallingford, UK.

Serghini, M.A., Fuchs, M., Pinck, M., Reinbolt, J., Walter, B. and Pinck, L. 1990. RNA2 of *Grapevine fanleaf virus*: Sequence analysis and coat protein cistron location. *Journal of General Virology*. 71: 1433-1441.

Sezonov, G., Joseleau-Petit, D. and D'Ari, R. 2007. *Escherichia coli* physiology in Luria-Bertani broth. *Journal of Bacteriology*. 189: 8746–8749.

Silhavy, D., Molnar, A., Lucioli, A., Szittyá, G., Hornyik, C., Tavazza, M. and Burgyan, J. 2002. A viral protein suppresses RNA silencing and binds silencing-generated, 21- to 25-nucleotide double-stranded RNAs. *EMBO Journal*. 21: 3070–3080.

Smith, D.B. and Johnson, K.S. 1988. Single-step purification of polypeptides expressed in *Escherichia coli* as fusions with glutathione S-transferase. *Gene*. 67: 31-40

South African Wine Industry and Systems (SAWIS). <http://www.sawis.co.za> (Accessed 01 November 2014).

Sparkes, I.A., Runions, J., Kearns, A. and Hawes, C. 2006. Rapid, transient expression of fluorescent fusion proteins in tobacco plants and generation of stably transformed plants. *Nature Protocols*. 1: 2019–2025.

Stephan D., Slabber, C., George, G., Ninov, V., Francis, K.P. and Burger, J.T. 2011. Visualization of plant viral suppressor silencing activity in intact leaf lamina by quantitative fluorescent imaging. *Plant Methods*. 7: 25.

Stewart, E.L., Qu, X.S., Overton, B.E., Gildow, F.E., Wenner, N.G., and Grove, D.S. 2007. Development of a real-time RT-PCR SYBR Green assay for *Tomato ring spot virus* in grape. *Plant Disease*. 91:1083-1088.

Stoger, E., Sack, M., Fischer, R., Christou, P. 2002. Plantbodies: Applications, advantages and bottlenecks. *Current Opinion in Biotechnology*. 13: 161-166.

Sun, Q.M., Chen, L.L., Cao, L., Fang, L., Chen, C. and Hua, Z.C. 2005. An improved strategy for high-level production of human vasostatin 120–180. *Biotechnology Progress*. 21: 1048–1052.

Swift, G.H., Peyton, M.J. and MacDonald, R.J. 2000. Assessment of RNA quality by semiquantitative RT-PCR of multiple regions of a long ubiquitous mRNA. *Biotechniques*. 28(3): 524-531.

Tamura, K., Peterson, D., Peterson, N., Stecher, G., Nei, M. and Kumar, S. 2011. MEGA5: molecular evolutionary genetics analysis using maximum likelihood, evolutionary distance, and maximum parsimony methods. *Molecular Biology and Evolution*. 28: 2731–2739.

Tang, W., Sun, Z.Y., Pannell, R., Gurewich, V. and Liu, J.N. 1997. An efficient system for production of recombinant urokinase-type plasminogen activator. *Protein Expression and Purification*. 11: 279–283.

Taylor, C.E. and Robertson, W.M. 1970. Sites of virus retention in the alimentary tract of the nematode vectors, *Xiphinema diversicaudatum* (Nicol.) and *X. index* (Thorne and Allen). *Annals of Applied Biology*. 66: 375-380.

Terlizzi, F., Biolchini, L. and Credi, R. 2004. Molecular characterization of Italian *Grapevine fanleaf virus* isolates. *Journal of Plant Pathology*. 86: 335

Torrance, L. 1998. Developments in serological methods to detect and identify plant viruses. *Plant Cell, Tissue and Organ Culture*. 52: 27-32.

Toye, B., Zhong, G.M., Peeling, R. and Brunham, R.C. 1990. Immunologic characterization of a cloned fragment containing the species-specific epitope from the major outer membrane protein of *Chlamydia trachomatis*. *Infection and Immunity*. 58(12): 3909-3913.

Vaira, A.M., Vecchiati, M., Masenga, V. and Accotto, G.P. 1996. A polyclonal antiserum against a recombinant viral protein combines specificity with versatility. *Journal of Virological Methods*. 56: 209-219.

Van Doorn, R., Szemes, M., Bonants, P., Kowalchuk, G.A., Salles, J.F., Ortenberg, E. and Schoen, C.D. 2007. Quantitative multiplex detection of plant pathogens using a novel ligation probe-based system coupled with universal, high-throughput realtime PCR on Open Arrays. *BMC Genomics*. 14: 276.

Van Regenmortel, M.H.V. and Dubs, M.C. 1993. Serological procedures. In: Matthews, R.E.F. (ed.), *Diagnosis of plant virus diseases*. 159-214. CRC Press, Florida, USA.

Van Zyl, S., Vivier, M.A. and Walker, M.A. 2012. *Xiphinema index* and its relationship to grapevines: a review. *South African Journal of Enology and Viticulture*. 33(1): 21-32

Vandesompele, J., De Paepe, A. and Speleman, F. 2002. Elimination of primer-dimer artifacts and genomic coamplification using a two-step SYBR green I real-time RT-PCR. *Analytical Biochemistry*. 303(1): 95-98.

Vaquero, C., Sack, M., Chandler, J., Drossard, J., Schuster, F., Monecke, M., Schillberg, S. and Fischer, R. 1999. Transient expression of a tumor-specific single-chain fragment and a chimeric antibody in tobacco leaves. *Proceedings of the National Academy of Sciences of the United States of America*. 96(20): 11128-11133.

Varga, A. and James, D. 2006. Real-time RT-PCR and SYBR Green I melting curve analysis for the identification of *Plum pox virus* strains C, E, A, and W: Effect of amplicon size, melt rate, and dye translocation. *Journal of Virological Methods*. 132: 146–153.

Veres, G., Gibbs, R.A., Scherer, S.E. and Caskey, C.T. 1987. The molecular basis of the sparse fur mouse mutation. *Science*. 237: 415-417.

- Vigne, E., Bergdoll, M., Guyader, S. and Fuchs, M. 2004. Population structure and genetic variability within isolates of *Grapevine fanleaf virus* from a naturally infected vineyard in France: evidence for mixed infection and recombination. *Journal of General Virology*. 85: 2435–2445.
- Vigne, E., Marmonier, A. and Fuchs, M. 2008. Multiple interspecies recombination events within RNA2 of *Grapevine fanleaf virus* and *Arabidopsis mosaic virus*. *Archives of Virology*. 153: 1771–1776.
- Voelkerding, K.V., Dames, S.A. and Durtschi, J.D. 2009. Next-generation sequencing: From basic research to diagnostics. *Clinical Chemistry*. 55: 641-658.
- Voinnet, O., Rivas, S., Mestre, P. and Baulcombe, D. 2003. An enhanced transient expression system in plants based on suppression of gene silencing by the p19 protein of tomato bushy stunt virus. *Plant Journal*. 33: 949-956.
- Voller, A., Bidwell, D. and Bartlett, A. 1976. Microplate immunoassay for the immunodiagnosis of virus infections. In: Rose, N.R. and Friedman, H.H. (eds.), *Handbook of Clinical Immunology*. 506-512. ASM Press, Washington D.C., USA.
- Wacker, M.J. and Godard, M.P. 2005. Analysis of one-step and two-step real-time RT-PCR using SuperScript III. *Journal of Biomolecular Techniques*. 16(3): 266-71.
- Walter, B. and Etienne, L. 1987. Detection of *Grapevine fanleaf virus* away from the period of vegetation. *Journal of Phytopathology*. 120: 335–364.
- Wang, A. and Sanfaçon, H. 2000. Diversity in the coding regions for the coat protein, VPg, protease, and putative RNA-dependent RNA polymerase among *Tomato ringspot nepovirus* isolates. *Canadian Journal of Plant Pathology*. 22: 145-149.
- Wang, A. and Sanfaçon, H. 2000a. Proteolytic processing at a novel cleavage site in the N-terminal region of the *Tomato ringspot nepovirus* RNA-1- encoded polyprotein *in vitro*. *Journal of General Virology*. 81: 2771–2781.

Ward, E., Foster, S.J., Fraaje, B.A. and McCartney, H.A. 2004. Plant pathogen diagnostics: immunological and nucleic acid-based approaches. *Annals of Applied Biology*. 145: 1-16.

Webster, C.G., Wylie, S.J. and Jones, M.G.K. 2004. Diagnosis of plant viral pathogens. *Current Science*. 86(12):1604-1607.

Wei, T. and Clover, G. 2008. Use of primers with 5' non-complementary sequences in RT-PCR for the detection of nepovirus subgroups A and B. *Journal of Virological Methods*. 153: 16–21.

Weickert, M.J., Doherty, D.H., Best, E.A. and Olins, P.O. 1996. Optimization of heterologous protein production in *Escherichia coli*. *Current Opinion in Biotechnology*. 7(5):494-499.

Wetzel, T., Candresse, T., Macquaire, G., Ravelonandro, M. and Dunez, J. 1992. A highly sensitive immunocapture polymerase chain reaction method for *Plum pox potyvirus* detection. *Journal of Virological Methods*. 39: 27–37.

Wetzel, T., Jardak, R., Meunier, L., Ghorbel, A., Reustle, G.M. and Krczal, G. 2002. Simultaneous RT-PCR detection and differentiation of *Arabis mosaic* and *Grapevine fanleaf nepoviruses* in grapevines with a single pair of primers. *Journal of Virological Methods*. 101: 63–69.

Wetzel, T., Meunier, L., Jaeger, U., Reustle, G. M. and Krczal, G. 2001. Complete nucleotide sequences of the RNAs 2 of German isolates of *Grapevine fanleaf* and *Arabis mosaic nepoviruses*. *Virus Research*. 75: 139-145.

White, E.J., Venter, M., Hiten, N.F. and Burger, J.T. 2008. Modified cetyltrimethylammonium bromide method improves robustness and versatility: the benchmark for plant RNA extraction. *Biotechnology Journal*. 3(11):1424-1428.

Wroblewski, T., Tomczak, A. and Michelmore, R. 2005. Optimization of *Agrobacterium*-mediated transient assays of gene expression in lettuce, tomato and Arabidopsis. *Plant Biotechnology Journal*. 3: 259–273.

Wylie, S.J., Li, H., Sivasithamparam, K. and Jones, M.G.K. 2014. Complete genome analysis of three isolates of *Narcissus late season yellows virus* and two of *Narcissus yellow stripe virus*: three species or one? *Archives of Virology*. 159: 1521–1525.

Wyss, U. 2000. *Xiphinema index*, maintenance and feeding in monoxenic cultures. In: Maramorosch, K. and Mahmood, F. (eds.), *Maintenance of human, animal, and plant pathogen vectors*. 251-281. Science Research Association, Chicago, USA.

Xu, H.J., Yang, Z.V., Wang, F. and Zhang, C.X. 2006. *Bombyx mori nucleopolyhedrovirus* ORF79 encodes a 28-kDa structural protein of the ODV envelope. *Archives of Virology*. 151: 681–695.

Yang, I.L., Deng, T.C. and Chen, M.J. 1986. Sap transmissible viruses associated with grapevine yellow mottle disease in Taiwan. *Journal of Agricultural Research of China*. 35: 504-510.

Yang, Y., Li, R. and Qi, M. 2000. *In vivo* analysis of plant promoters and transcription factors by agroinfiltration of tobacco leaves. *Plant Journal*. 22(6): 543-551.

Zottini, M., Barizza, E., Costa, A., Formentin, E., Ruberti, C., Carimi, C. and Lo Schiavo, F. 2008. Agroinfiltration of grapevine leaves for fast transient assays of gene expression and for long-term production of stable transformed cells. *Plant Cell Reports*. 27: 845–853.